



Water-soluble nitroxide biradicals for dynamic nuclear polarization

Anil Pandurang Jagtap



Faculty of Physical Sciences
School of Engineering and Natural Sciences
University of Iceland
2016

Water-soluble nitroxide biradicals for dynamic nuclear polarization

Anil Pandurang Jagtap

Dissertation submitted in partial fulfillment of a
Philosophiae Doctor degree in chemistry

Advisor
Professor Snorri Th. Sigurdsson

PhD Committee
Professor Guðmundur G. Haraldsson
Professor Már Másson

Opponents
Dr. Bela E. Bode
Dr. Stefán Jónsson

Faculty of physical sciences
School of Engineering and Natural Sciences
University of Iceland
Reykjavik, May 2016

Water-soluble nitroxide biradicals for dynamic nuclear polarization

Dissertation submitted in partial fulfillment of a *Philosophiae Doctor* degree in chemistry

Copyright © 2016 Anil Pandurang Jagtap
All rights reserved

Faculty of Physical Sciences
School of Engineering and Natural Sciences
University of Iceland
Dunhagi 3
107, Reykjavik
Iceland

Telephone: 525 4000

Bibliographic information:

Anil Pandurang Jagtap, 2016, Water-soluble nitroxide biradicals for dynamic nuclear polarization, PhD dissertation, Faculty of Physical Sciences, University of Iceland.

ISBN 978-9935-9140-9-5

Printing: Háskólaprent ehf.
Reykjavik, Iceland, June 2016

Abstract

Nuclear magnetic resonance (NMR) spectroscopy is a valuable analytical technique which has been applied in various fields. The most glaring limitation of NMR is its low sensitivity. Hyperpolarization techniques such as dynamic nuclear polarization can (DNP) increase the NMR signal intensities by several orders of magnitude. In DNP, polarization is usually transferred through the cross effect mechanism from biradicals to the nuclei that are being investigated. However, most of the known polarizing agents are hydrophobic and, therefore, cannot be used for samples that are soluble in aqueous-based solvents. The thesis describes the synthesis of three water-soluble spirocyclohexanoly biradicals, **bcTol**, **bcTol-M** and **cyolyl-TOTAPOL**. Both **bcTol** and **bcTol-M** showed exceptional solubility in water, much higher than any other known biradical, in addition to showing large DNP enhancements.

The reductive stability of various radicals was also investigated with the aim to use them as reporter groups for electron paramagnetic resonance (EPR) spectroscopic studies in cells, which contain natural reductants such as ascorbic acid and glutathione. A library of fifteen radicals was prepared and screened under different reducing conditions, including live cells. A tetraethylpyrrolidine-derived nitroxide was shown to be the most stable radical towards reduction. Tetraethylisoindoline-based radicals were also found to be reductively stable and due to their ease of synthesis were prepared for incorporation into nucleic acids. A new method for post-synthetic spin labeling of RNA with these labels was developed, utilizing the reaction of 2'-amino groups with aromatic isoindoline-based isothiocyanates in excellent yields.

Útdráttur

Kjarnsegulgreining (nuclear magnetic resonance, NMR) er mikilvæg litrófsgreiningaraðferð sem hefur verið notuð á mörgum sviðum vísinda. Helsta takmörkun NMR er lág næmni. Ein aðferð til að auka styrkleika NMR merkja um nokkrar stærðargráður er mögnun á kjarnskautun (dynamic nuclear polarization, DNP). Í DNP er skautunin venjulega yfirfærð frá tvístakeindum yfir á þann kjarna sem verið er að skoða með NMR. Hinsvegar eru flestar þekktar tvístakeindir vatnsfælnar og er því ekki hægt að nota þær fyrir sýni sem eru leysanleg í vatni. Þessi ritgerð lýsir smíði á þremur vatnsleysanlegum tvístakeindum, **bcTol**, **bcTol-M** og **cyolyl-TOTAPOL**. Bæði **bcTol** og **bcTol-M** sýna mjög góðan leysanleika í vatni, miklu hærri en hjá öðrum þekktum tvístakeindum, og sterk DNP áhrif.

Stöðugleiki mismunandi stakeinda gagnvart afoxun var einnig rannsakaður í því augnamiði að nota þær við rafeindasegulgreiningu (electron paramagnetic resonance, EPR) í frumum, sem hafa nátturulega afoxunarmiðla eins og askorbínsýru og glútaþíon. Fimmtán stakeindir voru smíðaðar og var stöðugleiki þeirra skoðaður í mismunandi afoxandi umhverfi, þar á meðal í lífandi frumum. Tetraetýlpyrrólídín-afleiddar nítroxíðstakeindir reyndust stöðugastar gagnvart afoxun. Tetraetýlisóindólín-afleiddar nítroxíðstakeindir voru einnig mjög stöðugar gagnvart afoxun og vegna auðveldra efnasmíða voru þær valdar til tengingar við kjarnsýrur. Í því skyni var ný aðferð þróuð til spunamerkingar á RNA þar sem 2'-amínó hópar í RNA voru hvarfaðir við ísóþíósýaníð virkniþópa á ísóindólín stakeindunum í mjög góðum heimtum.

Table of Contents

Abstract.....	iii
Útdráttur.....	v
Table of Contents	v
List of Figures.....	ix
List of Schemes	xi
List of Tables	xiii
List of Original Publications	xv
Abbreviations.....	xvi
Acknowledgements.....	xix
1 Objective and Scope of Ph.D. Thesis	1
2 Introduction	3
2.1 Nuclear magnetic resonance (NMR) spectroscopy	3
2.2 Dynamic nuclear polarization	6
2.2.1 Experimental set up of DNP	8
2.2.2 Mechanisms of DNP	10
2.2.3 Development of biradicals for polarization through the cross effect	12
2.2.4 Increasing DNP efficiency of existing biradicals by improving their electronic relaxation properties	16
2.2.5 Water-soluble biradicals for biological applications	18
2.3 Contribution of this Ph. D. thesis to the field of DNP	20
3 New water-soluble nitroxides: Early excursions	23

3.1	Modification at the α -position of the carbonyl group in 4-oxo-TEMPO.....	24
3.2	Modification at the α -position of the nitroxide group in 4-oxo-TEMPO.....	27
3.3	Conclusion	33
4	Water-soluble spirocyclohexanoly-deriv	35
4.1	Synthesis of bcTol [bis-(spirocyclohexyl-TEMPO-alcohol)-urea]	36
4.2	Synthesis of bcTol-M [bis-(spirocyclohexyl-TEMPO-alcohol)-urea-dimethyl]	38
4.3	Synthesis of cyolyl-TOTAPOL [spirocyclohexanoly-1-(TEMPO-4-oxy)-3-(TEMPO-4-amino) propan-2-ol]	40
4.4	DNP studies with bcTol , bcTol-M and cyolyl-TOTAPOL	42
4.5	Conclusion	43
5	Spin labels for in-cell EPR	45
5.1	Conclusion	49
6	Site-directed spin labeling of 2'-amino groups in RNA with reductively stable isoindoline-based nitroxides	51
6.1	Conclusion	54
7	Conclusions	55
	References	57
	Publications	71

List of Figures

Figure 2.1	A. A schematic diagram of MAS of a sample at the magic angle. B. A ^{13}C -NMR spectrum of polycrystalline glycine in static field. C. ss-NMR spectrum obtained with magic angle spinning at the frequency of 7.0 kHz. The Figure 2.1 B and C is printed with permission from <i>Annu. Rev. Chem.</i> , 2001 , 52, 575-606.	4
Figure 2.2	Relative populations of the energy levels for spin $I = \frac{1}{2}$ depending on the applied magnetic field strength B_0	5
Figure 2.3	First demonstration of the Overhauser effect in powdered Li samples. Top line: thermal equilibrium NMR spectrum of ^7Li ; middle line: Enhanced spectrum of ^7Li by electron saturation; bottom line: Proton resonance of a glycerine samples 8 times larger than the Li sample, used to estimate the enhancement. The Figure 2.3 is printed with permission from <i>Phys. Rev.</i> , 1953 , 92, 212–213.	7
Figure 2.4	Polarization of electron and proton spin reservoirs at different temperatures.	8
Figure 2.5	Commercial Bruker DNP solid-state NMR system. The Figure 2.5 is printed with permission from <i>Top. Curr. Chem.</i> , 2013 , 338, 181-228.	9
Figure 2.6	Representation of the EPR spectrum of the TEMPO radical along with the spectral width (Δ) and the homogenous linewidth (δ).	10
Figure 2.7	The solid effect with a trityl radical that has the homogeneous linewidth (δ).	11
Figure 2.8	The cross effect with a TEMPO radical.	12
Figure 2.9	The structures of carbon-centered trityl and BDPA radicals; Gd-DOTA ; nitroxide mono radicals TEMPOL and 4-amino TEMPO	13
Figure 2.10	A general structure of a nitroxide biradical. The nitroxides are shown in their respective coordinate systems.	14
Figure 2.11	Examples of nitroxide biradicals for DNP.	14

Figure 2.12	Trityl-nitroxide biradicals with varying length and flexibility of the linkers.	15
Figure 2.13	Spirocyclohexyl-derived bTbk biradicals.	17
Figure 2.14	Deuterated derivatives of bTbk and TOTAPOL	18
Figure 2.15	A. Host-guest formation of bTbk with cyclodextrin. B. Micelles formation of TEKPol with surfactant molecules.	19
Figure 2.16	Chemical modification of existing biradicals through incorporation of water soluble functional groups.	20
Figure 4.1	Structures of the new spirocyclohexanolyl biradicals bcTol , bcTol-M and cyolyl-TOTAPOL	36
Figure 4.2	Structures of PyPol and bcTol and their dimethyl derivatives PyPol-diMe and bcTol-M	39
Figure 4.3	A. ¹ H-DNP-signal enhancement (ϵ , filled symbols and T_1 open symbols) for proline, microcrystalline SH3 and channelrhodopsin as a function of temperature using bcTol as a polarizing agent. Proline (0.25 M) was uniformly ¹³ C-, ¹⁵ N- labeled. Spectra were recorded in glycerol- <i>d</i> ₈ /D ₂ O/H ₂ O (60/30/10 v/v/v) containing bcTol (10 mM), measured at 9.4 T in a 3.2 mm zirconia rotor at 8 kHz MAS. T_1 was measured via an inversion recovery experiment with ¹ H- ¹³ C-CP. B. A sample of SH3 (7.0 mg) containing bcTol (20 mM) (18.78 s recycle delay) measured with and without microwave irradiation at 9.4 T (110 K, 16 scans, 4 dummy scans, 5 W microwave power at end of probe waveguide). Insert shows a ribbon representation of the three-dimensional structure of the SH3 protein (PDB entry 1U06).	42
Figure 5.1	A. Reduction of selected radicals in presence of ascorbic acid, the EPR signal intensity is plotted as a function of time. B. Reduction of radicals in a cytosolic extract from <i>X. laevis</i> oocytes.	48
Figure 6.1	Reductive stabilities of TEMPO-labeled (circle), tetramethyl-labeled (triangle) and tetraethyl-labeled (square) RNA duplexes in ascorbic acid. Insert shows a longer time course (12 h) for tetraethyl-labeled RNA duplex.	54

List of Schemes

Scheme 3.1	Two approaches for making water-soluble biradicals by introducing hydrophilic groups at different sites in 1	23
Scheme 3.2	Examples of derivatization at the α -position with respect to the carbonyl group in 1 . A. Synthesis of carboxylate derivatives 2 and 3 . B. Michael reaction of enamine 4 with ethyl acrylate. C. Synthesis of proxyl radical (7) <i>via</i> a Favorskii rearrangement. D. Nucleophilic addition of morpholine to dimethylene derivative 8	24
Scheme 3.3	Synthesis of glycol-linked nitroxide precursors 14 and 16 through triacetoneamine (11).	25
Scheme 3.4	Synthesis of glycol-linked bTbk derivative 20	26
Scheme 3.5	Nucleophilic addition of morpholine A. on dimethylene TEMPO 8 . B. on dimethylene pentamethyl piperidone 23 . Dotted line indicates the projected plan.	27
Scheme 3.6	Various methods for preparation of α -substituted piperidine. A. From acetone (26). B. From α - β -unsaturated ketone 29 (mesityl oxide). C. From bisphosphonate 29 . D. From β -lactam 31 . E. From triacetoneamine (11).	28
Scheme 3.7	Condensation reaction of acetone-ketone 34 with triacetoneamine (11) and pentamethyl piperidone (22).	29
Scheme 3.8	A. Synthesis of mono-substituted derivative 35 from mesityl oxide (29). B. Mechanism for conversion of dihydroxyl compound 40 into tri-hydroxyl derivative 41 , postulated by Knoop <i>et al.</i> ^[101]	30
Scheme 3.9	A. Synthesis of the glycol-derived ketone 46 . B. Attempted condensation of ketone 46 with diacetoneamine (36) and pentamethyl piperidone (22).	31
Scheme 3.10	Synthesis of benzyl protected TOTAPOL derivative 54 , Bz: benzyl.	32

Scheme3.11	A. Attempted debenzylation of the disubstituted compound 50 . B. Hydrogenation of 1 . C. Hydrogenation of the proxyl radical 56	33
Scheme 4.1	Synthesis of spirocyclohexanolyl derived nitroxides. A. An unsuccessful approach using benzyl protected cyclohexanone 48 . B. New approach using the unprotected 4-hydroxyl cyclohexanone (57) for synthesizing diol derivative 58	35
Scheme 4.2	Synthesis of bcTol	37
Scheme 4.3	Improved synthesis of bcTol	38
Scheme 4.4	Urea formation of <i>N</i> -methyl derivative 65 by using carbonyldiimidazole (CDI).	39
Scheme 4.5	Synthesis of bcTol-M using triphosgene.	40
Scheme 4.6	Synthesis of cyolyl-TOTAPOL	41
Scheme 5.1	Reduction of a nitroxide group to an EPR inactive <i>N</i> -hydroxyl amine group. R is an alkyl group.	45
Scheme 5.2	Radicals used for evaluating their stability in reductive conditions. A. Piperidine-based nitroxides. B. Imidazolidine- and pyrrolidine-based nitroxides and a trityl radical. C. Isoindoline-based nitroxides.	47
Scheme 6.1	Spin labeling at the 2'-amino position of the oligonucleotide with isocyanate spin label 86	52
Scheme 6.2	A.Syntheses of isothiocyanate spin labels 89a and 89b . B. Reaction of spin labels 89a and 89b with RNA at 2'-amino position. C. Sequence of a spin-labeled duplex, U* indicates the spin-labeled uridine at 2'-amino position with 86 , 89a and 89b	53

List of Tables

Table 5.1	Extent of reduction of radicals by measuring EPR signal intensities after incubation (2 h) with ascorbic acid, in cell extract and inside oocyte cells.	48
------------------	--	----

List of Original Publications

This doctoral thesis is based on the following publications

- I. Jagtap AP, Krstic I, Kunjir NC, Hänsel R, Prisner TF and Sigurdsson ST, Sterically shielded spin labels for in-cell EPR spectroscopy: Analysis of stability in reducing environment, *Free Radical Res.* **2015**, 49, 78-85.
- II. Saha St, Jagtap AP† and Sigurdsson ST, Site-directed spin labeling of 2'-amino groups in RNA with isoindoline nitroxides that are resistant to reduction, *Chem. Commun.* **2015**, 51, 13142-13145.
(† These two authors contributed equally)
- III. Jagtap AP, Geiger M-A, Stöppler D, Oschkinat H and Sigurdsson ST, bcTol: A highly water-soluble biradical for efficient dynamic nuclear polarization of Biomolecules, *Chem. Commun.* **2016**, manuscript submitted.

Publications that are not part of the doctoral thesis

- IV. Saha S, Jagtap AP and Sigurdsson ST, In: Peter Z. Qin and Kurt Warncke, Editor(s), Chapter fifteen - Site-directed spin labeling of RNA by post-synthetic modification of 2'-amino groups, *Methods in Enzymol.*, Academic Press **2015**, 563, 397-414.

Abbreviations

BDPA	1,3-bisdiphenylene-2-phenylallyl
^{10m} SNR	signal-to-noise ratios per 10 minute
bcTol	bis-(spirocyclohexyl-TEMPO-alcohol)-urea
bcTol-M	bis-(spirocyclohexyl-TEMPO-alcohol)-urea-dimethyl
bTbk	bis-TEMPO-bis-ketal
BTnE	bis-TEMPO-n-ethylene oxide
bTurea	bis-TEMPO tethered by urea
CDI	1,1'-carbonyldiimidazole
CE	cross effect
CIDNP	chemically induced dynamic nuclear polarization
CP	cross polarization
cyolyl-TOTAPOL	spirocyclohexanolyl-1-(TEMPO-4-oxy)-3-(TEMPO-4-amino) propan-2-ol
DARR	¹³ C- ¹³ C dipolar-assisted-rotational-resonance
DMF	dimethylformamide
DMSO	dimethyl sulfoxide
DNP	dynamic nuclear polarization
EPR	electron paramagnetic resonance
GDH	<i>ds</i> -glycerol/D ₂ O/H ₂ O (60:30:10)
MALDI-TOF	matrix-assisted laser desorption/ionization time-of-flight mass spectrometry
MAS	magic angle spinning
<i>m</i> -CPBA	<i>meta</i> -chloroperoxybenzoic acid
NMR	nuclear magnetic resonance
OE	Overhauser effect
OP	optical pumping
OTP	<i>ortho</i> -terphenyl

PBS	phosphate-buffered saline
PDB	protein data bank
PELDOR	pulsed electron-electron double resonance
PHIP	para-hydrogen induced polarization
PRE	paramagnetic relaxation effects
<i>p</i> -TSA	<i>para</i> -toluenesulfonic acid
RNA	ribonucleic acid
SDSL	site-directed spin labeling
SE	solid effect
ss-NMR	solid-state nuclear magnetic resonance
TBAF	tetra- <i>n</i> -butylammonium fluoride
TBDMS-Cl	<i>tert</i> -butyldimethylsilyl chloride
TCE	1,1,2,2-tetrachloroethane
TE	thermal effect
TEMPO	2,2,6,6-Tetramethylpiperidin-1-yl)oxyl
TEMPOL	4-hydroxy-2,2,6,6-tetramethylpiperidin-1-oxyl
THF	tetrahydrofuran
TLC	thin layer chromatography
T_M	thermal denaturation
TM	thermal mixing
TMSOTf	trimethylsilyl trifluoromethanesulfonate
TOTAPOL	1-(TEMPO-4-oxy)-3-(TEMPO-4-amino) propan-2-ol

Acknowledgements

As time flies, Ph.D. study at University of Iceland becomes a very special part of my memories. During this period, colleagues, friends and family members brought me valuable life experience that encouraged me during the study. Therefore, I would like to express my deepest appreciation to them.

Firstly, I would like to express my sincere gratitude to my supervisor and mentor Prof. Snorri Th. Sigurdsson for offering me opportunity to do Ph. D. in his group. His guidance and trust were my major motivation throughout this Ph.D. study. Furthermore, I would like to thank him for the constructive discussions and his patience. Particularly, I would like to appreciate his support to my independent research work, which includes attendance to many important conferences.

Much of research work presented here was accomplished through collaborations. I want to thank my collaborators, Prof. Thomas Prisner and Prof. Hartmut Oschkinat for their valuable contributions and fruitful discussion during the collaborative projects. I also thank my all co-authors for their efforts and valuable insights during the joint projects.

My sincere thanks to members of the Doctoral committee, Prof. Guðmundur G. Haraldsson and Prof. Már Másson, for their encouragement and guidance. I also thank my opponents Dr. Bela E. Bode and Dr. Stefán Jónsson for accepting the invitation to become my opponents and for taking time to critically review my thesis.

I would like to thank past members of the Sigurdsson research group; Dr. Sandip Shelke, Dr. Ajaykumar Kale, Dr. Kristmann Gíslason, Dr. Dnyaneshwar Gophane, Gunnar Sandholt and Snædís Björgvinsdóttir. I also thank current members of the group; Dr. Nitin Kunjir, Dr. Marco Korner, Subham Saha, Nilesh Kamble, Haraldur Y. Júlíusson and Sucharita Mandal for their friendship, supportiveness and helpful discussion during these years.

Furthermore, I would like to thank Dr. Sigríður Jónsdóttir and Valgerður Edda Benediktsdóttir for NMR and mass analyses, as well as Svana Stefánsdóttir and Sverrir Guðmundsson for laboratory support. I am also grateful to the administrative staffs at the Science Institute for their assistances in various ways.

I wish to thank my former mentors Prof. Charansingh H. Gill, Prof. Bhausaheb K. Karale, Dr. Sanjeev Kulkarni, Dr. Anil S. Gajare and Dr. Sudhir S. Srivastava for their support and encouragement. I take this opportunity to express thanks to all my long time beloved friends, Vijay Kasture, Sandip Gavade, Sachin Mahangare, Nivrutti Waghmode, Rajesh Tanksali, Sandip Kulkarni, Mahesh Ekbote, Vijay Dhurandare, Gajanan Thakre and many more who have always been integral part of my life. I would like to also thank Kundan Raj Mishra, Thierry Vanessa Clemeur, Maximillian Riley, Tanya Helgason and their families for their support and help during our stay in Iceland.

I sincerely thank my both parents and mother-in-law for their encouragement and unwavering support of my academic pursuit. I also thank my sisters and their families for their unconditional love and support.

Last and most certainly not least, I want to thank my loving wife, Rajita, for being there at all times and taking care of our little family. I am very lucky to have her in my life. I am thankful to both lovely children, Sarvesh and Radhika who made my life richer and extra sweet.

To my wife Rajita

My children Sarvesh and Radhika

& my parents

1 Objective and Scope of Ph.D. Thesis

Nuclear magnetic resonance (NMR) is a widely used analytical method with major applications in chemistry, biochemistry and medicine. NMR experiments have been performed on both liquid and solid state of matter. In the solid-state, spectral lines become broader, compared with liquid-state, due to anisotropic interactions which are not averaged out due to restricted motion of the molecules. This line broadening in solid-state NMR can be eliminated by a method called magic angle spinning (MAS). However, MAS-NMR like other NMR methods are limited by its low sensitivity. Hyperpolarization techniques such as dynamic nuclear polarization (DNP) increases the NMR signal intensities by several orders of magnitude by transferring electron spin polarization of radicals to nuclear spins of the sample.

Designing new radicals for increasing DNP efficiency through the cross effect DNP mechanism, is an active area of research. Most of the aminoxyl-based (generally referred to as nitroxide-based) biradicals that have been reported are hydrophobic and thus, cannot be used for studying biological systems where aqueous-based solvents need to be used. Therefore, the design and synthesis of new water-soluble nitroxide biradicals with improved DNP properties are in high demand.

The project described in this doctoral thesis is mainly divided into three parts. The first part, which is the major part of this thesis, is the synthesis of water-soluble biradicals that give high DNP efficiency for studying biological systems. In **Chapter 2**, a brief introduction is given on DNP and its historical background, followed by experimental set up used for DNP. In the last section of **Chapter 2**, the development of biradicals for the cross-effect DNP mechanism is described. Our initial synthetic struggles in making new water-soluble biradicals are described in **Chapter 3**. The design and synthesis of three water-soluble spirocyclohexanonyl derived biradicals, called **bcTol**, **bcTol-M** and **cyolyl-TOTAPOL**, along with their DNP evaluation is described in **Chapter 4**. Both **bcTol** and **bcTol-M** showed exceptional high solubility in aqueous medium, more than any other known nitroxide-based biradicals. In addition, they all showed large DNP enhancements.

Determination of the structure and dynamics of biomacromolecules is crucial for understanding their physiological functions. Electron para-

magnetic resonance (EPR) spectroscopy has been used to study the structure and dynamics of nucleic acid through measurements between two covalently attached nitroxide radicals by site directed spin labeling (SDSL). It is of particular interest to study the structures of nucleic acids in cellular environments since they can be different than *in vitro* structures. However, *in vivo* applications of nitroxides and in-cell EPR are adversely affected by the presence of reducing agents inside cells, such as ascorbic acid and glutathione, that reduce nitroxide radicals to the corresponding EPR-silent hydroxylamines. The objective of the second part of my thesis was to find suitable spin labels that are stable inside cells to perform in-cell EPR studies. In **Chapter 5**, the design and synthesis of a library of 15 nitroxide-based radicals, along with a carbon-centered trityl radical is described, along with the evaluation of their reductive stabilities under different reducing conditions. A tetramethyl pyrrolidine-derived spin label was found to be most reductively stable radical among the radicals that we studied.

Tetraethylisoindoline-based nitroxide radicals were also found to be reductively stable and, therefore, chosen for incorporation into RNA, which was accomplished in collaboration with Mr. Subham Saha in our research group. **Chapter 6** describes a post-synthetic spin labeling method of 2'-amino groups of RNA with aromatic isoindoline-based isothiocyanates, *via* formation of thiourea linkage, in excellent yields. These spin labels exhibited limited mobility in RNA, making them promising candidates for distance measurements by pulsed EPR.

2 Introduction

2.1 Nuclear magnetic resonance (NMR) spectroscopy

Over the past few decades, nuclear magnetic resonance (NMR) spectroscopy has grown into an indispensable analytical tool to perform chemical analysis and for studying structure and dynamics of biological macromolecules at atomic resolution. It is commonly used for a wide range of applications from the characterization of synthetic products to the study of molecular structures of systems such as polymers, proteins and catalysts.^[1,2] NMR experiments can be performed on three states of matter, i.e. liquid, solid and gas. However, NMR experiments performed on liquid and solid states are more common.^[3]

In solution-state, rapid tumbling motions of molecules results in averaging of the anisotropic interactions, giving rise to sharp lines in the resulting NMR spectra. For performing liquid-state NMR experiments, the sample under study needs to be soluble in a given solvent up to a concentration of 100 μM .^[4] This is not possible for biomolecules that either have a larger size or form aggregates or complexes. NMR-studies of such systems can be achieved by solid-state NMR (ss-NMR) experiments, which has no molecular size limit. However, in case of ss-NMR, molecules do not undergo any molecular motions and thus, anisotropic interactions are not averaged out as observed in liquid-state NMR. As a result of this, the spectral lines in a ss-NMR spectrum are broad, giving rise to a low-resolution spectrum, displaying a so-called “powder pattern”.^[3,5,6] These powder patterns carry valuable structural and dynamic information about the sample. To eliminate the anisotropic interactions that are causing line broadening in solid phase samples, a method called “magic angle spinning” (MAS) is used.^[7,8] In MAS, the sample is rotated rapidly around an axis of 54.74° with respect to the static magnetic field, resulting in averaging out the anisotropy of nuclear interactions (**Figure 2.1A**). A powder spectrum of polycrystalline glycine (5% of ^{13}C enrichment at the carboxyl site) in static

field is shown in **Figure 2.1B**. Under the MAS conditions, the spectrum shows a single sharp line for the carboxylate group at 180 ppm and for the methylene group at 40 ppm (**Figure 2.1C**).

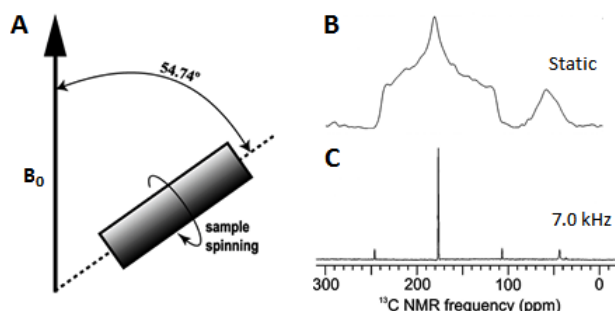


Figure 2.1 A. A schematic diagram of MAS of a sample at the magic angle. B. A ^{13}C -NMR spectrum of polycrystalline glycine in static field. C. ss-NMR spectrum obtained with magic angle spinning at the frequency of 7.0 kHz. The **Figure 2.1 B** and **C** is printed with permission from *Annu. Rev. Chem.*, **2001**, 52, 575-606.

The MAS-NMR technique has been used to acquire high-resolution data on solid samples, among them are many biological systems,^[9,10] e.g. amyloid,^[11-13] nanocrystalline^[14,15] and membrane proteins.^[16-20] However, MAS-NMR, like other NMR techniques is limited by its low sensitivity which is a major drawback and restricts its application. This low sensitivity is due to the small energy difference between the nuclear spin states in the applied magnetic field, resulting in virtually equal numbers of spins in the upper (β state) and lower energy levels (α state). To understand this low sensitivity, consider, a spin $\frac{1}{2}$ nucleus being placed in an external magnetic field. There are two energy states associated with alignment of nuclear spins along or opposite to magnetic field, nuclear spins α and β respectively. The α state has lower energy and thus, it is always more populated than the β state. At thermal equilibrium, the spin populations follow a Boltzmann distribution as given in equation 1, where N_1 and N_2 represent the spin population of the α - and β -energy levels respectively. ΔE is the energy difference between the two spin states, k_B is the Boltzmann constant and T is the temperature in Kelvin.

$$\frac{N_1}{N_2} = e^{-\frac{\Delta E}{k_B T}} = e^{-\frac{h\nu}{k_B T}} \quad (1)$$

The polarization P is defined as the ratio of the difference of number of spins and total number of spins in the two states, given by equation 2, where γ is the gyromagnetic ratio of the nucleus, h is Plank's constant divided by 2π , B_0 is the magnetic field strength, k_B is the Boltzmann constant and T is the temperature in Kelvin.

$$P = \frac{N_2 - N_1}{N_2 + N_1} = \tanh \frac{\gamma \hbar B_0}{2k_B T} \quad (2)$$

Therefore, the sensitivity of NMR spectroscopy depends on the population ratio of the nuclei. **Figure 2.2** shows how the polarization, varies with the applied external magnetic field. To picture this low population difference of nuclei in NMR, consider about two million hydrogen nuclei which yield a population ratio of 0.999872 in a magnetic field of 800 MHz at room temperature. That means for every 1,000,000 nuclei in the β state, there are 1,000,128 nuclei in the lower α state. This small population difference poses a significant sensitivity problem for NMR because only the difference between these populations (i.e. 128 of 2,000,000 spins) is detected, as the others effectively cancel one another.^[21]

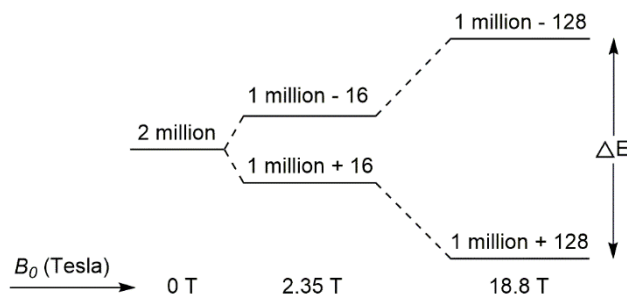


Figure 2.2 Relative populations of the energy levels for spin $I = \frac{1}{2}$ depending on the applied magnetic field strength B_0 .

The sensitivity of NMR experiments has been dramatically increased throughout the lifetime of this technique by instrumental as well as methodological developments. One of the methods to increase the polarization of nuclear spins is to increase the applied magnetic field. This has been the method of choice for two to three decades and has increased NMR signal intensities of up to four orders of magnitude.^[22] Lowering the temperature is an alternative, brute force approach for polarizing spins. At 0.1 K, the polarization of protons reaches 23%. However, this is not very practical because of the technical difficulty of reaching such low temperature. Isotopic enrichments of nuclear spins through chemical modification of the sample is another method which increases NMR signal intensities of nuclei with low natural abundance of magnetically active nuclei such as ^{13}C , ^{15}N and ^{17}O . In addition to these methods, cross polarization (CP) has been frequently used to polarize low γ nuclei (e.g. ^{13}C and ^{15}N) through polarization transfer from high γ -nuclei (e.g. ^1H).

In addition to the approaches which are mentioned above, the sensitivity of NMR can also be increased by several orders of magnitude, well beyond the Boltzmann distribution by a technique which is termed as hyperpolarization. Several hyperpolarization methods have been used in this context, such as chemically induced dynamic nuclear polarization (CIDNP), para-hydrogen induced polarization (PHIP), optical pumping (OP) and dynamic nuclear polarization (DNP). The first two methods (CIDNP and PHIP) produce hyperpolarized states by performing chemical reactions, while optical pumping is limited to noble gases. However, DNP is substantially more general in terms of its applicability in which large polarization from electrons is transferred to nuclei, leading to an enhancement of nuclear polarization. The work described in this thesis is related to this method, which will be explained in more detail in the upcoming sections.

2.2 Dynamic nuclear polarization

DNP is almost as old as NMR spectroscopy. However, development and application of DNP was restricted for a long time, due to a lack of instrumentation required to generate high-frequency microwaves like the gyrotron. DNP was first proposed by Overhauser in 1953.^[23] He predicted that a polarization transfer can occur between the electron spins and the nuclei in metal by irradiating the electron spins at their EPR (electron paramagnetic resonance) frequency. This phenomenon was demonstrated by Slichter and Carver on powdered Li samples, with an enhancement of the ^7Li signal by a factor of ca. 100 (**Figure 2.3**). Later this effect was termed as the Overhauser effect (OE).^[24] In 1955, Abragam extended this effect to non-metals.^[25] In 1956, a DNP experiment in the liquid state was carried by Carver and Slichter.^[26] They dissolved sodium in anhydrous liquid ammonia and saturated the EPR transition of the dissolved free electrons. As a result, more than 400 times increased proton polarization of ammonia was observed.

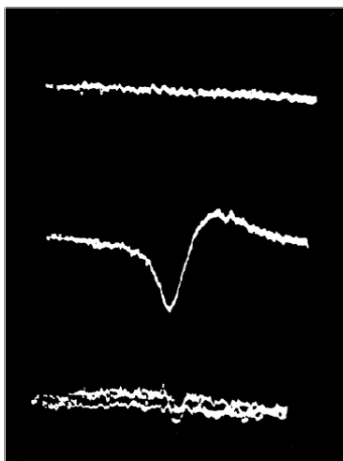


Figure 2.3 First demonstration of the Overhauser effect in powdered Li samples. Top line: thermal equilibrium NMR spectrum of ${}^7\text{Li}$; middle line: Enhanced spectrum of ${}^7\text{Li}$ by electron saturation; bottom line: Proton resonance of a glycerine samples 8 times larger than the Li sample, used to estimate the enhancement. The **Figure 2.3** is printed with permission from *Phys. Rev.*, **1953**, 92, 212–213.

Figure 2.4 shows the polarization of electron- and proton-spin reservoirs at different temperatures. At 90 K and 14 T, the polarization of electron spins is 10.541%, while it is 0.016% for proton spins. Through DNP, this considerably larger electron spin polarization can be transferred to the nuclei of interest by microwave irradiation of the sample at the EPR frequency. Aminoxyl radicals (also called nitroxide radicals), carbon-centered radicals^[22,27-30] as well as paramagnetic metal ions^[31] have been used as the source of electron spins in this context. The polarization transfer from core nuclei to the bulk nuclei propagates through spin diffusion resulting in an increase in NMR signal intensities. The theoretical enhancement (ϵ_{\max}) is given by the ratio of the gyromagnetic ratios (γ) of the electron spin and the nuclear spin. The theoretical enhancement values for proton (${}^1\text{H}$), fluorine (${}^{19}\text{F}$), carbon (${}^{13}\text{C}$) and nitrogen (${}^{15}\text{N}$) nuclei are 660, 700, 2600 and 6494, respectively.

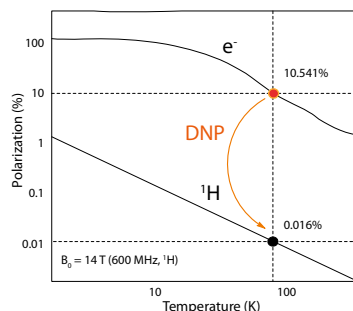


Figure 2.4 Polarization of electron and proton spin reservoirs at different temperatures.

The DNP enhancement factor (ϵ) is quantified conventionally as the ratio between the NMR signal intensities obtained with and without microwave irradiation ($\epsilon_{on/off}$) for a sample that contain radicals. However, Tycko *et al.* observed a 5-6 fold reduction in NMR signal intensities for MAS experiments with a polarizing agent in absence of microwave which was termed as the “depolarization effect”.^[32] They further concluded that intermolecular electron-electron dipolar interaction plays an important role in the depolarization effect under MAS conditions. By considering the depolarization effect, the value of NMR signal intensities under the “microwave off” condition may not be significant and thus, the conventional DNP enhancement factor ($\epsilon_{on/off}$) might be larger than the actual enhancement value. After accounting for this depolarization effect in MAS experiments, one can say that conditions that produce the largest ratio of signal with and without microwaves may not be the same as conditions that maximize NMR sensitivity.^[32,33]

2.2.1 Experimental set up of DNP

The implementation of DNP experiments requires the addition of four pieces of instrumentation to an existing NMR spectrometer: a suitable microwave (μW) source (a gyrotron), a wave guide to transmit the microwaves from the source to the NMR cavity, a multiple frequency NMR probe with a waveguide to irradiate the sample and a cooling cabinet to perform DNP experiments at lower temperatures (**Figure 2.5**). In a gyrotron, an electron beam is guided by a strong magnetic field, produced by a superconducting magnet, and injected into a radiofrequency resonant cavity. As the beam passes through this cavity, its energy is then converted into microwave radiation. Transmitting the microwaves to the sample with a minimal loss of power was a major challenge. This challenge was addressed by Woskov *et al.* by the introduction of waveguides.^[34] Nitrogen and helium gases have been

used for cooling samples to perform DNP experiments at lower temperatures.^[35-37] Most recently, it has been shown by Saint-Bonnet *et al.* that sample spinning with helium gas permits much higher MAS frequencies than the traditional nitrogen gas and at much lower temperatures, which significantly increases the hyperpolarization efficiency.^[38]

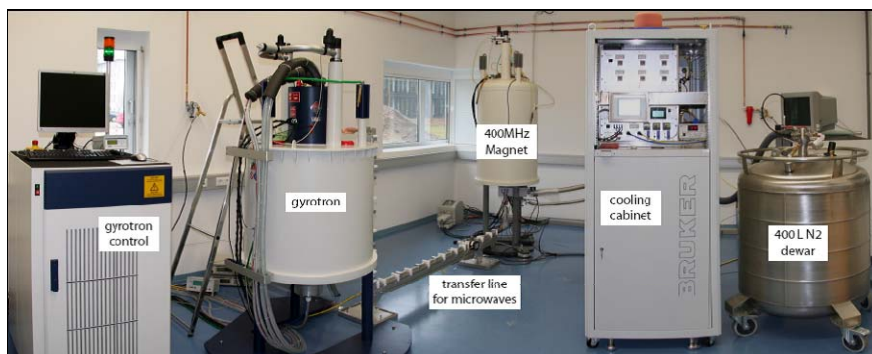


Figure 2.5 Commercial Bruker DNP solid-state NMR system. The **Figure 2.5** is printed with permission from *Top. Curr. Chem.*, **2013**, 338, 181-228.

Sample preparation is an important step for achieving sufficient DNP enhancement. A glass-forming solvent is necessary to avoid the formation of ice crystals that cryoprotects the sample at lower temperature and ensures a uniform distribution of the polarizing agent in the sample.^[35,39] Glycerol-water mixtures are usually used for studying protein samples^[40] in DNP experiments that use water-soluble polarizing agents.^[41,42] However, solvents like 1,1,2,2-tetrachloroethane (TCE), polystyrene, *ortho*-terphenyl (OTP) or a mixture of solvents like DMSO/water or dichloromethane/MeOH have been used for DNP experiments with hydrophobic biradicals.^[39,43-46] Deuterated solvents have also been used to enhance the sensitivity in DNP experiments.^[47,48] However, a minimum concentration of protons is required to distribute the polarization across the entire sample through ^1H - ^1H spin diffusion.^[49,50] It was demonstrated by Rosay *et al.* that a significant increase in DNP efficiency was achieved by using d_8 -glycerol/ D_2O / H_2O (60:30:10; sometimes referred as “DNP juice” or GDH).^[50] Apart from this, the deuterated solvent mixtures that have been used in many DNP experiments are d_6 -DMSO/ D_2O / H_2O (60:34:6),^[39] d_{14} -OTP/OTP (95:5),^[45] and d_4 -MeOH/TCE (4:96).^[51] It has been shown that the DNP enhancement in a fully protonated solvent matrix (glycerol/ H_2O) is smaller than the enhancement that is obtained in a mostly deuterated solvent matrix (d_6 -DMSO/ H_2O).^[50] Recently, Takahashi *et al.* introduced a “matrix-free” sample preparation approach to study the dry compounds, wetting the sample with radical without any a cryoprotecting solution (glycerol, dimethyl sulfoxide, etc.).^[52,53]

2.2.2 Mechanisms of DNP

The type of mechanism that is operational during the DNP experiments depends on the type and concentration of the radical used, as well as on its EPR properties. There are four types of mechanisms through which electron spin polarization is transferred to nuclear spins: The Overhauser effect (OE), the thermal effect or thermal mixing (TE or TM), the solid effect (SE) and the cross effect (CE). The EPR parameters that determine the DNP mechanism are the inhomogeneous breadth of the EPR spectrum (Δ), the homogeneous EPR linewidth (δ), and the nuclear Larmor frequency (ω_{0I}). The inhomogeneous linewidth (Δ) indicates the breadth of entire EPR spectrum and the homogeneous linewidth (δ) represents the linewidth of a single electron orientation element from the whole spectrum (**Figure 2.6**). ω_{0I} is the Larmor- or the precessional-frequency and refers to the rate of precession of the magnetic moment of the nuclear spin around the axis of the external magnetic field.

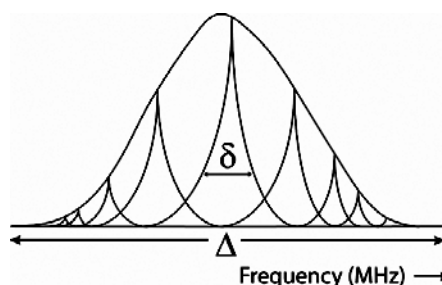


Figure 2.6 Representation of the EPR spectrum of the TEMPO radical along with the spectral width (Δ) and the homogenous linewidth (δ).

2.2.2.1 The Overhauser effect

The OE was first theoretically described in the revolutionary paper published by Albert Overhauser in 1953, who predicted for metals that “if the electron spin resonance of the conducting electrons is saturated, the nuclei will be polarized to the same degree they would if their gyromagnetic ratio were that of electron spin”.^[23] This effect was further proven experimentally, not only for metals,^[24] but also for insulators doped with paramagnetic impurities.^[25] In the OE, polarization is based on the spin flip-flop transitions in two spin systems consisting of one electron and one nuclear spin. This polarization is driven by the electron spin relaxation process that polarizes the nuclear spin. Recently, it was shown that this effect is possible in an insulating solid with narrow line radicals like SA-BDPA and BDPA.^[44] Further, it has been observed that this effect increases with increasing magnetic field.^[45]

2.2.2.2 The thermal effect

The thermal effect^[54,55] is a three-spin facilitated polarization transfer mechanism that occurs when the homogeneously broadened EPR linewidth is larger than the nuclear Larmor frequency ($\delta > \omega_{0I}$). This situation is typically observed at high radical concentrations that increase the overall dipolar couplings of electrons and broaden the δ . Generally, the TM mechanism is more efficient at high magnetic field compared to the SE (Section 2.2.2.3), but smaller compared to the CE (Section 2.2.2.4).

2.2.2.3 The solid effect

The solid effect was proposed by Jeffries in 1957,^[56] and further demonstrated and named by Abragam.^[57] The SE is dominant for radicals having relatively narrow EPR lines compared to the nuclear Larmor frequency ($\delta \approx \Delta < \omega_{0I}$) (Figure 2.7). The polarizing agent is often a radical with high molecular symmetry e.g., carbon-centered radicals like BDPA,^[28,29] trityl^[22,58] and paramagnetic metal ions like Gd-DOTA.^[31] The solid effect is a two spin process, involving one electron and one nucleus. The SE is more favorable at low magnetic fields. For this effect, the microwave frequency should be equal to the relative difference between electron Larmor frequency and the nuclear Larmor frequency or sum of both frequencies ($\omega_e \pm \omega_{0I}$).

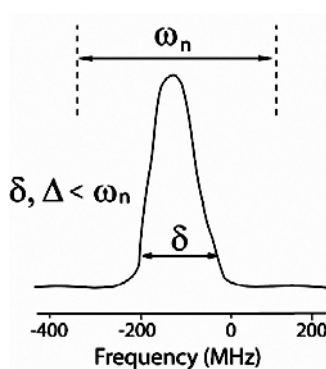


Figure 2.7 The solid effect with a trityl radical that has the homogeneous linewidth (δ).

2.2.2.4 The cross effect

The cross effect is a three spin process (two electrons and one nucleus) that requires a strongly dipole-dipole coupled electron pair and a nucleus. It was discovered by Kessenikh *et al.* in 1963^[59] and further investigated by Hwang and Hill.^[60,61] The CE occurs when the homogenous EPR linewidth is smaller than the nuclear Larmor frequency, and the inhomogeneous breadth of EPR spectrum is larger than ω_{0I} ($\delta < \omega_{0I} < \Delta$).^[62] (Figure 2.8). The efficiency of polarization is maximal when the difference between the Larmor frequencies

of two electrons equals the Larmor frequency of the nucleus ($\omega_{e1} - \omega_{e2} = \omega_{0I}$), which is also known as the frequency matching condition.

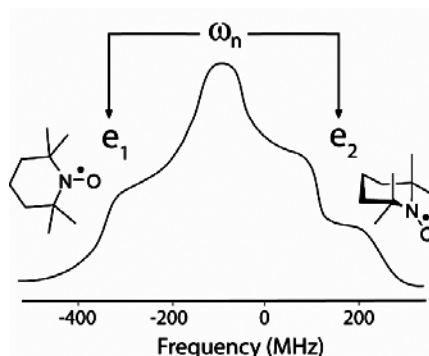


Figure 2.8 The cross effect with a TEMPO radical.

In the CE, microwave radiation is used to excite one electron, which excites other electron that is dipolar coupled, followed by excitation of the nuclear spin if the frequency matching condition is fulfilled. A radical with a broad EPR linewidth, for example a nitroxide satisfies this condition. The CE is more effective when the inter-electron distance and the relative orientation between two nitroxide radicals are optimized, which will be explained in detail in **Section 2.2.3**. CE is the most efficient mechanism at high field and used frequently in MAS-DNP experiments.

2.2.3 Development of biradicals for polarization through the cross effect

Polarizing agents represent a core resource for DNP. They must exhibit a long lifetime for the unpaired electron, along with good solubility in the solvent matrix that is used for DNP experiments. Further, they should be capable of polarizing a large array of samples, ranging from small molecules to proteins. The most commonly used polarizing agents are nitroxide radicals and carbon-centered radicals such as trityl and BDPA (**Figure 2.9**). Furthermore, paramagnetic metal ions like Mn^{2+} and Gd^{3+} have also been used as a polarizing agents (**Figure 2.9**).^[31]

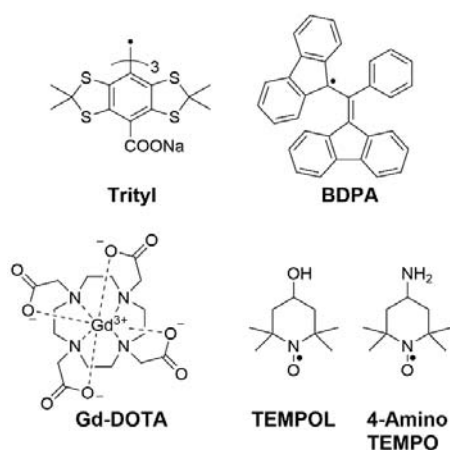


Figure 2.9 The structures of carbon-centered **trityl** and **BDPA** radicals; **Gd-DOTA**; nitroxide mono radicals **TEMPOL** and **4-amino TEMPO**.

Nitroxide monoradicals, such as **TEMPOL** and **4-amino TEMPO** (**Figure 2.9**) have been used in early high field DNP experiments. The use of monoradical requires a high concentration of radicals, up to 40mM.^[35,63] However, at high concentration, paramagnetic relaxation effects (PRE) dominates, resulting into line-broadening and signal quenching (also called “the bleaching effect”).^[52,64,65] A high concentration of radicals also directly affects the intensity of the detectable NMR signal as it leads to increased nuclear spin relaxation rates of nearby nuclei, thus broadening the NMR resonance of close nuclei beyond the limit of detection.^[33] A DNP experiment that is performed using monoradicals will have a lower number of molecules that satisfy the frequency matching condition ($\omega_{e1} - \omega_{e2} = \omega_{0l}$), which is essential for getting maximal DNP enhancement through the CE. To improve the efficiency of CE, biradicals were introduced which ensure that the frequency matching condition is satisfied. The use of biradicals enables a lower concentration of radicals to be used, compared with monoradicals, which reduces the PRE.

Much effort has been devoted to the design and synthesis of more efficient biradicals for DNP. For the design of biradicals, two structural factors are important and need to be considered. First, the two radicals should be tethered at an optimal interspin distance, which guarantees electron-electron dipolar coupling between the two radicals. The second factor which also has an influence on the DNP efficiency, is the relative orientation between the two nitroxide radicals. **Figure 2.10** shows a schematic representation of a biradical, where two nitroxide radicals in their coordinate systems, are placed at a distance R .

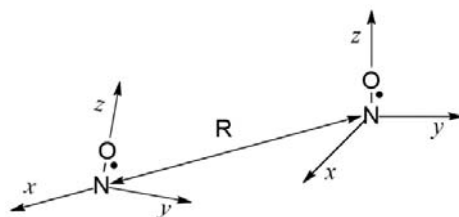


Figure 2.10 A general structure of a nitroxide biradical. The nitroxides are shown in their respective coordinate systems.

As stated in **Section 2.2**, the enhancement factor (ϵ) is the ratio of the NMR signal intensities obtained with and without microwave irradiation. The values of the enhancements for biradicals are always compared with other known biradicals, because the absolute value may differ for the same biradical. The reason is that the enhancement values depend on the experimental conditions under which it was determined, such as the strength of the magnetic field, the temperature and the solvent matrix, which varies from experiment to experiment. A comparative screening of all biradicals under the same experimental condition would be the ideal way for comparing their DNP efficiencies, but has not been reported to date.

In order to find the optimal distance between two TEMPO radicals, Hu *et al.* synthesized a series **bis-TEMPO-*n*-ethylene oxide (BTnE)** biradicals with a varying length of ethylene glycol chains by $n = 2-4$ units.^[47] It was found that if two nitroxide units are linked with two ethylene glycol units (**BT2E**, **Figure 2.11**), optimal enhancement (ϵ) of 175 among this series of biradicals was observed, which is almost 4 times higher than the monoradical TEMPO ($\epsilon \approx 45$). **Bis-TEMPO** tethered by **urea (bTurea**, **Figure 2.11**) is another biradical in which two TEMPO moieties were linked with urea linkage. It was first described in 1965^[66] and tested as DNP polarizing agent by Hu *et al.*^[48] It was 3 times more efficient than TEMPO.

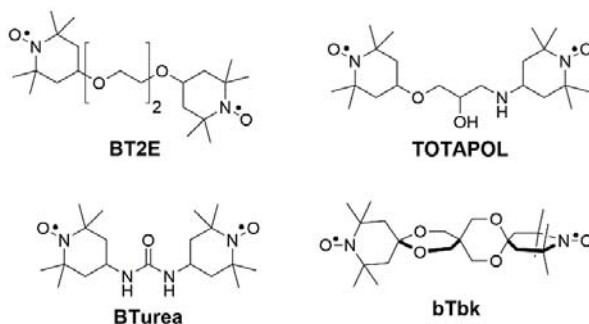


Figure 2.11 Examples of nitroxide biradicals for DNP.

More recently, Mathies *et al.* have screened trityl-TEMPO biradicals (**Figure 2.12**) that have linkers of different lengths and flexibility.^[67] Among these biradicals, **TEMTriPol-1** showed an enhancement of 65, which is the largest enhancement achieved at 18.8 T (800 MHz) in this series. However, other biradicals in this series performed poorly, probably due to the length and/or flexibility of the linker.

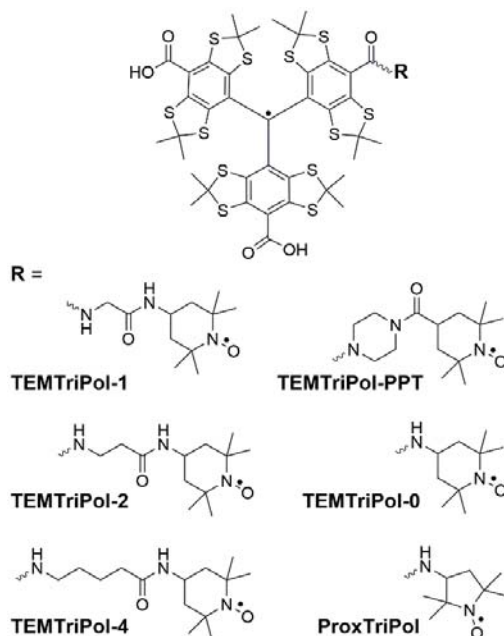


Figure 2.12 Trityl-nitroxide biradicals with varying length and flexibility of the linkers.

The first water-soluble biradical, 1-(TEMPO-4-oxy)-3-(TEMPO-4-amino) propan-2-ol (**TOTAPOL**, **Figure 2.11**), was introduced by Song *et al.* It contains two TEMPO moieties linked by a tether that has a secondary hydroxyl and an amino group, that increase its aqueous solubility.^[41] This biradical is one of the most frequently used water-soluble biradicals for studying biological systems and showed similar enhancement as **BT2E**.

Bis-TEMPO-bis-ketal (bTbk, Figure 2.11) was designed to improve the relative orientation of the tethered nitroxide radicals.^[39] In this biradical, two TEMPO units are placed nearly orthogonal to each other by using a rigid bis-ketal tether. Orthogonal orientation between two nitroxide radicals is considered to be the ideal angle in order to satisfy the frequency matching condition for the cross effect.^[68] This biradical gave a 1.4 times higher enhancement than **TOTAPOL**.

2.2.4 Increasing DNP efficiency of existing biradicals by improving their electronic relaxation properties

The DNP efficiency of the biradicals that are mentioned in **Section 2.2.3** can be improved further by increasing the electronic relaxation (T_{1e} and T_{2e}) of the radicals, which is another parameter that affects the DNP performance. The T_{1e} relaxation time (also known as longitudinal relaxation, or relaxation along the z-direction, or spin-lattice relaxation) is a measure of how quickly the net magnetization recovers to its ground state in the direction of the applied magnetic field. Longer T_{1e} facilitates saturation of EPR transitions with spins, resulting in an increase in DNP efficiency. Another relaxation time which influences the DNP performance is the spin-spin relaxation time (T_{2e} , sometimes called transverse relaxation, or relaxation along xy plane) and referred to the rate of decay of magnetization within xy plane. This relaxation is caused by molecular motion.

Methyl groups that are present at the α -position to the nitroxide group are known to create relaxation pathways of the radical by generating fluctuating dipolar fields through their rotation.^[69] Rotation of these methyl groups can also induce effective transverse relaxation that result in shorter T_{1e} . Further, these methyl groups have been called “polarization sink”, as a lot of polarization has been used by protons from methyl groups.^[70] Removing these methyl groups by replacing them with other groups can lead to longer relaxation times, which is also known to increase the time constant for the echo decay (T_m , also termed as phase memory time) which increases the T_{1e} and ultimately increases DNP performance.^[68] In **bCTbk** (**Figure 2.13**), the methyl groups that are present at the α -position to the nitroxide group, have been replaced with spirocyclohexyl groups which resulted into increase in relaxation time T_{1e} by a factor of two, compared with **bTbk**.^[71] This increase in T_{1e} of **bCTbk** resulted in a DNP enhancement of about 4 compared to the parent **bTbk** biradical.

A series of seven high molecular weight biradicals that are derivatives of **bTbk** has been synthesized to study the impact of radical relaxation time on the DNP enhancement.^[68] Out of these biradicals, **TEKPol** (**Figure 2.13**) showed 2.5 times higher DNP enhancement than **bCTbk** and was found to be a very efficient polarizing agent in this series. It was hypothesized that lessened molecular motions of these high molecular weight-containing biradicals slows the electronic relaxation of radicals, and thus gives longer phase memory relaxation time (T_m). **TEKPol2** (**Figure 2.13**) is another biradical that possesses high molecular weight and recently has been synthesized by Kubicki *et al.*^[51] In this biradical, two phenyl rings are placed at the meta position with respect to each other on the spirocyclohexyl moieties of **TEKPol**. This biradical showed slightly higher enhancement than

TEKPol and the highest enhancement of all known nitroxide-based biradicals.

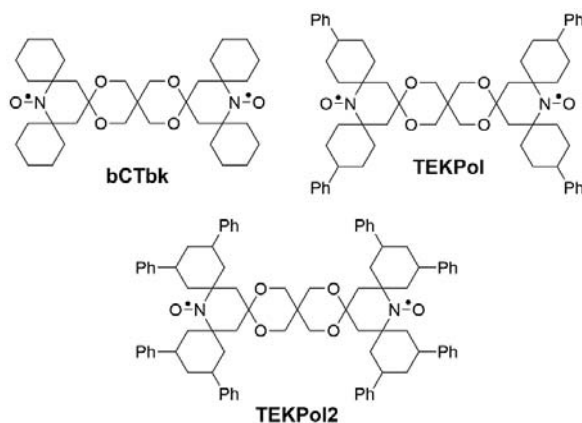


Figure 2.13 Spirocyclohexyl-derived **bTbk** biradicals.

Instead of replacing the methyl groups, their protons can also be replaced by deuteration, which is another way to increase DNP efficiency. As a result of deuteration, less polarization will be spent on repolarizing the rapidly relaxing protons of the methyl groups that are present at α -position to the nitroxide group. Replacement of these protons by deuteration eliminates the ^1H spins that are close to the radical which increases phase memory time (T_m).^[51]

Deuterated derivatives of **bTbk** and **TOTAPOL** biradicals (**Figure 2.14**) have been synthesized by Perras et al.^[70] Up to 70% increase in DNP enhancement has been observed after performing deuteration for both biradicals. A similar increment in DNP enhancement was obtained by Kubicki *et al.* for a deuterated derivative of **bTbk**.^[51] Deuteration can also be carried out on the sample which is under study rather than the polarizing agent, to improve its DNP enhancement. For instance, it was observed that a deuterated SH3 protein gave larger DNP enhancement than the corresponding protonated form of the protein.^[49]

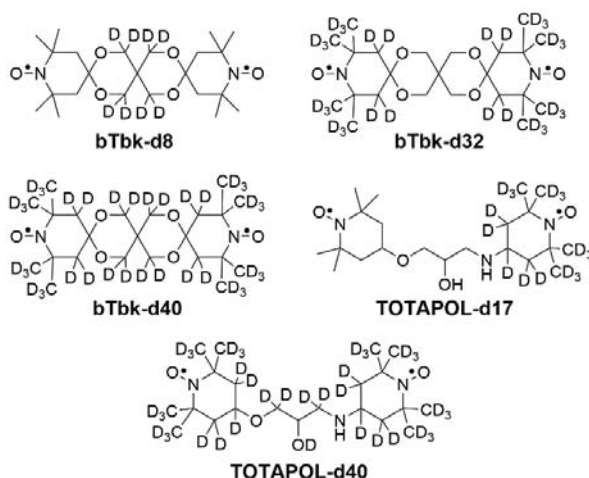


Figure 2.14 Deuterated derivatives of **bTbk** and **TOTAPOL**.

2.2.5 Water-soluble biradicals for biological applications

Although the biradicals mentioned in Sections 2.2.3 and 2.2.4 showed good enhancements, they are all hydrophobic in nature, except **TOTAPOL**. These biradicals are sparingly soluble in DMSO/water mixtures, hence their use is limited to DNP/ss-NMR applications carried out in organic solvents.^[71,72] As these biradicals are not soluble in aqueous systems, they can't be used for studying biological systems that ultimately require more polar solvents (glycerol/water mixtures).

In order to use hydrophobic radicals, that are efficient polarizers, for biological applications, two strategies have been used. The first strategy was to prepare a noncovalent complex of hydrophobic biradicals with water-soluble entities. For instance, **bTbk** was mixed with cyclic oligosaccharides such as cyclodextrins, that can form host-guest complexes (**CAP-bTbk**, **Figure 2.15A**), increasing its water-solubility up to 20 mM in DNP juice.^[73] In another example, hydrophobic radicals such as **bTbk** and **TEKPol** were mixed with surfactant molecules that form micelles, to improve their water-solubility.^[74,75] With this strategy, aqueous solutions of micelles containing **bTbk** (**Figure 2.15B**), **TEKPol** biradicals have been prepared in concentration of up to 30 mM and 8 mM in DNP juice, respectively.

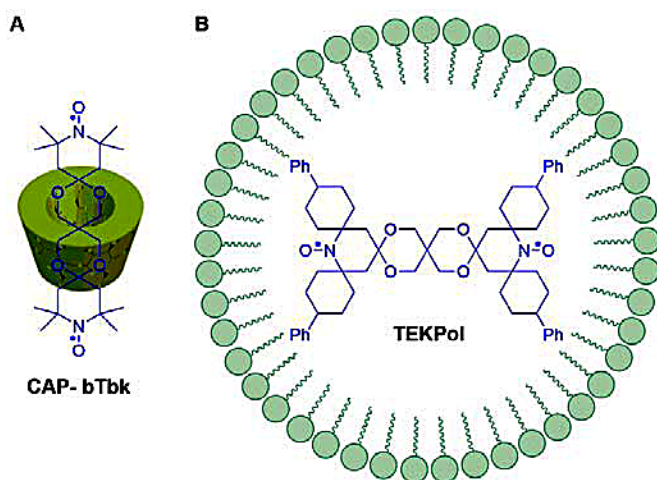


Figure 2.15 **A.** Host-guest formation of **bTbk** with cyclodextrin. **B.** Micelles formation of **TEKPol** with surfactant molecules.

Water-solubility can also be increased by performing chemical modification of known biradicals. The first example of chemical modification was done on the **bTbk** biradical, where oxygen atoms from the bisketal tether were replaced with sulfur atoms in order to introduce hydrophilic groups through oxidation.^[76] However, oxidation of these sulfur atoms gave a complex mixture of various oxidized products that were difficult to isolate (**bTbtk**, **Figure 2.16**). This biradical mixture was soluble up to 20 mM in DNP juice and showed 1.1 times higher DNP enhancement than **TOTAPOL**. **bTbtk-py** (**Figure 2.16**) was also synthesized in a similar manner and gave a 1.2 times higher DNP enhancement than **TOTAPOL**.^[77] However, the DNP enhancements values for both biradicals (**bTbtk** and **bTbtk-py**) were smaller than their parent biradical **bTbk**, which was 1.4 times higher than **TOTAPOL**.^[39] The reason for their lower performance is presumably due to a change in the inter-radical distance after replacing the oxygen atoms by sulfur atoms.

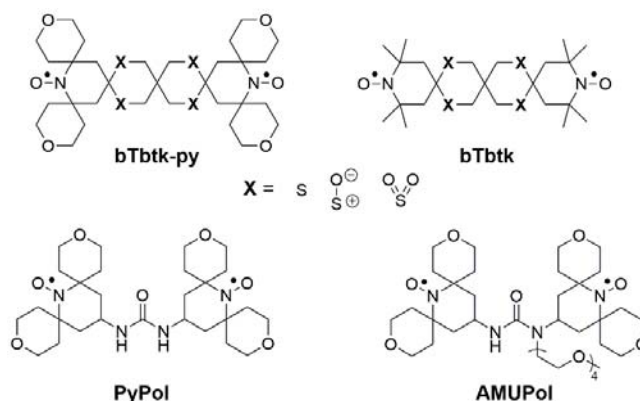


Figure 2.16 Chemical modification of existing biradicals through incorporation of water soluble functional groups.

Another example of a chemical modification that has been performed on **bTurea** is replacement of α -methyl groups with tetrahydropyran moieties. With this strategy, two water-soluble derivatives, **AMUPol** and **PyPol** (Figure 2.16) have been synthesized, showing an improved water-solubility up to 25 mM in DNP juice.^[42] The difference between the structures of **AMUPol** and **PyPol** is the presence of a tetraethylene glycol chain at the urea tether in **AMUPol**, which was added to increase its water-solubility. **AMUPol** performed better than **PyPol** and showed a 4 times higher DNP performance than **TOTAPOL**. This is currently the best water-soluble biradical among all nitroxide-based biradicals and known to be the “gold standard biradical”.^[33]

2.3 Contribution of this Ph. D. thesis to the field of DNP

Designing and synthesizing new biradicals for DNP is an active area of research, particularly for the cross effect mechanism, since it is currently the most efficient DNP mechanism at high field and low temperature. Although, a few water-soluble biradicals have been reported for biological applications, there is still need to design and synthesize new water-soluble biradicals with improved DNP properties.

The project described in this doctoral thesis is mainly divided into three parts. The first part, which is the major part of this thesis, is the design

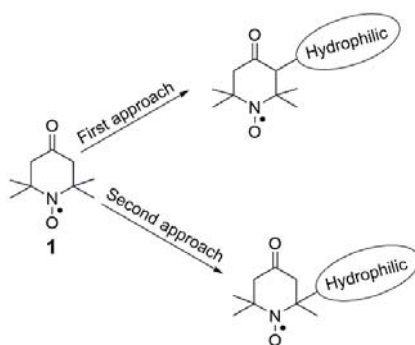
and synthesis of water-soluble nitroxides biradicals for DNP. Initial synthetic efforts and findings towards the synthesis of water-soluble biradicals is explained in **Chapter 3**. Design and syntheses of three water-soluble biradicals, **bcTol**, **bcTol-M** and **cyolyl-TOTAPOL**, along with their DNP investigation is described in **Chapter 4**. Biradical **bcTol** and **bcTol-M** exhibited exceptionally high solubility in water, much higher than the currently known nitroxide-based biradicals.

Various *in vivo* applications of nitroxides such as in-cell EPR and PELDOR studies, are adversely affected by cellular reductants present in the cell, which reduces the nitroxide radicals. The goal of second part of my thesis is to identify a suitable spin label that is stable inside cells for performing in-cell EPR studies. **Chapter 5** describes the design and synthesis of a library containing fifteen different nitroxide-based radicals along with a carbon-centered trityl radical. **Chapter 5** also describes the reductive stability of these radicals under different reducing conditions, including inside cells. A tetraethyl-pyrrolidine spin label was found to be the most reductively stable radical among the radicals that we studied.

The last part of my thesis describes my collaboration with Mr. Subham Saha to incorporate reductively stable radicals into RNA. We developed a spin-labeling method that enabled incorporation of isoindoline-based nitroxides, shown in **Chapter 6** to be resistant towards reduction. We utilized post-synthetic modification of 2'-amino groups of RNA with aromatic isothiocyanates.

3 New water-soluble nitroxides: Early excursions

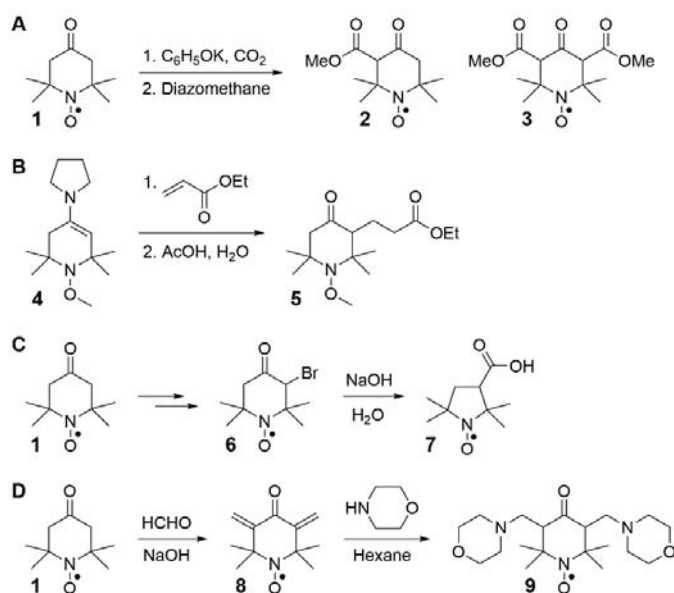
Nitroxide-based biradicals are known to be the best suited biradicals for the cross effect due to their broad EPR spectra, which brings them closer to the frequency matching condition ($\omega_{e1} - \omega_{e2} = \omega_{0l}$) that is required to get a maximal DNP enhancement (Section 2.2.2.4). A useful precursor for synthesizing such nitroxide-based biradicals is the radical 4-oxo-TEMPO (**1**, Scheme 3.1). For synthesizing water-soluble biradicals, this building block needs to be modified prior to being used for making biradicals. However, there are only two sites available for modifications in **1**, as shown in Scheme 3.1, apart from the carbonyl group that is normally used for conjugation to another molecule. In the first approach, hydrophilic functional groups are introduced at the α -position, with respect to the carbonyl of **1**. In the second approach, hydrophilic functional groups are introduced at the position α to the nitroxide group in **1**.



Scheme 3.1 Two approaches for making water-soluble biradicals by introducing hydrophilic groups at different sites in **1**.

3.1 Modification at the α -position of the carbonyl group in 4-oxo-TEMPO

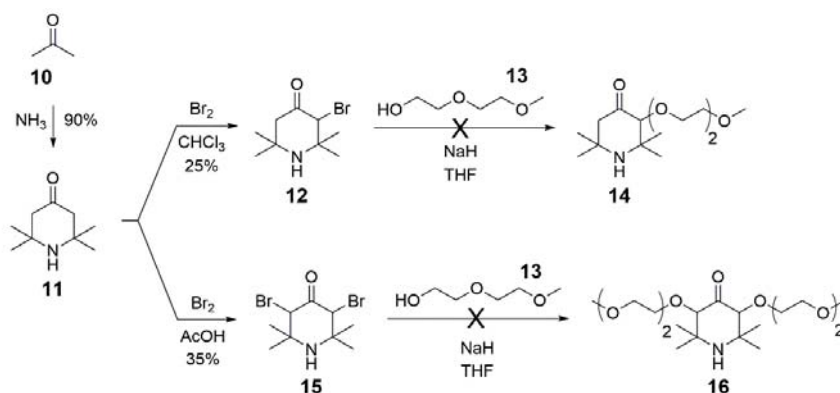
The α -position of the carbonyl group (referred as the “active methylene group”) can be derivatized easily by forming an enol or an enolate intermediate that can react with variety of electrophiles to introduce other functional groups and is what we intended to do for 4-oxo-TEMPO (**1**). There are a few reported examples of derivatization of the α -position of the carbonyl group in **1**. Mori *et al.* described carboxylation of **1** (**Scheme 3.2A**) using potassium phenoxide and carbon dioxide, which was followed by the treatment with diazomethane, leading to the production of mono-carboxylate **2** and di-carboxylate **3** in low yields.^[78] In another example, enamine **4** (**Scheme 3.2B**) was treated with ethyl acrylate, which underwent a Michael-type reaction that yielded δ -keto esters **5**.^[79] Yamada *et al.* synthesized a 3-bromo derivative **6** (**Scheme 3.2C**) from **1** in three steps, which underwent Favorskii rearrangement under alkaline conditions that gave a ring-contracted five membered 3-carboxy proxyl radical (**7**).^[80,81] Nucleophilic addition of various secondary amines was performed at the α -position to the carbonyl group by Malievskii *et al.* on the dimethylene intermediate **8** (**Scheme 3.2D**) which was synthesized by the condensation of **1** with formaldehyde in an alkaline medium.^[82]



Scheme 3.2 Examples of derivatization at the α -position with respect to the carbonyl group in **1**. **A.** Synthesis of carboxylate derivatives **2** and **3**. **B.** Michael reaction of enamine

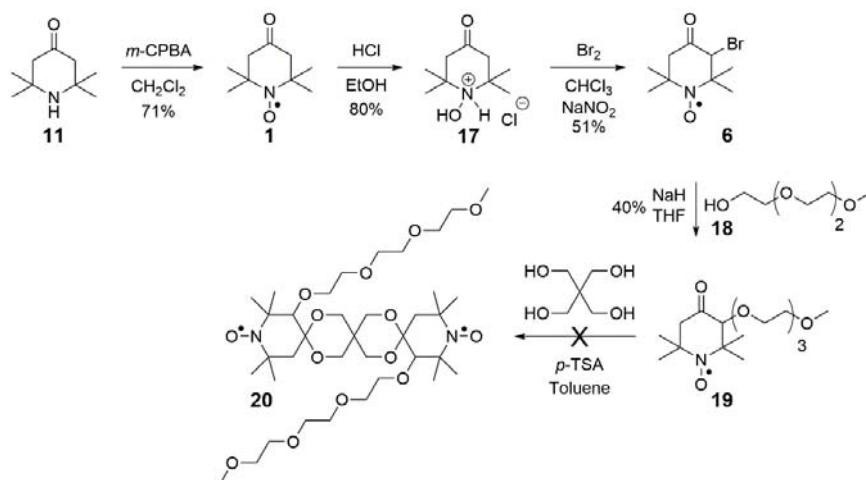
4 with ethyl acrylate. C. Synthesis of proxyl radical (7) *via* a Favorskii rearrangement. D. Nucleophilic addition of morpholine to dimethylene derivative 8.

Bromo-derivative **6** (Figure 3.2C) was chosen as the first compound in order to explore derivatizations at the α -position to the carbonyl group. To obtain the starting material for this approach, triacetoneamine (**11**, Scheme 3.3) was synthesized by bubbling ammonia gas in acetone (**10**) in presence of NH_4Cl .^[83] Monobromo- (**12**) and dibromo- (**15**) derivatives were obtained by the addition of stoichiometric amounts of bromine to triacetoneamine (**11**). Nucleophilic displacements of the bromo groups in **12** and **15** were attempted by using monomethyl glycol **13** in presence of NaH, but did not yield the desired glycol-linked derivatives **14** and **16** respectively. It is likely that a ring-contracted product might have formed during this reaction due to the presence of both the secondary amine and the bromo group in the same molecule.^[84] Therefore, a protecting group for the secondary amine in **11** was employed to avoid the formation of the unwanted ring contraction product.



Scheme 3.3 Synthesis of glycol-linked nitroxide precursors **14** and **16** through triacetoneamine (**11**).

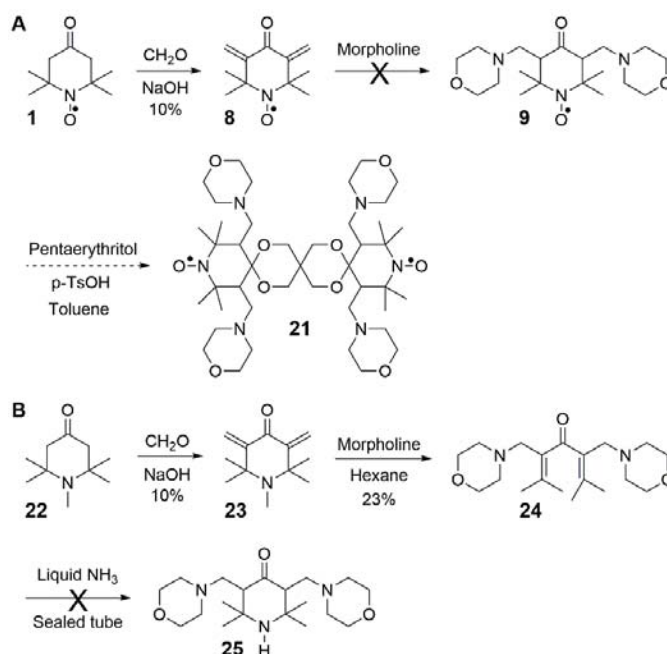
A nitroxide group was chosen as a protecting group for the amine. Nitroxide radical **1**^[80] was synthesized with a slight modification of the reported protocol (Scheme 3.4). It was prepared by the oxidation of triacetoneamine (**11**), which on treatment with hydrochloric acid gave the salt **17**. Bromination of **17** followed by treatment with sodium nitrate gave monobromo derivative **6**. Nucleophilic displacement of the bromo group in **6** with monomethyl triethylene glycol (**18**) resulted in **19** in 40% yield.



Scheme 3.4 Synthesis of glycol-linked **bTbk** derivative **20**.

After introducing the triethylene group at the α -position to the carbonyl in **1**, we decided to prepare its **bTbk** (Chapter 2, Figure 2.11) derivative which is known to have ideal orthogonal orientation of the two nitroxides, similar to **TEKPol** (Chapter 2, Figure 2.13) giving maximum DNP enhancement.^[68] Bisketal formation was tried by using *p*-TSA/toluene using Dean-stark apparatus (Scheme 3.4), but it did not work even after varying the reaction conditions, including the temperature, duration of the reaction and trying several other reagents such as sulphamic acid,^[85] TiCl_4 ,^[86] TMSOTf ^[87] and by performing reactions in sulfonic acid-functionalized ionic liquid.^[88] We also evaluated bisketal formation with other different starting materials such as **1**, **17** and **6**, but none of the reactions worked; either the starting material remained intact or no bisketal derivatives of these compounds were observed. Substituents at the α -position to the carbonyl group might slow the reaction due to steric hindrance and hence, making it difficult to form a bisketal.

In parallel, we explored the incorporation of a different group at the α -position to the carbonyl for bisketal formation reaction, preparing the morpholine derivative **9**.^[82] Di-methylene derivative **8** (Scheme 3.5) was prepared by the treatment of 4-oxo-TEMPO (**1**) with formaldehyde in low yield.^[82] However, in contradiction to the published report,^[82] nucleophilic addition of morpholine to **8** was unsuccessful. In an attempt for improvement, pentamethyl piperidone (**22**) was applied for the preparation of its dimethylene derivative **23** by using formaldehyde in an aqueous solution.^[82] However, nucleophilic addition of morpholine to **23**, gave the β -elimination product **24**. Condensing this product with ammonia in a sealed container to prepare **25**, proved to be unsuccessful.



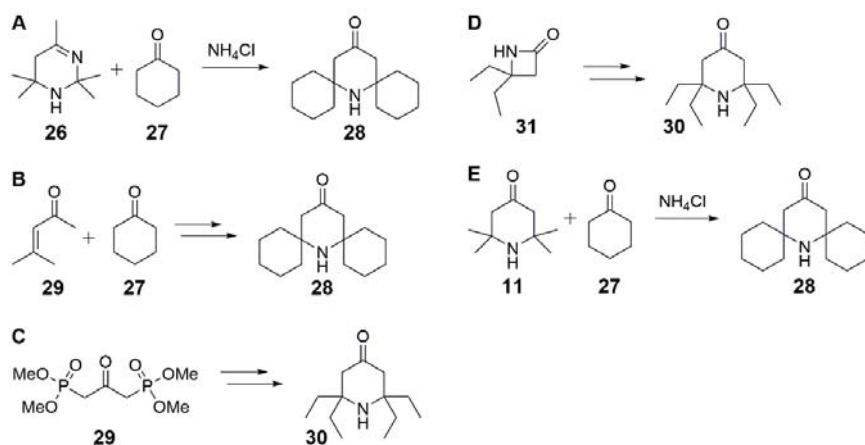
Scheme 3.5 Nucleophilic addition of morpholine **A.** on di-methylene TEMPO **8.** **B.** on di-methylene pentamethyl piperidone **23.** Dotted line indicates the projected plan.

To conclude on our first approach for introducing polar groups into **1**, a glycol chain was successfully introduced at the α -position to the carbonyl group (**19**), but preparing its bisketal derivative **20** was not possible. However, in case of morpholine-based derivatization, although we obtained a β -elimination product **24**, we were not able to prepare its ring-closed product **25** for the synthesis of the bisketal derivative **21**.

3.2 Modification at the α -position of the nitroxide group in 4-oxo-TEMPO

In 4-oxo-TEMPO (**1**, **Scheme 3.1**), the α -position of the nitroxide group is another position that could be modified. This position is not close to the carbonyl group and, therefore, we did not expect any steric hindrance, which we faced while forming the bisketal with the carbonyl group of **19** (**Scheme 3.4**). Therefore, we selected the α -position of the nitroxide group for modification with hydrophilic groups.

Different methods have been used to synthesize α -substituted derivatives with respect to the nitroxide in **1**. Synthesis of α -substituted piperidine derivatives (*e.g.* **28**) have been reported from acetone (26, **Scheme 3.6A**) by Ma *et al.*^[89] Subsequently, various α -substituted piperidines have been synthesized using this approach, such as **28**.^[90-92] The other main approach is a stepwise synthesis from the appropriate starting materials (**Schemes 3.6B, C and D**). For example, Yoshioka *et al.* reported the synthesis of spirocyclohexyl derived compounds (*e.g.* **28**) by using the α , β -unsaturated ketone **29** (mesityl oxide, **Scheme 3.6B**).^[93] In addition, focusing on synthesis of tetraethyl derivative **30** (**Schemes 3.6C and D**), Wetter *et al.* reported its stepwise synthesis through a bisphosphonate **29**.^[94] β -Lactam **31** has also been used as a starting material for obtaining **30** on a larger scale, which involved several synthetic steps including a high pressure reaction.^[95] Recently, an alternative synthetic method has been developed by Sakai *et al.* that involved a single step synthesis of an α -substituted derivative (**28**).^[96] This method, described in **Scheme 3.6E**, involved triacetoneamine (**11**) as a starting material and has been used to synthesize various α -substituted piperidine derivatives.^[97,98]

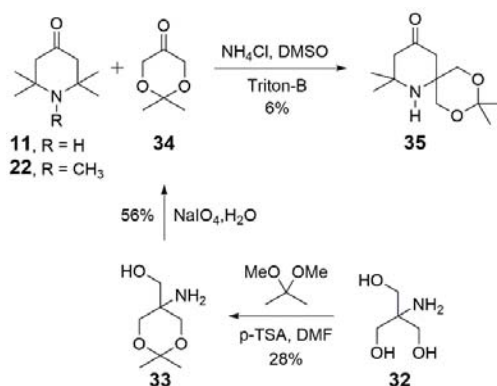


Scheme 3.6 Various methods for preparation of α -substituted piperidine. **A.** From acetone (**26**). **B.** From α , β -unsaturated ketone **29** (mesityl oxide). **C.** From bisphosphonate **29**. **D.** From β -lactam **31**. **E.** From triacetoneamine (**11**).

Although there are variety of methods available for preparing α -derived nitroxides, only two of them (**Schemes 3.6A and E**) involve a one-step synthesis while the remaining methods require multiple steps (**Schemes 3.6B, C and D**). Out of these two methods, the protocol described by Sakai *et al.* looked the most promising (**Scheme 3.6E**), as the starting material triacetoneamine (**11**) can be easily prepared and it is more stable than acetone (**26**).^[89] Also, yields of α -substituted derivatives that are reported

with this method, such as **28** (Scheme 3.6E), are better than those obtained from acetone (26) as a starting material (Scheme 3.6A). Therefore, this method was applied for derivatization of the α -position.

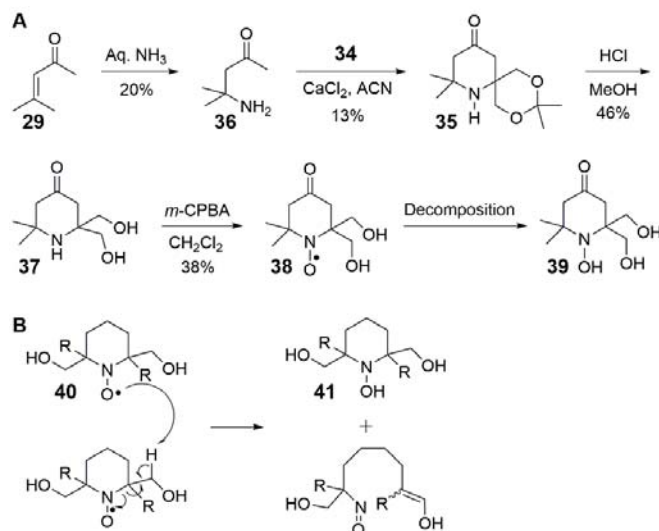
The acetonide ketone **34**, which was chosen for the condensation reaction, contains a ketal which on deprotection could generate polar hydroxymethyl groups. Therefore, acetonide-ketone **34** (Scheme 3.7) was synthesized following the reported procedure.^[99] Condensation of acetonide-ketone **34** with pentamethyl piperidone (**22**) gave mono-substituted derivative **35** in 6% yield. In order to get the desired disubstituted product, condensation of **34** with triacetoneamine (**11**) was attempted at various temperatures and reaction times, but always gave the monosubstituted product **35**.



Scheme 3.7 Condensation reaction of acetonide-ketone **34** with triacetoneamine (**11**) and pentamethyl piperidone (**22**).

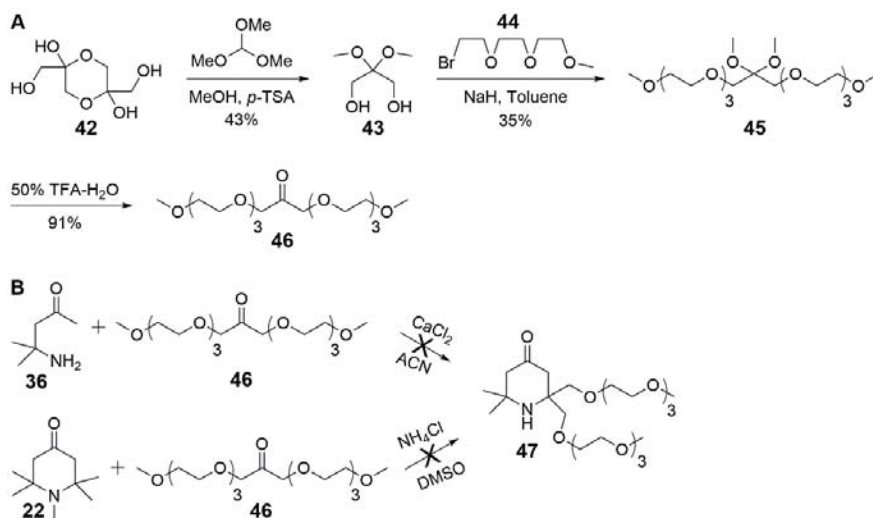
The low yield of the condensation reaction between triacetoneamine (**11**) and acetonide-ketone **34** (Scheme 3.7) was the limiting factor in the synthesis of the mono-substituted derivative **35**. To increase the yield of the condensation reaction, another route was therefore followed, wherein mesityl oxide (**29**, Scheme 3.8A) was used as the starting material. Michael addition with ammonia to the α , β -unsaturated ketone **29** yielded diacetoneamine (**36**), which was isolated as an oxalate salt.^[100] Condensation of diacetoneamine (**36**) with the acetonide ketone **34** in the presence of calcium chloride, gave the mono-substituted derivative **35** in 13% yield, which was two times higher than that reported with the earlier protocol (Scheme 3.6). Deprotection of the ketal was achieved by methanolic HCl to give diol **37**, which on oxidation in the presence of *m*-CPBA yielded dihydroxyl-nitroxide **38**. However, nitroxide **38** was not stable and decomposed to the trihydroxyl derivative **39** within a few hours. A similar decomposition was described by Knoop *et.al* for the hydroxyl-derived TEMPO derivative **40** (Scheme 3.8B)

which was converted into its trihydroxyl derivative **41** through a bimolecular process.^[101] We hypothesized that a similar kind of decomposition might be taking place with our compound **38**.



Scheme 3.8 A. Synthesis of mono-substituted derivative **35** from mesityl oxide (**29**). B. Mechanism for conversion of di-hydroxyl compound **40** into tri-hydroxyl derivative **41**, postulated by Knoop *et al.*^[101]

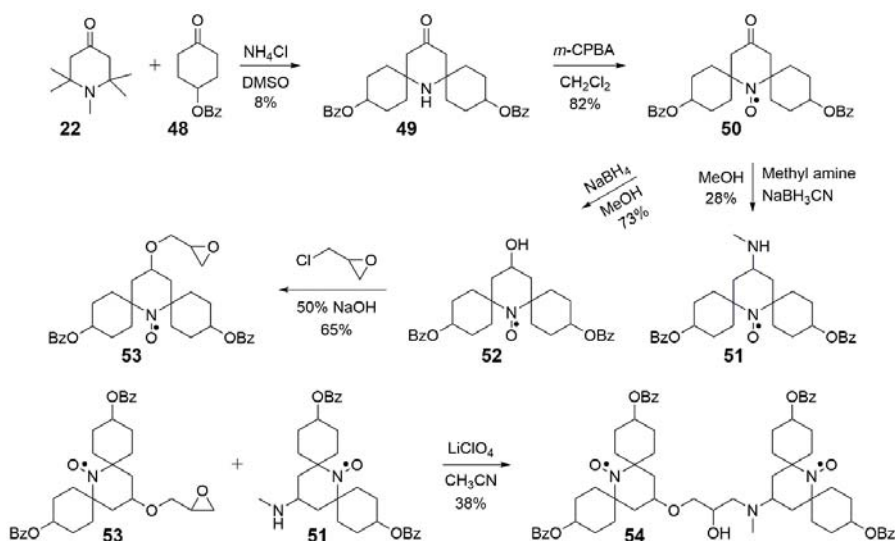
Owing to the instability of the dihydroxyl compound **38** (**Scheme 3.8A**), we decided to change our approach yet again and avail hydroxymethyl groups adjacent to the nitroxide. The glycol-derived aliphatic ketone **46** was chosen, since in that case the methylene groups are present in the form of poly-ethylene glycol. Dimethyl acetal-protected **43** (**Scheme 3.9**) was synthesized from the dihydroxyl-acetone dimer **42**, following a reported procedure.^[102] The hydroxyl groups were alkylated using bromo triethylene glycol **44** in the presence of NaH in toluene to obtain **45**, which on deprotection of the dimethyl acetal groups with trifluoroacetic acid yielded ethylene glycol-derived ketone **46** in 91% yield. Condensation reactions of **46** with both diacetoneamine (**36**) and pentamethyl piperidone (**22**) were tried, but we could not detect any formation of the desired product **47**. Even after trying a variety of different conditions, by changing the temperature, reaction time and the stoichiometric ratio of the reagents, the reactions did not work.



Scheme 3.9 A. Synthesis of the glycol-derived ketone **46**. B. Attempted condensation of ketone **46** with diacetoneamine (**36**) and pentamethyl piperidone (**22**).

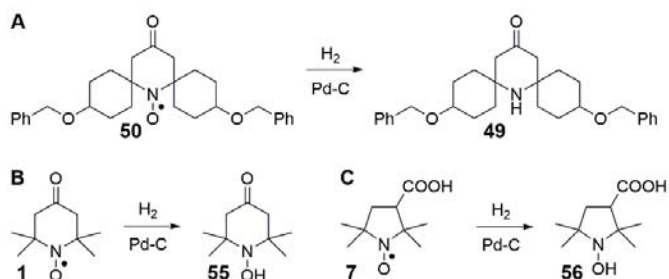
In the next attempt, spirocyclohexanol groups were incorporated at the α -positions to the nitroxide in 4-oxo-TEMPO (**1**). The presence of spirocyclohexyl groups at this position has been shown to increase the electronic relaxation properties of the radical (T_{1e} , **Chapter 2.2.4**) and thereby increase its DNP efficiency.^[68,71] The hydroxyl groups would contribute to solubility in water. Benzyl-protected ketone **48** was chosen as a precursor for introducing spirocyclohexanol groups; deprotection of the benzyl groups would unmask the hydroxyl groups. As a first application of this strategy, spirocyclohexanol derivative **49** (**Scheme 3.10**) was prepared and applied for the synthesis of **TOTAPOL**.

Benzyl-protected ketone **48**^[103] was condensed with pentamethyl piperidone (**22**, **Scheme 3.10**) to yield the disubstituted derivative **49** in 8% yield. It was challenging to isolate this disubstituted derivative **49** from its monosubstituted analogue and often several chromatographic purifications were required. Oxidation of **49** with *m*-CPBA yielded **50**, which on reductive amination with methylamine and NaBH₃CN gave amino derivative **51**. Disubstituted derivative **50** was reduced and further alkylated using epichlorohydrin to give **53**. Coupling of **53** and **51** was done in presence of LiClO₄ to give benzyl-protected **TOTAPOL** derivative **54**, and now only deprotection of the benzyl groups remained to be done.



Scheme 3.10 Synthesis of benzyl protected TOTAPOL derivative **54**, Bz: benzyl.

We chose **50** as a model compound for debenzylation and performed the debenzylation reaction with hydrogenation in the presence of Pd-C (**Scheme 3.11A**). It was surprising to see that the benzyl groups remained intact and that the nitroxide group was reduced to an amine **49**. However, we tried other debenzylation conditions such as Pd-C with acetic acid, ammonium formate, $\text{PPH}_3\cdot\text{HBr}$,^[104] BBr_3 ,^[105] and $\text{BF}_3\cdot\text{etherate}$,^[106] but none of the reactions worked. Either the starting material remained intact or formation of any debenzylated product was not observed. Observation of reduction of the nitroxide group of **50** to its amine derivative **49** during hydrogenation reaction, was contrary to the reported literature, where the nitroxide had reportedly been reduced to a hydroxylamine, which can be readily oxidized back to the nitroxide.^[107-109] For example, hydrogenation of **1** has been performed with Pd-C to obtain *N*-hydroxylamine derivative **55** (**Scheme 3.11B**) in 80% yield.^[107,108] A similar kind of hydrogenation was performed on the proxyl radical **7** by Yan'shole *et al.* to yield *N*-hydroxyl derivative **56** (**Scheme 3.11C**).^[109]



Scheme 3.11 A. Attempted debenzylation of the disubstituted compound 50. B. Hydrogenation of 1. C. Hydrogenation of the proxyl radical 7.

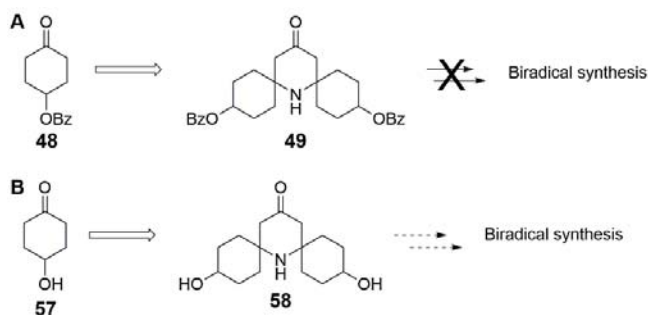
3.3 Conclusion

Two approaches were tried for introducing hydrophilic groups in 4-oxo-TEMPO (1). Triethylene glycol units were introduced at the α -position with respect to the ketone group in 19, but could not be converted into the **bTbk** derivative 20. Hydroxymethyl groups were successfully introduced at the adjacent position to the nitroxide group in 1, but the decomposition of the nitroxide radical for the compound 38 was observed. A benzyl-protected spirocyclohexanol derivative of **TOTAPOL** 54 was synthesized, which is the first example of a spirocyclohexyl derived **TOTAPOL** derivative. However, benzyl groups of 50 could not be removed, even after trying different debenzylation reactions, which appeared to be the bottleneck for this approach.

Introduction of spirocyclohexanol groups into radicals is a promising approach for synthesizing water-soluble biradicals. Therefore, we decided to concentrate on this approach, which is described in **Chapter 4**. We were able to accomplish this task by using an unprotected version of 48, i.e. 4-hydroxyl cyclohexanone (57) for the condensation reaction.

4 Water-soluble spirocyclohexanoly-derivived biradicals

As discussed in **Chapter 3**, we developed a novel strategy wherein the methyl groups at the α -position to the nitroxide group in a TEMPO unit were replaced with spirocyclohexanoly moiety that had a benzyl protecting group for the hydroxyls (**Scheme 4.1A**). However, removal of the benzyl groups did not work despite several attempts. Therefore, in order to avoid the debenzylation reaction, we decided to use 4-hydroxyl cyclohexanone (**57**, **Scheme 4.1B**), which is an unprotected version of **48**. Diol derivative **58** could in principle be assembled to yield different biradicals.



Scheme 4.1 Synthesis of spirocyclohexanoly derived nitroxides. **A.** An unsuccessful approach using benzyl protected cyclohexanone **48**. **B.** New approach using the unprotected 4-hydroxyl cyclohexanone (**57**) for synthesizing diol derivative **58**.

We chose the biradicals **bTurea** and **TOTAPOL** to demonstrate the application of this approach, using 4-hydroxyl cyclohexanone (**57**). Three spirocyclohexanoly radicals, **bcTol**, **bcTol-M** and **cyoly-TOTAPOL** (**Figure 4.1**) were designed and the synthesis of each biradical will be described in the following sections.

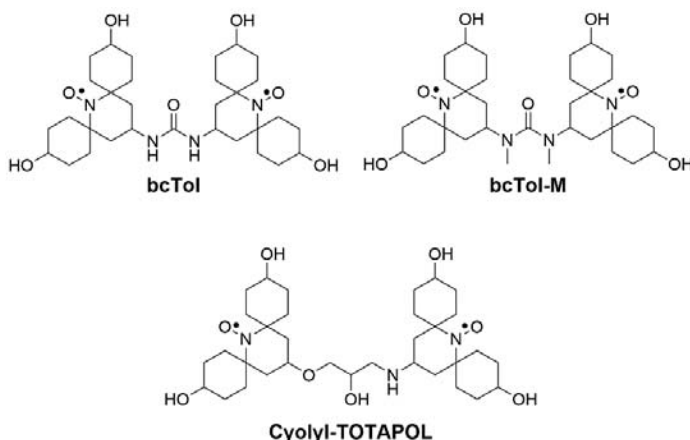


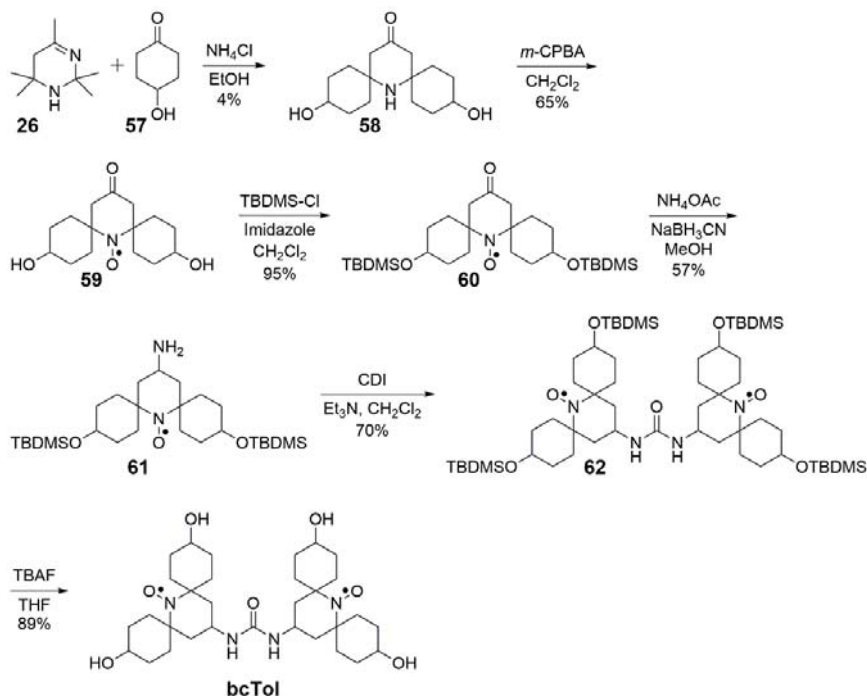
Figure 4.1 Structures of the new spirocyclohexanoly biradicals **bcTol**, **bcTol-M** and **cyolyl-TOTAPOL**.

4.1 Synthesis of **bcTol** [bis-(spirocyclohexyl-TEMPO-alcohol)-urea]

The synthesis of the first spirocyclohexanoly-derived **bTurea**-derivative **bcTol** is shown in **Scheme 4.2**. Condensation of acetone^[89] (**26**) with 4-hydroxy cyclohexanone^[110] (**57**) in the presence of ammonium chloride gave dihydroxy derivative **58** in 4% yield, which on further oxidation with *m*-CPBA yielded diol **59**.^[111] The hydroxyl groups of **59** were protected with TBDMS groups to obtain di-TBDMS derivative **60**. Ketone **60** was subjected to reductive amination in the presence of NH_4OAc and NaBH_3CN to yield amino derivative **61** in 57% yield. Amino derivative **61** was reacted with 1,1'-carbonyldiimidazole (CDI) to obtain a urea-linked derivative **62**. Deprotection of the hydroxyl groups with TBAF afforded **bcTol** as a yellow crystalline solid.

The extremely low yield of the first reaction hampered its practical use. To increase the yield of the condensation reaction (**Scheme 4.2**), we tested several conditions, including variation in the temperatures and reaction times, but none of the attempts improved the yield of the reaction. Further, we found that the yield of this step was not reproducible and varied from 0 to 4%. Isolation of diol **58** from the crude mixture was highly laborious due to the presence of multiple unidentified impurities in the reaction mixture. In addition to this, we observed that the starting material

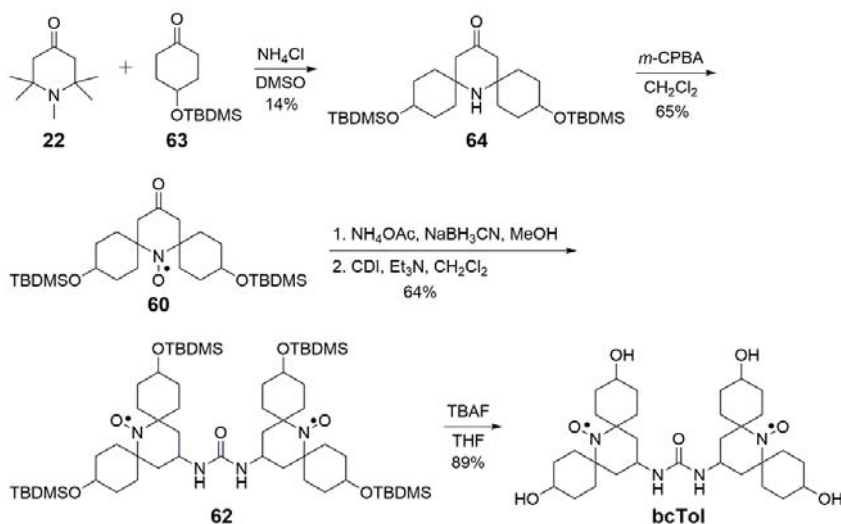
acetone (26) was stable for only a few days and therefore, needed to be freshly prepared before the condensation reaction.^[89]



Scheme 4.2 Synthesis of **bcTol**.

In an attempt to improve the ease of the synthesis of **bcTol**, we adopted a different method (Scheme 4.3) using pentamethyl piperidone (**22**) as a starting material which is more stable than acetone (**26**, Scheme 4.2). Another change was that the TBDMS group was used as a protection group for the hydroxyl group in **57** (Scheme 4.2), to avoid the arduous purification that was associated with the polar-dihydroxyl compound **58**.

Condensation of **22** with **63** in the presence of ammonium chloride gave di-TBDMS protected compound **64** in 14% yield, which was a great improvement over the yield in the earlier condensation reaction (4%, Scheme 4.2). Compound **64** was oxidized by using $m\text{-CPBA}$ to give **60**, which was subjected to the series of similar reactions that were performed in Scheme 4.2 to obtain **bcTol**.

Scheme 4.3 Improved synthesis of **bcTol**.

After the successful synthesis of **bcTol**, we checked its solubility in water and water-based solutions. **bcTol** exhibited excellent solubility of up to 150 mM in GDH (60:30:10 mixture of glycerol/D₂O/H₂O, also termed “DNP juice”) and in water (100 mM) which is five times more soluble than the current “gold standard” **AMUPol** (30 mM). Also, **bcTol** does not require sonication for dissolution, as is the case for **AMUPol**.^[42] This high solubility, along with the fact that it is crystalline, gives practical advantages to **bcTol** over **AMUPol**, in that it simplifies the handling, preparation of stock solutions and helps minimizing precipitation of the biradical at high concentrations.

4.2 Synthesis of **bcTol-M** [bis-(spirocyclohexyl)-TEMPO-alcohol)-urea-dimethyl]

As described in Section 2.2.3 (Chapter 2), the inter-radical distance and the relative orientation between the two nitroxide radicals are two important parameters that need to be considered while designing new biradicals for DNP. With regards to orientation, it has been postulated that an orthogonal orientation between the two nitroxides is an ideal situation for obtaining a maximal DNP efficiency, as in the case of **bTbk**^[39] (Section 2.2.3, Figure 2.10). Along the same lines, Kubicki *et al.* showed that *N*-methylation of the

urea functional group connecting the two radicals in **bTurea**-based biradicals, changes the dihedral angle between the two nitroxide radicals from 56° (for **PyPol**, **Figure 4.2**) to 89° (**PyPol-diMe**). The change in the dihedral angle towards orthogonality in **PyPol-diMe** yielded three times more DNP enhancement than the non-methylated urea version (**PyPol**).^[51] In order to apply a similar strategy to increase the DNP-efficiency of **bcTol**, we decided to synthesize its *N,N*-dimethyl derivative, which we named **bcTol-M** (**Figure 4.2**).

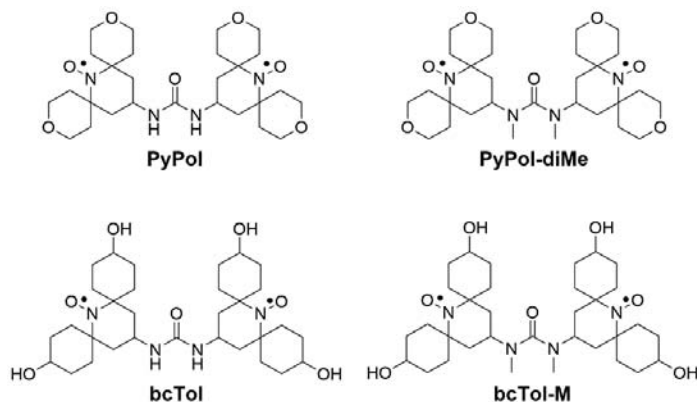
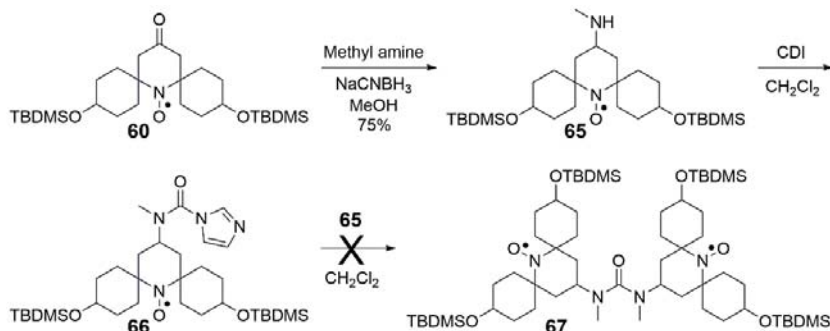


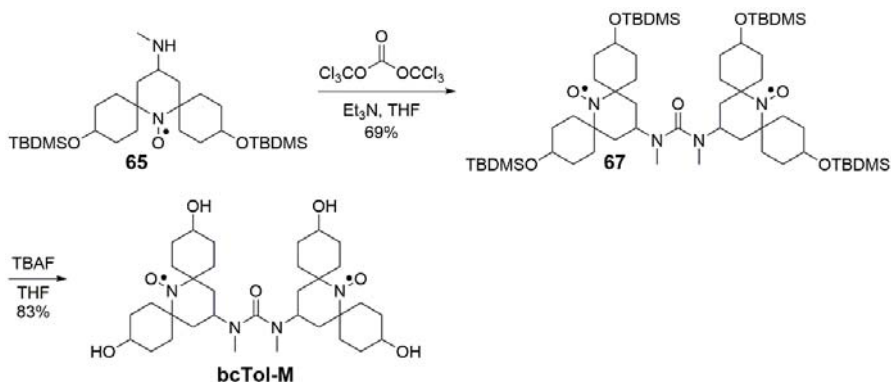
Figure 4.2 Structures of **PyPol** and **bcTol** and their dimethyl derivatives **PyPol-diMe** and **bcTol-M**.

Synthesis of **bcTol-M** started with the reductive amination of ketone **60** (**Scheme 4.4**) with methylamine hydrochloride to yield amino methyl derivative **65**. Treatment of **65** with 1,1'-carbonyldiimidazole only gave an imidazole-linked intermediate **66**, rather than the expected *N*-methyl urea derivative **67**. The imidazole-linked intermediate **66** was heated with **65** for prolonged duration, but did not give the desired *N*-methyl urea derivative **67**.



Scheme 4.4 Urea formation of *N*-methyl derivative **65** by using carbonyldiimidazole (CDI).

In the second attempt to build the *N*-methyl urea derivative **67**, we reacted the amino methyl derivative **65** with triphosgene in THF at 27°C for 12 h, followed by addition of another portion of amino methyl derivative **65**. The resulting solution was heated to reflux for 12 h to give *N*-methyl urea derivative **67** (**Scheme 4.5**) in 69% yield. Deprotection of hydroxyl groups from **67** with TBAF, yielded **bcTol-M** as a yellow crystalline solid.



Scheme 4.5 Synthesis of **bcTol-M** using triphosgene.

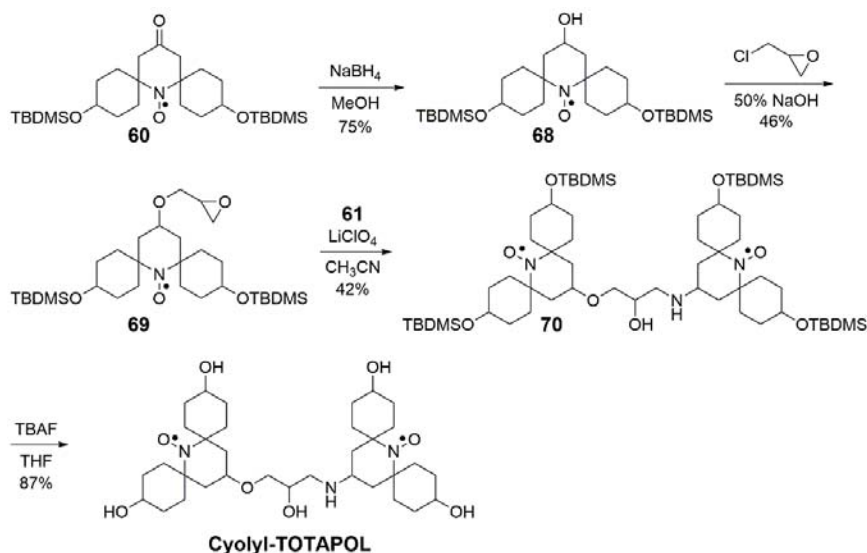
bcTol-M showed exceptionally high solubility in GDH (250 mM) and in water (170 mM) which is eight times more soluble than **AMUPol** (30 mM) and 1.6 times more than **bcTol**. To the best of our knowledge, **bcTol-M** has by far the highest water-solubility among all known nitroxide-based biradicals.

4.3 Synthesis of cyolyl-TOTAPOL [spirocyclohexanol-1-(TEMPO-4-oxy)-3-(TEMPO-4-amino) propan-2-ol]

TOTAPOL is one of the most frequently used water-soluble biradicals for studying biological systems by DNP. The effect of the longer relaxation time T_{1e} of **TOTAPOL** biradical on DNP-efficiency, by replacing the methyl groups adjacent to the nitroxide group in TEMPO unit with spirocyclohexanolyl groups, has not been studied yet. To explore this effect, we decided to apply our strategy on **TOTAPOL** and designed a spirocyclohexanolyl **TOTAPOL** derivative which we named **cyolyl-**

TOTAPOL. In addition, the intermediates **60** and **61** (Scheme 4.2) that we used for synthesizing **bcTol** and **bcTol-M**, could be used to synthesize a novel biradical, **cyolyl-TOTAPOL**.

Synthesis of **cyolyl-TOTAPOL** (Scheme 4.6) began with the reduction of **60** by NaBH_4 to obtain **68**, which was alkylated with epichlorohydrin to give epoxide **69**. Amino derivative **61** was treated with epoxide **69** to obtain **70** in moderate yield. Deprotection of hydroxyl groups from **70** with TBAF, yielded **cyolyl-TOTAPOL** as a yellow solid.



Scheme 4.6 Synthesis of **cyolyl-TOTAPOL**.

Cyolyl-TOTAPOL showed a lower solubility in GDH (17 mM) than **bcTol**, which was surprising, since it has one additional hydroxyl group and one amine compared with **bcTol**. In fact, the solubility exhibited by **cyolyl-TOTAPOL** is similar to the parent biradical-**TOTAPOL** in GDH (15 mM).^[112] The low solubility of **cyolyl-TOTAPOL** might be attributed to the formation of aggregates or clusters of molecules due to greater flexibility of the linker than in **bcTol**.

4.4 DNP studies with bcTol, bcTol-M and cyolyl-TOTAPOL

DNP measurements were carried in Prof. Oschkinat's research group at the Leibniz-Institut für Molekulare Pharmakologie (FMP), Berlin. The DNP performance of **bcTol** was evaluated using three different systems: a sample of proline, the SH3 protein^[14] and the membrane protein channelrhodopsin.^[113]

At 110 K, **bcTol** exhibits an enhancement ($\epsilon_{\text{on/off}}$) of 221 ± 8 (**Figure 4.3A**) for proline in GDH, which decreased with temperature to around 21 ± 5 at 181 K. Under similar conditions, **TOTAPOL** and **AMUPOL** gave enhancements of 52 ± 2 and 215 ± 9 respectively. Thus, **bcTol** showed similar enhancement values to that of **AMUPOL**, while four times higher value than **TOTAPOL**. The proton T_1 values were plotted in **Figure 4.3A** and decreased with increase in temperature.

The performance of **bcTol** was tested with the membrane protein channelrhodopsin^[113] at 100 K (**Figure 4.3A**) and showed enhancement of 36, which is three times higher than **TOTAPOL** ($\epsilon \approx 10$). In the case of SH3 at 110 K, **bcTol** gave an enhancement of 244 ± 5 (**Figure 4.3A and B**), which is 1.3 times higher than **AMUPOL** ($\epsilon \approx 181 \pm 4$) under similar conditions.

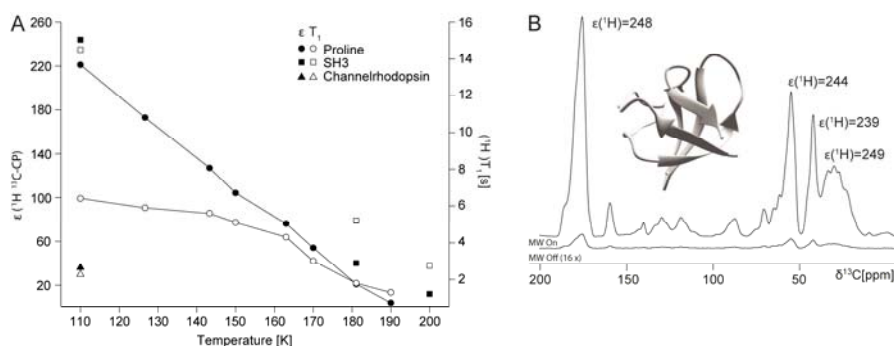


Figure 4.3 A. ^1H -DNP-signal enhancement (ϵ , filled symbols and T_1 open symbols) for proline, microcrystalline SH3 and channelrhodopsin as a function of temperature using **bcTol** as a polarizing agent. Proline (0.25 M) was uniformly ^{13}C -, ^{15}N - labeled. Spectra were recorded in glycerol- d_8 /D $_2$ O/H $_2$ O (60/30/10 v/v/v) containing **bcTol** (10 mM), measured at 9.4 T in a 3.2 mm zirconia rotor at 8 kHz MAS. T_1 was measured via an inversion recovery experiment with ^1H - ^{13}C -CP. **B.** A sample of SH3 (7.0 mg) containing **bcTol** (20 mM) (18.78 s recycle delay) measured with and without microwave irradiation at 9.4 T (110 K, 16 scans, 4 dummy scans, 5 W microwave power at end of probe waveguide). Insert shows a ribbon representation of the three-dimensional structure of the SH3 protein (PDB entry 1U06).

The depolarization effect (**Chapter 2, Section 2.2**)^[32,33] is important to take into account for determining the real enhancement. Signal-to-noise ratios were determined in 10 minute-intervals (^{10m}SNR) at 110, 181 and 200 K and normalized with respect to the amount of SH3 protein. At 110 K, **bcTol** showed a similar $^{10m}\text{SNR}/\text{mg}$ value to that of **AMUPol** (≈ 1320). However, at 181 K, the value for **bcTol** (238 ± 11) was significantly higher than that of **AMUPol** (147 ± 7). We also determined $^{10m}\text{SNR}_{\text{off}}/\text{mg}$ values for **AMUPol** (6.8) and **bcTol** (6.4) samples with that of a sample without radical (12.5) at 110 K, which highlights the depolarization effect of the radicals.

In order to evaluate the PRE effect^[65] (**Chapter 2, Section 2.2.3**) of **bcTol**, ^{13}C - ^{13}C dipolar-assisted-rotational-resonance (DARR) correlations of SH3 samples was measured at 181 K and showed relatively low PRE. DNP enhancement values obtained with **bcTol** clearly showed that it is particularly well suited for studying biological systems by DNP with ss-NMR spectroscopy. DNP evaluation of **bcTol-M** and **cyolyl-TOTAPOL** are currently under investigation in Prof. Oschkinat's research group in Berlin.

4.5 Conclusion

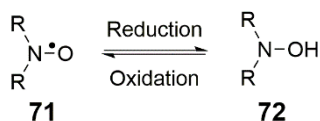
We established a new strategy to convert hydrophobic radicals into hydrophilic radicals through incorporation of spirocyclohexanol-yl groups adjacent to the nitroxide group. Furthermore, we demonstrated the usefulness of this strategy by synthesizing **bcTol**, **bcTol-M** and **cyolyl-TOTAPOL**. Both **bcTol** and **bcTol-M** showed remarkable increase in their water-solubility compared with the other known nitroxide-based biradicals, while, **cyolyl-TOTAPOL** showed similar water solubility as that of the parent biradical-**TOTAPOL**.

bcTol showed 1.3 times higher DNP enhancement than **AMUPol** for a sample of the SH3 protein, while exhibiting similar enhancements for proline sample at 110 K. A comparable signal-to-noise ratio (^{10m}SNR) was observed for **bcTol** and **AMUPol** at 110 K, while it was higher for **bcTol** than **AMUPol** at 181 K for SH3 protein.

5 Spin labels for in-cell EPR

Elucidating the structure and dynamics of biomacromolecules, for example, proteins and nucleic acid, is crucial for understanding their physiological functions. Beside widespread techniques, such as nuclear magnetic resonance (NMR) spectroscopy,^[114] X ray crystallography^[115] and fluorescence spectroscopy,^[116] sophisticated electron paramagnetic resonance (EPR) methods have been successfully used to study the structure and dynamics of nucleic acids through distance measurements between two nitroxide radicals, covalently attached by site-directed spin labeling (SDSL).^[117-119] However, structures of nucleic acids in a cellular environment can be different than *in vitro* structures. They also depend on various factors such as concentrations of ions or small molecules and molecular crowding, all of which may have a crucial role in determining the biologically relevant conformations of the nucleic acid of interest.^[120-122] The development of analytical tools for revealing native nucleic acid structures inside cells is an ongoing challenge, which has begun to be addressed by in-cell spectroscopy.^[123]

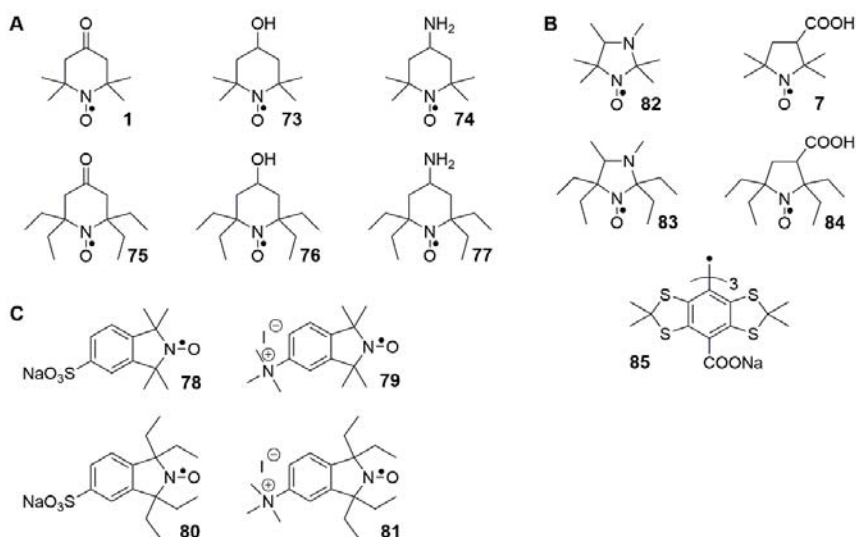
EPR spectroscopy is well-suited for investigation of living systems because there is no background interference, as can be the case with fluorescence spectroscopy. In fact, in-cell PELDOR has been used to study nucleic acids inside *X. laevis* oocytes by using nitroxides.^[124-127] In addition to the use of nitroxide radicals for in-cell EPR spectroscopy, nitroxides have also been used to determine the partial pressure of oxygen,^[128] pH values^[129] and redox states^[130] in living tissues. However, the applications of nitroxides under cellular conditions or in biological fluids are greatly hampered by the presence of different reducing agents (e.g. ascorbic acid and glutathione) inside cells that reduce nitroxide radicals into a corresponding EPR-silent *N*-hydroxylamine (72, **Figure 5.1**).^[131-133]



Scheme 5.1 Reduction of a nitroxide group to an EPR inactive *N*-hydroxyl amine group. R is an alkyl group.

In order to increase the stability of nitroxide radicals in cellular environments, extensive efforts have been directed towards the synthesis of nitroxides that have structures that render them more resistant to reduction.^[89,96] Many factors such as ring size, substituents (neutral or charged) and the alkyl groups present adjacent to the nitroxide group affect the stability of nitroxide radicals. The stability of nitroxide radicals has been studied in presence of ascorbic acid^[133-136] and under different biologically relevant conditions.^[137-141] However, each of these biostability studies has focused only on a small number of radicals and conditions vary between studies. Therefore, to conclusively investigate reductive stabilities of variety of radicals on a broader level in terms of number of radicals, we synthesized a library (**Figure 5.1**) containing fifteen different radicals to compare their stabilities under the same conditions. In this library, we included a piperidine-, pyrrolidine-, isoindoline- and imidazolidine-based nitroxides, along with a carbon-centered trityl radical. The reducing conditions that we chose were ascorbic acid, a cytosolic extract from *X. laevis* oocytes and inside oocyte cells.^[142]

Tetramethyl-derived spin labels **1**, **73**, **74** and pyrrolidine spin label **7** were purchased, while tetraethyl piperidine derivatives **75-77**,^[141,143] isoindoline derivatives **78-81**^[142,144] and compounds **82-85**^[145-148] were synthesized using slightly modified procedures, compared with the published protocols. Stability studies of these radicals under different reducing agents were carried out by Dr. Ivan Krstić in Prof. Prisner's research group at Goethe University in Frankfurt am Main, Germany.



Scheme 5.2 Radicals used for evaluating their stability in reductive conditions. **A.** Piperidine-based nitroxides. **B.** Imidazolidine- and pyrrolidine-based nitroxides and a trityl radical. **C.** Isoindoline-based nitroxides.

To comparatively investigate the stability of radicals in presence of ascorbic acid, we incubated the radicals (200 μM) with ascorbic acid (5 mM) in PBS buffer (pH 7.2) and monitored the decay of intensity of the low-field nitroxide line of the EPR signal as a function of time. Normalized intensities of the EPR signals for different radicals were plotted against time (**Figure 5.2A**, **Table 5.1**) and showed that the substituents that are present at the α -position to the nitroxide had the largest impact on the stability of the radicals. Tetraethyl-substituted piperidine nitroxides **75-77** were found to be ca. 100 times more stable against reduction than the corresponding tetramethyl-derivatives **1**, **73**, **74**. Further, we observed that five-membered nitroxide radicals, were three- to ten-fold more stable than the six-membered piperidine derivatives. The slowest reduction rate was found with tetraethyl pyrrolidine derivative **84**, which remained 94% intact after 2 h (**Table 5.1**).

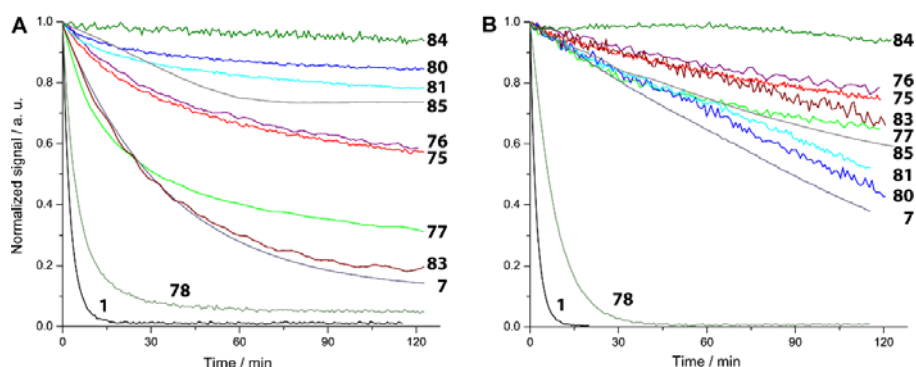


Figure 5.1 A. Reduction of selected radicals in presence of ascorbic acid, the EPR signal intensity is plotted as a function of time. B. Reduction of radicals in a cytosolic extract from *X. laevis* oocytes.

Table 5.1 Extent of reduction of radicals by measuring EPR signal intensities after incubation (2 h) with ascorbic acid, in cell extract and inside oocyte cells.

Radicals	Extent of reduction ^a		
	In ascorbic acid	In cytosolic extract	Inside cells
1	1	0	-
75	57	75	34
73	1	0	-
76	58	78	15
74	1	0	-
77	31	65	66
78	5	0	-
80	84	45	51
79	5	0	-
81	78	52	55
82	5	0	-
83	19	66	25
7	14	38	-
84	94	94	88
85	74	60	70

^a listed as a percentage, after reaction time of 2 h.

Stability of different radicals was also investigated in cytosolic extract from *X. laevis* oocytes (**Figure 5.2B**, **Table 5.1**). Again, the most resistant radical in the cytosolic extract was found to be the pyrrolidine derivative **84**, which was 94% intact after 2 h. Tetraethyl piperidine derivatives **75** and **76**

(75%), tetraethyl isoindoline **77** (65%) and trityl **85** (60%) were also more stable than the remaining radicals.

Stability of radicals inside cells is a crucial test for radicals to be used for in-cell EPR studies. Charged radicals **77**, **80**, **81**, **84** and **85** gave very similar reduction profiles (**Table 5.1**) to those recorded in cytosolic extract, while non-charged radicals **75**, **76** and **83** were more reduced inside cells than in cytosolic extract. Pyrrolidine derivative **84** was the most stable radical and remained 88% intact, whereas the trityl radical (**85**) remained 70% intact after 2 h.

5.1 Conclusion

Radicals that have ethyl groups adjacent to the nitroxide radical were found to be more stable than the corresponding methyl derivatives. It was observed that tetraethyl-pyrrolidine derivative **84** was the most stable radical with respect to reduction among the radicals studied, including a trityl radical (**85**). Thus, **84** is a good candidate for performing in-cell EPR studies. Tetraethyl isoindoline spin labels **80** and **81** were comparatively less stable than pyrrolidine spin label **84** but more stable than the other remaining radicals. Hence, we chose isoindolines for spin-labeling of RNA, utilizing the high-yielding reaction of aromatic isothiocyanates with 2'-amino groups in RNA (**Chapter 6, Figure 6.2**), since conjugation of **84** to RNA would be more difficult.

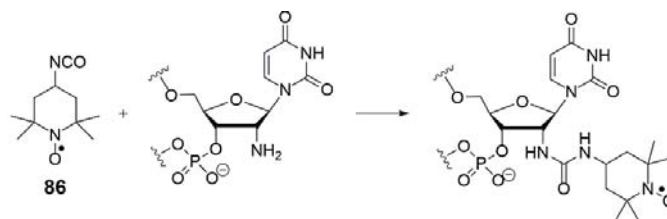
6 Site-directed spin labeling of 2'-amino groups in RNA with reductively stable isoindoline-based nitroxides

As mentioned in **Chapter 5**, EPR has routinely been applied to study the structure and dynamics of nucleic acid through distance measurements.^[117-119] Nucleic acids are not intrinsically paramagnetic and, therefore, it is necessary to modify them with paramagnetic atoms or groups, which are referred as spin labels. Incorporating spin labels into nucleic acids at specific sites is termed site-directed spin labeling (SDSL)^[149-152] and is achieved by three methods. Two of these strategies for SDSL are accomplished by formation of covalent bonds, i.e. the phosphoramidite approach and post-synthetic labeling, while the third is spin label binding through noncovalent interactions.^[153-157]

One of the methods for covalent spin labeling is the phosphoramidite approach, which utilizes spin-labeled phosphoramidites as building blocks for automated synthesis of the spin-labeled oligonucleotide.^[158] This approach usually requires a substantial synthetic effort and the spin label is exposed to the reagents used during oligonucleotide synthesis, which may result in partial reduction of the nitroxide radical.^[159,160] Post-synthetic spin labeling is the other method for covalent incorporation of spin labels at specific sites, wherein a spin-labeling reagent reacts with a specific reactive functional group within the nucleic acid.^[161-165] This strategy is less laborious than the phosphoramidite method and can often be executed with commercially available reagents.

Post-synthetic labeling of 2'-amino groups in RNA is a facile and selective approach for spin labeling.^[166,167] This method is very attractive, as 2'-amino modified phosphoramidites are commercially available or can be synthesized in-house on an automated synthesizer using commercially available 2'-amino-modified phosphoramidites. The first example of spin labeling at a 2'-position in RNA was performed to incorporate TEMPO radicals at specific sites through the reaction of 2'-amino groups with 4-isocyanato-TEMPO (**86**, **Scheme 6.1**) by forming a urea linkage.^[163] However, this method has a few limitations, *e.g.* special precautions are required while handling the isocyanates due to its high reactivity, making it prone to

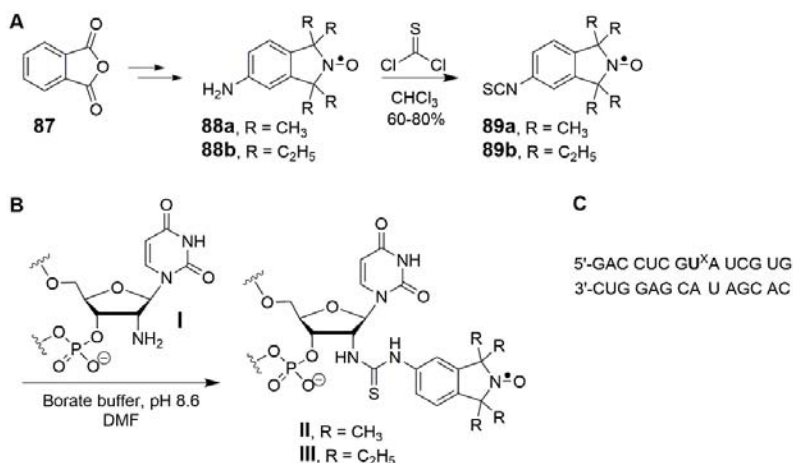
hydrolysis. As a result of this high reactivity, the labeling reaction needs to be performed at low temperature, which in turn can lead to formation of secondary structures for longer RNAs which may slow down the labeling reaction and lead to incomplete labeling.



Scheme 6.1 Spin labeling at the 2'-amino position of the oligonucleotide with isocyanate spin label **86**.

It has been shown that 2'-amino groups in RNA can react efficiently with aromatic isothiocyanates.^[168,169] Further, aromatic isothiocyanates are less reactive than aliphatic isocyanates and thus, special care is not required while handling isothiocyanates. In order to use aromatic isothiocyanates for spin labeling at 2'-amino positions, we employed spin labels **89a** and **89b** that are isoindoline-based isothiocyanates.^[170] Further, due to the low reactivity of the isothiocyanate group, the labeling reaction can be carried out at “ambient” or “elevated” temperatures which minimizes the chance of incomplete labeling, which has been observed using isocyanate **86**. We included tetraethyl isoindoline-based spin label **89b**, as it has been proven to be resistant towards different reducing conditions as described in **Chapter 5**.

Amino isoindolines **89a** and **89b** were synthesized from phthalic anhydride (**87**), which involved six steps for their synthesis.^[142,171] Isothiocyanate spin-labeling reagents **89a** and **89b** were synthesized from their corresponding amines **88a** and **88b** upon treatment with thiophosgene (**Scheme 6.2A**). Labeling of **89a** and **89b** to the 14-mer RNA sequence 5'-GAC CUC G(2'-NH₂U)A UCG UG (**I**, **Scheme 6.2B**) and its analysis was performed by Mr. Subham Saha.^[170]



Scheme 6.2 A. Syntheses of isothiocyanate spin labels **89a** and **89b**. B. Reaction of spin labels **89a** and **89b** with RNA at 2'-amino position. C. Sequence of a spin-labeled duplex, U* indicates the spin-labeled uridine at 2'-amino position with **86**, **89a** and **89b**.

Monitoring of the spin-labeling reaction of RNA showed that tetramethyl-derivative **89a** had reacted faster than tetraethyl-derivative **89b**, to form the corresponding spin-labeled sequences **II** and **III**. To determine the site-specificity of the spin labeling, isothiocyanates **89a** and **89b** were treated with an unmodified RNA sequence (that does not have 2'-amino groups). We did not detect any formation of spin-labeled products with the unmodified sequence, which confirmed the high selectivity of the spin labeling reaction at 2'-amino groups in RNA sequence. MALDI-TOF analysis of the RNA sequences showed the expected mass for the spin labeled RNA sequences **II** and **III**. Thermal denaturation (T_M) experiments showed a minor destabilization of 1.2 °C and 2 °C for the tetramethyl- and tetraethyl-RNA duplexes (**Scheme 6.2C**), relative to an unmodified sequence. However, TEMPO-labeled RNA duplex (**Scheme 6.2C**) was found to be less stable ($\Delta T_M = -5.3$ °C).

In-cell EPR spectroscopy, as mentioned in **Chapter 5**, is a promising technique which has been used to study nucleic acids in cellular conditions.^[124,125,127] However, scope of in-cell EPR is limited due to the reduction of the nitroxide radical in the reductive environment inside cells. In order to evaluate the reductive stabilities of spin-labeled RNA sequences, we incubated RNA duplexes (**Scheme 6.2C**) with ascorbic acid solution and monitored the decay of the respective EPR intensity of the low-field nitroxide line as a function of time. Normalized intensities of signals for the different spin-labeled RNA duplexes (**Scheme 6.2C**) were plotted against time (**Figure 6.1**). It was found that TEMPO-labeled RNA duplex was completely reduced within 10 min while tetramethyl-duplex was reduced within 1 h. A

remarkable reductive stability was shown by tetraethyl-duplex which remained 90% intact after 10 h (**Figure 6.1**).^[170]

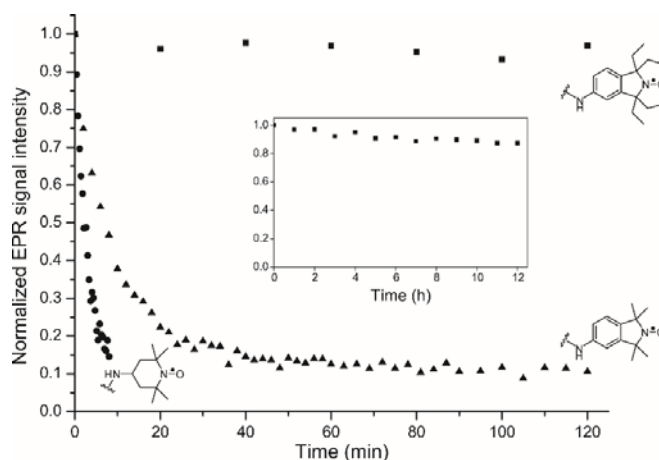


Figure 6.1 Reductive stabilities of TEMPO-labeled (circle), tetramethyl-labeled (triangle) and tetraethyl-labeled (square) RNA duplexes in ascorbic acid. Insert shows a longer time course (12 h) for tetraethyl-labeled RNA duplex.

6.1 Conclusion

An efficient post-synthetic spin labeling of 2'-amino groups in RNA with reductively stable isoindolines spin labels **89a** and **89b** was described. The reductive stability of spin-labeled RNA duplexes in ascorbic acid was investigated, showing that tetraethyl isoindoline spin label **89b** is a promising candidate for performing in-cell EPR studies.

7 Conclusions

We have introduced a strategy to convert hydrophobic biradicals into water-soluble biradicals by substituting methyl groups that are adjacent to the nitroxide group in 4-oxo-TEMPO by spirocyclohexanolyl groups. We successfully applied this strategy for the biradicals **bTurea** and **TOTOPOL** by synthesizing three water-soluble biradicals, which we named **bcTol**, **bcTol-M** and **cyolyl-TOTAPOL**. Out of these biradicals, **bcTol** and **bcTol-M** showed exceptionally high solubility in aqueous-based solvents compared with all other known nitroxide-based biradicals. However, **cyolyl-TOTAPOL** showed similar water solubility as that of the parent biradical-**TOTAPOL**.

DNP measurements were carried in Prof. Oschkinat's research group at the Leibniz-Institut für Molekulare Pharmakologie (FMP), Berlin. DNP evaluation of **bcTol** revealed 1.3 times higher DNP enhancement than currently gold-standard biradical **AMUPol** for a sample of an SH3 protein, while showing similar enhancement for proline at 110 K under similar conditions. A comparable signal-to-noise ratio (10m SNR) was observed for **bcTol** and **AMUPol** at 110 K, while it was higher for **bcTol** than **AMUPol** at 181 K for SH3 protein. DNP performance of **bcTol-M** and **cyolyl-TOTAPOL** are currently in progress.

In-cell stabilities of fifteen different radicals were also performed in order to evaluate which spin label would be suitable for in-cell EPR studies. Stability studies of these radicals in the presence of different reducing agents were carried in Prof. Prisner's research group at Goethe University in Frankfurt am Main. A tetraethyl pyrrolidine-derived nitroxide showed exceptionally high stability and remained 85% intact inside cells after 2 h at 125 K, which was higher than the carbon-centered trityl radical (70%). Tetraethyl isoindoline-based radicals were also found to be reductively stable and therefore, chosen for incorporation into RNA which was performed with in-house collaborator Mr. Subham Saha. In the process, we developed a highly efficient post-synthetic spin labeling method of 2'-amino groups of RNA with aromatic isoindoline-based isothiocyanates in excellent yields. Reductive stability of tetraethyl isoindoline labeled RNA duplex in ascorbic acid showed that 90% of the spin-labeled duplex remained intact after 10 h, demonstrating a promising candidate for performing in-cell EPR studies.

References

1. Polenova T, Gupta R and Goldbourt A, Magic angle spinning NMR spectroscopy: A versatile technique for structural and dynamic analysis of solid-phase systems, *Anal. Chem.* **2015**, *87*, 5458-5469.
2. Laws DD, Bitter HML and Jerschow A, Solid-state NMR spectroscopic methods in chemistry, *Angew. Chem. Int. Ed.* **2002**, *41*, 3096-3129.
3. Mehring M In *Principles of high resolution NMR in solids*; Springer: 1983, p 8-62.
4. Tycko R, Biomolecular solid state NMR: Advances in structural methodology and applications to peptide and protein fibrils, *Annu. Rev. Phys. Chem.* **2001**, *52*, 575-606.
5. Haeberlen U *High resolution NMR in solids: selective averaging*. New York: Academic; Elsevier, 2012.
6. Pake G, Nuclear resonance absorption in hydrated crystals: fine structure of the proton line, *J. Chem. Phys.* **1948**, *16*, 327-336.
7. Andrew ER, Bradbury A and Eades RG, Nuclear magnetic resonance spectra from a crystal rotated at high speed, *Nature* **1958**, *182*, 1659-1659.
8. Lowe I, Free induction decays of rotating solids, *Phys. Rev. Lett.* **1959**, *2*, 285-287.
9. Griffin RG, Dipolar recoupling in MAS spectra of biological solids, *Nat. Struct. Biol.* **1998**, *5*, 508-512.
10. McDermott AE, Structural and dynamic studies of proteins by solid-state NMR spectroscopy: rapid movement forward, *Curr. Opin. Struct. Biol.* **2004**, *14*, 554-561.
11. Jaroniec CP, Macphee CE, Bajaj VS, McMahon MT, Dobson CM and Griffin RG, High-resolution molecular structure of a peptide in an amyloid fibril determined by magic angle spinning NMR spectroscopy, *Proc. Natl. Acad. Sci. USA* **2004**, *101*, 711-716.
12. Wasmer C, Lange A, Van Melckebeke H, Siemer AB, Riek R and Meier BH, Amyloid fibrils of the HET-s(218-289) prion form a beta solenoid with a triangular hydrophobic core, *Science* **2008**, *319*, 1523-1526.

13. Tycko R, Characterization of amyloid structures at the molecular level by solid state nuclear magnetic resonance spectroscopy, *Meth. Enzymol.* **2006**, 413, 103-122.
14. Castellani F, Van Rossum B, Diehl A, Schubert M, Rehbein K and Oschkinat H, Structure of a protein determined by solid-state magic-angle-spinning NMR spectroscopy, *Nature* **2002**, 420, 98-102.
15. Nieuwkoop AJ, Wylie BJ, Franks WT, Shah GJ and Rienstra CM, Atomic resolution protein structure determination by three-dimensional transferred echo double resonance solid-state nuclear magnetic resonance spectroscopy, *J. Chem. Phys.* **2009**, 131, 095101.
16. Renault M, Bos MP, Tommassen J and Baldus M, Solid-state NMR on a large multidomain integral membrane protein: the outer membrane protein assembly factor BamA, *J. Am. Chem. Soc.* **2011**, 133, 4175-4177.
17. Lange V, Becker-Baldus J, Kunert B, Van Rossum BJ, Casagrande F, Engel A, Roske Y, Scheffel FM, Schneider E and Oschkinat H, A MAS NMR study of the bacterial ABC transporter artMP, *ChemBioChem* **2010**, 11, 547-555.
18. Franks WT, Linden AH, Kunert B, Van Rossum BJ and Oschkinat H, Solid-state magic-angle spinning NMR of membrane proteins and protein-ligand interactions, *Eur. J. Cell Biol.* **2012**, 91, 340-348.
19. Shahid SA, Bardiaux B, Franks WT, Krabben L, Habeck M, Van Rossum BJ and Linke D, Membrane-protein structure determination by solid-state NMR spectroscopy of microcrystals, *Nat. Methods* **2012**, 9, 1212-1217.
20. Park SH, Das BB, Casagrande F, Tian Y, Nothnagel HJ, Chu MN, Kiefer H, Maier K, De Angelis AA, Marassi FM and Opella SJ, Structure of the chemokine receptor CXCR1 in phospholipid bilayers, *Nature* **2012**, 491, 779-783.
21. James TL, Fundamentals of NMR, online textbook: Department of pharmaceutical chemistry, University of California, San Francisco, **1998**, 1-31.
22. Ardenkjær-Larsen JH, Fridlund B, Gram A, Hansson G, Hansson L, Lerche MH, Servin R, Thaning M and Golman K, Increase in signal-to-noise ratio of > 10,000 times in liquid-state NMR, *Proc. Natl. Acad. Sci. USA* **2003**, 100, 10158-10163.
23. Overhauser AW, Polarization of nuclei in metals, *Phys. Rev.* **1953**, 92, 411-415.
24. Carver TR and Slichter CP, Polarization of nuclear spins in metals, *Phys. Rev.* **1953**, 92, 212-213.
25. Abragam A, Overhauser effect in nonmetals, *Phys. Rev.* **1955**, 98, 1729-1735.
26. Carver TR and Slichter CP, Experimental verification of the Overhauser nuclear polarization effect, *Phys. Rev.* **1956**, 102, 975-981.

27. Ardenkjaer-Larsen JH, Laursen I, Leunbach I, Ehnholm G, Wistrand LG, Petersson JS and Golman K, EPR and DNP properties of certain novel single electron contrast agents intended for oximetric imaging, *J. Magn. Reson.* **1998**, 133, 1-12.
28. Lumata L, Jindal AK, Merritt ME, Malloy CR, Sherry AD and Kovacs Z, DNP by thermal mixing under optimized conditions yields > 60 000-fold enhancement of Y-89 NMR signal, *J. Am. Chem. Soc.* **2011**, 133, 8673-8680.
29. Lumata L, Ratnakar SJ, Jindal A, Merritt M, Comment A, Malloy C, Sherry AD and Kovacs Z, BDPA: An efficient polarizing agent for fast dissolution dynamic nuclear polarization NMR spectroscopy, *Chem. Eur. J.* **2011**, 17, 10825-10827.
30. Koelsch C, Syntheses with triarylvinylmagnesium bromides. α , γ -Bisdiphenylene- β -phenylallyl, a stable free radical, *J. Am. Chem. Soc.* **1957**, 79, 4439-4441.
31. Corzilius B, Smith AA, Barnes AB, Luchinat C, Bertini I and Griffin RG, High-field dynamic nuclear polarization with high-spin transition metal ions, *J. Am. Chem. Soc.* **2011**, 133, 5648-5651.
32. Thurber KR and Tycko R, Perturbation of nuclear spin polarizations in solid state NMR of nitroxide-doped samples by magic-angle spinning without microwaves, *J. Chem. Phys.* **2014**, 140, 184201.
33. Mentink-Vigier F, Paul S, Lee D, Feintuch A, Hediger S, Vega S and De Paëpe G, Nuclear depolarization and absolute sensitivity in magic-angle spinning cross effect dynamic nuclear polarization, *Phys. Chem. Chem. Phys.* **2015**, 17, 21824-21836.
34. Woskov PP, Bajaj VS, Hornstein MK, Temkin RJ and Griffin RG, Corrugated waveguide and directional coupler for CW 250-GHz gyrotron DNP experiments, *IEEE Trans. Microw. Theory Tech.* **2005**, 53, 1863-1869.
35. Hall DA, Maus DC, Gerfen GJ, Inati SJ, Becerra LR, Dahlquist FW and Griffin RG, Polarization-enhanced NMR spectroscopy of biomolecules in frozen solution, *Science* **1997**, 276, 930-932.
36. Carravetta M, Johannessen OG, Levitt MH, Heinmaa I, Stern R, Samoson A, Horsewill A, Murata Y and Komatsu K, Cryogenic NMR spectroscopy of endohedral hydrogen-fullerene complexes, *J. Chem. Phys.* **2006**, 124, 104507.
37. Macho V, Kendrick R and Yannoni CS, Cross polarization magic-angle spinning NMR at cryogenic temperatures, *J. Magn. Reson.* **1983**, 52, 450-456.
38. Bouleau E, Saint-Bonnet P, Mentink-Vigier F, Takahashi H, Jacquot J-F, Bardet M, Aussenac F, Pureau A, Engelke F and Hediger S, Pushing NMR sensitivity limits using dynamic nuclear polarization with closed-loop cryogenic helium sample spinning, *Chem. Sci.* **2015**, 6, 6806-6812.

39. Matsuki Y, Maly T, Ouari O, Karoui H, Le Moigne F, Rizzato E, Lyubenova S, Herzfeld J, Prisner T, Tordo P and Griffin RG, Dynamic nuclear polarization with a rigid biradical, *Angew. Chem. Int. Ed.* **2009**, *48*, 4996-5000.
40. Maly T, Miller AF and Griffin RG, In situ high-field dynamic nuclear polarization—direct and indirect polarization of ^{13}C nuclei, *ChemPhysChem* **2010**, *11*, 999-1001.
41. Song C, Hu K-N, Joo C-G, Swager TM and Griffin RG, TOTAPOL: A biradical polarizing agent for dynamic nuclear polarization experiments in aqueous media, *J. Am. Chem. Soc.* **2006**, *128*, 11385-11390.
42. Sauvée C, Rosay M, Casano G, Aussenac F, Weber RT, Ouari O and Tordo P, Highly efficient, water-soluble polarizing agents for dynamic nuclear polarization at high frequency, *Angew. Chem. Int. Ed.* **2013**, *52*, 10858-10861.
43. Zagdoun A, Rossini AJ, Gajan D, Bourdolle A, Ouari O, Rosay M, Maas WE, Tordo P, Lelli M, Emsley L, Lesage A and Coperet C, Non-aqueous solvents for DNP surface enhanced NMR spectroscopy, *Chem. Commun.* **2012**, *48*, 654-656.
44. Can TV, Caporini MA, Mentink-Vigier F, Corzilius B, Walish JJ, Rosay M, Maas WE, Baldus M, Vega S, Swager TM and Griffin RG, Overhauser effects in insulating solids, *J. Chem. Phys.* **2014**, *141*, 064202.
45. Lelli M, Chaudhari SR, Gajan D, Casano G, Rossini AJ, Ouari O, Tordo P, Lesage A and Emsley L, Solid-state dynamic nuclear polarization at 9.4 and 18.8 T from 100 K to room temperature, *J. Am. Chem. Soc.* **2015**, *137*, 14558-14561.
46. Eaton GR, Eaton SS, Barr DP and Weber RT *Quantitative EPR*; Springer Vienna, 2010.
47. Hu K-N, Yu H-H, Swager TM and Griffin RG, Dynamic nuclear polarization with biradicals, *J. Am. Chem. Soc.* **2004**, *126*, 10844-10845.
48. Hu K-N, Song C, Yu H-H, Swager TM and Griffin RG, High-frequency dynamic nuclear polarization using biradicals: A multifrequency EPR lineshape analysis, *J. Chem. Phys.* **2008**, *128*, 052302.
49. Akbey Ü, Franks WT, Linden A, Lange S, Griffin RG, Van Rossum BJ and Oschkinat H, Dynamic nuclear polarization of deuterated proteins, *Angew. Chem. Int. Ed.* **2010**, *49*, 7803-7806.
50. Rosay M, Tometich L, Pawsey S, Bader R, Schauwecker R, Blank M, Borchard PM, Cauffman SR, Felch KL, Weber RT, Temkin RJ, Griffin RG and Maas WE, Solid-state dynamic nuclear polarization at 263 GHz: spectrometer design and experimental results, *Phys. Chem. Chem. Phys.* **2010**, *12*, 5850-5860.

51. Kubicki DJ, Casano G, Schwarzwald M, Abel S, Sauvee C, Ganesan K, Yulikov M, Rossini AJ, Jeschke G, Coperet C, Lesage A, Tordo P, Ouari O and Emsley L, Rational design of dinitroxide biradicals for efficient cross-effect dynamic nuclear polarization, *Chem. Sci.* **2016**, 7, 550-558.
52. Takahashi H, Lee D, Dubois L, Bardet M, Hediger S and De Paëpe G, Rapid natural-abundance 2D ^{13}C - ^{13}C correlation spectroscopy using dynamic nuclear polarization enhanced solid-state NMR and matrix-free sample preparation, *Angew. Chem. Int. Ed.* **2012**, 51, 11766-11769.
53. Takahashi H, Hediger S and De Paepe G, Matrix-free dynamic nuclear polarization enables solid-state NMR ^{13}C - ^{13}C correlation spectroscopy of proteins at natural isotopic abundance, *Chem. Commun.* **2013**, 49, 9479-9481.
54. Atsarkin VA, Dynamic polarization of nuclei in solid dielectrics, *Sov Physics Uspekhi* **1978**, 21, 725-745.
55. Wind RA, Duijvestijn MJ, Vanderlugt C, Manenschijn A and Vriend J, Applications of dynamic nuclear-polarization in ^{13}C Nmr in Solids, *Prog. Nucl. Magn. Reson. Spectrosc.* **1985**, 17, 33-67.
56. Jeffries C, Polarization of nuclei by resonance saturation in paramagnetic crystals, *Phys. Rev.* **1957**, 106, 164-165.
57. Abragam A and Proctor WG, Une nouvelle méthode de polarisation dynamique des noyaux atomiques dans les solides, *Comptes Rendus Hebdomadaires Des Seances De L Academie Des Sciences* **1958**, 246, 2253-2256.
58. Hu K-N, Bajaj VS, Rosay M and Griffin RG, High-frequency dynamic nuclear polarization using mixtures of TEMPO and trityl radicals, *J. Chem. Phys.* **2007**, 126, 044512.
59. Kessenikh AV, Lushchikov VI, Manenkov AA and Taran YV, Proton polarization in irradiated polyethylenes, *Soviet Phys.-Solid State (English Transl.)* **1963**, 5, 321-329.
60. Hwang CF and Hill DA, Phenomenological model for the new effect in dynamic polarization, *Phys. Rev. Lett.* **1967**, 19, 1011-1014.
61. Hwang CF and Hill DA, New effect in dynamic polarization, *Phys. Rev. Lett.* **1967**, 18, 110-112.
62. Maly T, Debelouchina GT, Bajaj VS, Hu K-N, Joo C-G, Mak-Jurkauskas ML, Sirigiri JR, Van Der Wel PCA, Herzfeld J, Temkin RJ and Griffin RG, Dynamic nuclear polarization at high magnetic fields, *J. Chem. Phys.* **2008**, 128, 052211.
63. Becerra LR, Gerfen GJ, Bellew BF, Bryant JA, Hall DA, Inati SJ, Weber RT, Un S, Prisner TF, Mcdermott AE, Fishbein KW, Kreischer KE, Temkin RJ, Singel DJ and Griffin RG, A spectrometer for dynamic nuclear-polarization and electron-paramagnetic-resonance at high-frequencies, *J. Magn. Reson., Ser A* **1995**, 117, 28-40.

64. Rossini AJ, Zagdoun A, Hegner F, Schwarzwald M, Gajan D, Coperet C, Lesage A and Emsley L, Dynamic nuclear polarization NMR spectroscopy of microcrystalline solids, *J. Am. Chem. Soc.* **2012**, *134*, 16899-16908.
65. Bertini I, Luchinat C and Parigi G *Solution NMR of paramagnetic molecules: applications to metalloproteins and models*; Elsevier, 2001; Vol. 2.
66. Rozantsev EG, Golubev VA, Neiman MV and Kokhanov YV, *Izv. Akad. Nauk Arm. SSR Khim. Nauki* **1965**, 572-573.
67. Mathies G, Caporini MA, Michaelis VK, Liu YP, Hu K-N, Mance D, Zweier JL, Rosay M, Baldus M and Griffin RG, Efficient dynamic nuclear polarization at 800 MHz/527 GHz with trityl-nitroxide biradicals, *Angew. Chem. Int. Ed.* **2015**, *54*, 11770-11774.
68. Zagdoun A, Casano G, Ouari O, Schwarzwald M, Rossini AJ, Aussenac F, Yulikov M, Jeschke G, Coperet C, Lesage A, Tordo P and Emsley L, Large molecular weight nitroxide biradicals providing efficient dynamic nuclear polarization at temperatures up to 200 K, *J. Am. Chem. Soc.* **2013**, *135*, 12790-12797.
69. Smith AN and Long JR, Dynamic nuclear polarization as an enabling technology for solid state nuclear magnetic resonance spectroscopy, *Anal. Chem.* **2015**, *88*, 122-132.
70. Perras FA, Reinig RR, Slowing II, Sadow AD and Pruski M, Effects of biradical deuteration on the performance of DNP: towards better performing polarizing agents, *Phys. Chem. Chem. Phys.* **2016**, *18*, 65-69.
71. Zagdoun A, Casano G, Ouari O, Lapadula G, Rossini AJ, Lelli M, Baffert M, Gajan D, Veyre L, Maas WE, Rosay M, Weber RT, Thieuleux C, Coperet C, Lesage A, Tordo P and Emsley L, A slowly relaxing rigid biradical for efficient dynamic nuclear polarization surface-enhanced NMR spectroscopy: expeditious characterization of functional group manipulation in hybrid materials, *J. Am. Chem. Soc.* **2012**, *134*, 2284-2291.
72. Rossini AJ, Zagdoun A, Lelli M, Canivet J, Aguado S, Ouari O, Tordo P, Rosay M, Maas WE, Coperet C, Farrusseng D, Emsley L and Lesage A, Dynamic nuclear polarization enhanced solid-state NMR spectroscopy of functionalized metal-organic frameworks, *Angew. Chem. Int. Ed.* **2012**, *51*, 123-127.
73. Mao J, Akhmetzyanov D, Ouari O, Denysenkov V, Corzilius B, Plackmeyer J, Tordo P, Prisner TF and Glaubitz C, Host-guest complexes as water-soluble high-performance DNP polarizing agents, *J. Am. Chem. Soc.* **2013**, *135*, 19275-19281.
74. Lelli M, Rossini AJ, Casano G, Ouari O, Tordo P, Lesage A and Emsley L, Hydrophobic radicals embedded in neutral surfactants for dynamic nuclear polarization of aqueous environments at 9.4 Tesla, *Chem. Commun.* **2014**, *50*, 10198-10201.

75. Kieseewetter MK, Michaelis VK, Walish JJ, Griffin RG and Swager TM, High field dynamic nuclear polarization NMR with surfactant sheltered biradicals, *J. Phys. Chem. B* **2014**, 118, 1825-1830.
76. Dane EL, Corzilius B, Rizzato E, Stocker P, Maly T, Smith AA, Griffin RG, Ouari O, Tordo P and Swagert TM, Rigid orthogonal bis-TEMPO biradicals with improved solubility for dynamic nuclear polarization, *J. Org. Chem.* **2012**, 77, 1789-1797.
77. Kieseewetter MK, Corzilius B, Smith AA, Griffin RG and Swager TM, Dynamic nuclear polarization with a water-soluble rigid biradical, *J. Am. Chem. Soc.* **2012**, 134, 4537-4540.
78. Mori H, Ohara M and Kwan T, Carboxylation of the nitroxide radical of 2,2,6,6-tetramethyl-4-piperidone-1-oxyl with carbon-dioxide and potassium phenoxide, and the physical-properties of the products, *Chem. Pharm. Bull.* **1980**, 28, 3178-3183.
79. Fischer W, Basbas A-I, Schoening K-U and Hauck S, Synthesis of 3-substituted derivatives of 2,2,6,6-tetramethylpiperidine-n-alkoxyamine ethers: novel alkoxyamine building blocks, *Synthesis* **2010**, 2010, 3873-3878.
80. Yamada KI, Kinoshita Y, Yamasaki T, Sadasue H, Mito F, Nagai M, Matsumoto S, Aso M, Suemune H and Sakai K, Synthesis of nitroxyl radicals for overhauser-enhanced magnetic resonance imaging, *Arch. Pharm.* **2008**, 341, 548-553.
81. Sosnovsky G and Cai Z-W, A study of the Favorskii rearrangement with 3-bromo-4-oxo-2, 2, 6, 6-tetramethylpiperidine-1-oxyl, *J. Org. Chem.* **1995**, 60, 3414-3418.
82. Malievskii AD, Shapiro AB, Yakovleva IV and Koroteev SV, Quantitative study of nucleophilic-addition of secondary-amines to 3,5-dimethylene-2,2,6,6-tetramethyl-4-oxopiperidine-1-oxyl, *B Acad Sci Ussr Ch+* **1988**, 37, 542-548.
83. Orban I, Lind H, Brunetti H, Rody J and Rasberger M; Ciba-Geigy Corporation, US 3,959,295: 1976.
84. Krinitskaya LA, Synthesis and properties of bicyclic aziridines, derivatives of triacetoneamine, *Russ. Chem. Bull.* **2007**, 56, 527-531.
85. Wang B, Gu Y, Song G, Yang T, Yang L and Suo J, An efficient procedure for protection of carbonyls catalyzed by sulfamic acid, *J. Mol. Catal. A: Chem.* **2005**, 233, 121-126.
86. Clerici A, Pastori N and Porta O, Mild acetalisation of mono and dicarbonyl compounds catalysed by titanium tetrachloride. Facile synthesis of β -keto enol ethers, *Tetrahedron* **2001**, 57, 217-225.
87. Wessig P, Möllnitz K and Eiserbeck C, Oligospiroketales as novel molecular rods, *Chem. Eur. J.* **2007**, 13, 4859-4872.
88. Wang Y, Gong X, Wang Z and Dai L, SO₃H-functionalized ionic liquids as efficient and recyclable catalysts for the synthesis of pentaerythritol diacetals and diketals, *J. Mol. Catal. A: Chem.* **2010**, 322, 7-16.

89. Ma ZK, Huang QT and Bobbitt JM, Oxoammonium salts .5¹ A new synthesis of hindered piperidines leading to unsymmetrical tempo-type nitroxides - synthesis and enantioselective oxidations with chiral nitroxides and chiral oxoammonium salts, *J. Org. Chem.* **1993**, *58*, 4837-4843.
90. Miura Y, Nakamura N and Taniguchi I, Low-temperature "living" radical polymerization of styrene in the presence of nitroxides with spiro structures, *Macromolecules* **2001**, *34*, 447-455.
91. Miura Y, Ichikawa A and Taniguchi I, 'Living' radical polymerization of styrene mediated by spiro ring-substituted piperidiny-N-oxyl radicals. The effect of the spiro rings on the control of polymerization, *Polymer* **2003**, *44*, 5187-5194.
92. Mannan MA, Ichikawa A and Miura Y, Living radical polymerization of styrene mediated by a piperidiny-N-oxyl radical having very bulky substituents, *Polymer* **2007**, *48*, 743-749.
93. Yoshioka T, Higashid.S and Murayama K, Studies on stable free-radicals .VIII. synthesis and oxidation of hindered 4-oxopiperidine derivatives, *Bull. Chem. Soc. Jpn.* **1972**, *45*, 636-638.
94. Wetter C, Gierlich J, Knoop CA, Muller C, Schulte T and Studer A, Steric and electronic effects in cyclic alkoxyamines - synthesis and applications as regulators for controlled/living radical polymerization, *Chem. Eur. J.* **2004**, *10*, 1156-1166.
95. Schulte T, Siegenthaler KO, Luftmann H, Letzel M and Studer A, Nitroxide-mediated polymerization of N-isopropylacrylamide: Electrospray ionization mass spectrometry, matrix-assisted laser desorption ionization mass spectrometry, and multiple-angle laser light scattering studies on nitroxide-terminated poly-N-isopropylacrylamides, *Macromolecules* **2005**, *38*, 6833-6840.
96. Sakai K, Yamada K, Yamasaki T, Kinoshita Y, Mito F and Utsumi H, Effective 2,6-substitution of piperidine nitroxyl radical by carbonyl compound, *Tetrahedron* **2010**, *66*, 2311-2315.
97. Yamasaki T, Mito F, Ito Y, Pandian S, Kinoshita Y, Nakano K, Murugesan R, Sakai K, Utsumi H and Yamada K-I, Structure-reactivity relationship of piperidine nitroxide: electrochemical, ESR and computational studies, *J. Org. Chem.* **2010**, *76*, 435-440.
98. Yamasaki T, Ito Y, Mito F, Kitagawa K, Matsuoka Y, Yamato M and Yamada K-I, Structural concept of nitroxide as a lipid peroxidation inhibitor, *J. Org. Chem.* **2011**, *76*, 4144-4148.
99. Gonzalez-Garcia EM, Grognum J, Wahler D and Reymond JL, Synthesis and evaluation of chromogenic and fluorogenic analogs of glycerol for enzyme assays, *Helv. Chim. Acta* **2003**, *86*, 2458-2470.
100. Haeseler PR, Preparation of Diacetonamine, *J. Am. Chem. Soc.* **1925**, *47*, 1195-1196.

101. Knoop CA and Studer A, Hydroxy- and silyloxy-substituted TEMPO derivatives for the living free-radical polymerization of styrene and n-butyl acrylate: Synthesis, kinetics, and mechanistic studies, *J. Am. Chem. Soc.* **2003**, *125*, 16327-16333.
102. Zelikin AN, Zawaneh PN and Putnam D, A functionalizable biomaterial based on dihydroxyacetone, an intermediate of glucose metabolism, *Biomacromolecules* **2006**, *7*, 3239-3244.
103. Dibble DJ, Ziller JW and Woerpel KA, Spectroscopic and X-ray crystallographic evidence for electrostatic effects in 4-substituted cyclohexanone-derived hydrazones, imines, and corresponding salts, *J. Org. Chem.* **2011**, *76*, 7706-7719.
104. Ramanathan M and Hou D-R, Cleavage of benzyl ethers by triphenylphosphine hydrobromide, *Tetrahedron Lett.* **2010**, *51*, 6143-6145.
105. Bang HB, Han SY, Choi DH, Hwang JW and Jun J-G, High yield total syntheses of XH-14 derivatives using Sonogashira coupling reaction, *Arkivoc* **2009**, *2*, 112-125.
106. Cao Y, Yang X, Du D, Xu X, Song F and Xu L, New system of deprotection step for the hydroxide radicals: boron trifluoride etherate/sodium iodide, *Int. J. Chem.* **2011**, *3*, 113-117.
107. Sen' VD, Tikhonov IV, Borodin LI, Pliss EM, Golubev VA, Syroeshkin MA and Rusakov AI, Kinetics and thermodynamics of reversible disproportionation-comproportionation in redox triad oxoammonium cations – nitroxyl radicals – hydroxylamines, *J. Phys. Org. Chem.* **2015**, *28*, 17-24.
108. Babič A and Pečar S, Synthesis of novel bicyclic nitroxides using partial Favorskii rearrangement, *Synlett* **2008**, *2008*, 1155-1158.
109. Yan'shole V, Kirilyuk I, Grigor'ev I, Morozov S and Tsentalovich YP, Antioxidative properties of nitroxyl radicals and hydroxylamines in reactions with triplet and deaminated kynurenine, *Russ. Chem. Bull.* **2010**, *59*, 66-74.
110. Marti F, Chadwick J, Amewu RK, Burrell-Saward H, Srivastava A, Ward SA, Sharma R, Berry N and O'Neill PM, Second generation analogues of RKA182: synthetic tetraoxanes with outstanding in vitro and in vivo antimalarial activities, *Med. Chem. Commun.* **2011**, *2*, 661-665.
111. Okazaki S, Mannan MA, Sawai K, Masumizu T, Miura Y and Takeshita K, Enzymatic reduction-resistant nitroxyl spin probes with spirocyclohexyl rings, *Free Radical Res.* **2007**, *41*, 1069-1077.
112. Yau WM, Thurber KR and Tycko R, Synthesis and evaluation of nitroxide-based oligoradicals for low-temperature dynamic nuclear polarization in solid state NMR, *J. Magn. Reson.* **2014**, *244*, 98-106.

113. Bruun S, Stoeppler D, Keidel A, Kuhlmann U, Luck M, Diehl A, Geiger M-A, Woodmansee D, Trauner D, Hegemann P, Oschkinat H, Hildebrandt P and Stehfest K, Light-dark adaptation of channelrhodopsin involves photoconversion between the all-trans and 13-cis retinal isomers, *Biochemistry* **2015**, 54, 5389-5400.
114. Scott LG and Hennig M In *Bioinformatics: Data, Sequence Analysis and Evolution*; JM Keith, Ed.; Humana Press: Totowa, NJ, 2008, p 29-61.
115. Holbrook SR, Structural principles from large RNAs, *Annu. Rev. Biophys.* **2008**, 37, 445-464.
116. Blanchard SC, Single-molecule observations of ribosome function, *Curr. Opin. Struct. Biol.* **2009**, 19, 103-109.
117. Milov AD, Ponomarev AB and Tsvetkov YD, Electron double-resonance in electron-spin echo-model biradical systems and the sensitized photolysis of decalin, *Chem. Phys. Lett.* **1984**, 110, 67-72.
118. Schiemann O, Mapping global folds of oligonucleotides by pulsed electron-electron double resonance, *Meth. Enzymol.* **2009**, 469, 329-351.
119. Sowa GZ and Qin PZ, Site-directed spin labeling studies on nucleic acid structure and dynamics, *Prog. Nucleic Acid Res. Mol. Biol.* **2008**, 82, 147-197.
120. Miyoshi D and Sugimoto N, Molecular crowding effects on structure and stability of DNA, *Biochimie* **2008**, 90, 1040-1051.
121. Leipply D, Lambert D and Draper DE, Ion-RNA interactions: thermodynamic analysis of the effects of mono- and divalent ions on RNA conformational equilibria, *Meth. Enzymol.* **2009**, 469, 433-463.
122. Kilburn D, Roh JH, Guo L, Briber RM and Woodson SA, Molecular crowding stabilizes folded RNA structure by the excluded volume effect, *J. Am. Chem. Soc.* **2010**, 132, 8690-8696.
123. Hänsel R, Luh LM, Corbeski I, Trantirek L and Dötsch V, In-Cell NMR and EPR Spectroscopy of Biomacromolecules, *Angew. Chem. Int. Ed.* **2014**, 53, 10300-10314.
124. Krstić I, Hänsel R, Romainczyk O, Engels JW, Dötsch V and Prisner TF, Long-range distance measurements on nucleic acids in cells by pulsed EPR spectroscopy, *Angew. Chem. Int. Ed.* **2011**, 50, 5070-5074.
125. Azarkh M, Okle O, Singh V, Seemann IT, Hartig JS, Dietrich DR and Drescher M, Long-range distance determination in a DNA model system inside *Xenopus laevis* oocytes by in-cell spin-label EPR, *ChemBioChem* **2011**, 12, 1992-1995.

126. Azarkh M, Okle O, Eyring P, Dietrich DR and Drescher M, Evaluation of spin labels for in-cell EPR by analysis of nitroxide reduction in cell extract of *Xenopus laevis* oocytes, *J. Magn. Reson.* **2011**, 212, 450-454.
127. Azarkh M, Singh V, Okle O, Seemann IT, Dietrich DR, Hartig JS and Drescher M, Site-directed spin-labeling of nucleotides and the use of in-cell EPR to determine long-range distances in a biologically relevant environment, *Nat. Protoc.* **2013**, 8, 131-147.
128. Swartz HM and Clarkson RB, The measurement of oxygen in vivo using EPR techniques, *Phys. Med. Biol.* **1998**, 43, 1957-1975.
129. Khrantsov VV, Grigor'ev IA, Foster MA, Lurie DJ and Nicholson I, Biological applications of spin pH probes, *Cell. Mol. Biol.* **2000**, 46, 1361-1374.
130. Chen K, Morse PD and Swartz HM, Kinetics of enzyme-mediated reduction of lipid soluble nitroxide spin labels by living cells, *Biochim. Biophys. Acta-Biomembranes* **1988**, 943, 477-484.
131. Levine M, Padayatty SJ and Espey MG, Vitamin C: A concentration-function approach yields pharmacology and therapeutic discoveries, *Adv. Nutr.* **2011**, 2, 78-88.
132. Kocherginsky N and Swartz HM *Nitroxide spin labels: reactions in biology and chemistry*; CRC Press, 1995.
133. Bobko AA, Kirilyuk IA, Grigor'ev IA, Zweier JL and Khrantsov VV, Reversible reduction of nitroxides to hydroxylamines: roles for ascorbate and glutathione, *Free Radical Biol. Med.* **2007**, 42, 404-412.
134. Marx L, Chiarelli R, Guiberteau T and Rassat A, A comparative study of the reduction by ascorbate of 1,1,3,3-tetraethylisindolin-2-yloxy and of 1,1,3,3-tetramethylisindolin-2-yloxy, *J. Chem. Soc. Perkin Trans. I* **2000**, 1181-1182.
135. Blinco JP, Hodgson JL, Morrow BJ, Walker JR, Will GD, Coote ML and Bottle SE, Experimental and theoretical studies of the redox potentials of cyclic nitroxides, *J. Org. Chem.* **2008**, 73, 6763-6771.
136. Kavala M, Boca R, Dlhán L, Brezova V, Breza M, Kozisek J, Fronc M, Herich P, Svorec L and Szolcsanyi P, Preparation and spectroscopic, magnetic and electrochemical studies of mono-/biradical TEMPO derivatives, *J. Org. Chem.* **2013**, 78, 6558-6569.
137. Belkin S, Mehlhorn RJ, Hideg K, Hankovsky O and Packer L, Reduction and destruction rates of nitroxide spin probes, *Arch. Biochem. Biophys.* **1987**, 256, 232-243.
138. Couet WR, Eriksson UG, Tozer TN, Tuck LD, Wesbey GE, Nitecki D and Brasch RC, Pharmacokinetics and metabolic-fate of two nitroxides potentially useful as contrast agents for magnetic-resonance imaging, *Pharm. Res.* **1984**, 203-209.
139. Sentjurs M, Pecar S, Chen K, Wu M and Swartz H, Cellular-metabolism of proxyl nitroxides and hydroxylamines, *Biochim. Biophys. Acta* **1991**, 1073, 329-335.

140. Eriksson UG, Tozer TN, Sosnovsky G, Lukszo J and Brasch RC, Human-erythrocyte membrane-permeability and nitroxyl spin-label reduction, *J. Pharm. Sci.* **1986**, 75, 334-337.
141. Kinoshita Y, Yamada K, Yamasaki T, Mito F, Yamato M, Kosem N, Deguchi H, Shirahama C, Ito Y, Kitagawa K, Okukado N, Sakai K and Utsumi H, In vivo evaluation of novel nitroxyl radicals with reduction stability, *Free Radical Biol. Med.* **2010**, 49, 1703-1709.
142. Jagtap AP, Krstić I, Kunjir NC, Hänsel R, Prisner TF and Sigurdsson ST, Sterically shielded spin labels for in-cell EPR spectroscopy: Analysis of stability in reducing environment, *Free Radical Res.* **2015**, 49, 78-85.
143. Siegenthaler KO, Schafer A and Studer A, Chemical surface modification via radical C-C bond-forming reactions, *J. Am. Chem. Soc.* **2007**, 129, 5826-5827.
144. Huang WL, Charleux B, Chiarelli R, Marx L, Rassat A and Vairon JP, Synthesis of water-soluble nitroxides and their use as mediators in aqueous-phase controlled radical polymerization, *Macromol. Chem. Phys.* **2002**, 203, 1715-1723.
145. Kirilyuk IA, Bobko AA, Grigor'ev IA and Khramtsov VV, Synthesis of the tetraethyl substituted pH-sensitive nitroxides of imidazole series with enhanced stability towards reduction, *Org. Biomol. Chem.* **2004**, 2, 1025-1030.
146. Volodarsky LB, Reznikov VA and Grigor'ev IA, Chemical properties of hetetrocyclic nitroxides, *Imidazoline nitroxides*, ed. L. B. Volodarsky, CRC Press, Boca Raton, Florida **1988**, 1, 5-23.
147. Paletta JT, Pink M, Foley B, Rajca S and Rajca A, Synthesis and reduction kinetics of sterically shielded pyrrolidine nitroxides, *Org. Lett.* **2012**, 14, 5322-5325.
148. Liu Y, Villamena FA, Sun J, Xu Y, Dhimitruka I and Zweier JL, Synthesis and characterization of ester-derivatized tetrathiatriarylmethyl radicals as intracellular oxygen probes, *J. Org. Chem.* **2008**, 73, 1490-1497.
149. Sowa GZ and Qin PZ, Site-directed spin labeling studies on nucleic acid structure and dynamics, *Prog. Nucleic Acid Res. Mol. Biol.* **2008**, 82, 147-197.
150. Shelke SA and Sigurdsson ST In *Structural information from spin-labels and intrinsic paramagnetic centres in the biosciences*; Springer: 2013, p 121-162.
151. Ding Y, Nguyen P, Tangprasertchai NS, Reyes CV, Zhang X and Qin PZ In *electron paramagnetic resonance*; The Royal Society of Chemistry: 2015; Vol. 24, p 122-147.
152. Saha S, Jagtap AP and Sigurdsson ST In *Meth. Enzymol.*; ZQ Peter, Kurt, W, Eds.; Academic Press: 2015; Vol. 563, p 397-414.

153. Belmont P, Chapelle C, Demeunynck M, Michon J, Michon P and Lhomme J, Introduction of a nitroxide group on position 2 of 9-phenoxyacridine: Easy access to spin labelled DNA-binding conjugates, *Bioorg. Med. Chem. Lett.* **1998**, *8*, 669-674.
154. Maekawa K, Nakazawa S, Atsumi H, Shiomi D, Sato K, Kitagawa M, Takui T and Nakatani K, Programmed assembly of organic radicals on DNA, *Chem. Commun.* **2010**, *46*, 1247-1249.
155. Shelke SA and Sigurdsson ST, Noncovalent and site-directed spin labeling of nucleic acids, *Angew. Chem. Int. Ed.* **2010**, *49*, 7984-7986.
156. Shelke SA, Sandholt GB and Sigurdsson ST, Nitroxide-labeled pyrimidines for non-covalent spin-labeling of abasic sites in DNA and RNA duplexes, *Org. Biomol. Chem.* **2014**, *12*, 7366-7374.
157. Chalmers BA, Saha S, Nguyen T, Mcmurtrie J, Sigurdsson ST, Bottle SE and Masters K-S, TMIO-pyrImid hybrids are profluorescent, site-directed spin labels for nucleic acids, *Org. Lett.* **2014**, *16*, 5528-5531.
158. Spaltenstein A, Robinson BH and Hopkins PB, A rigid and nonperturbing probe for duplex DNA motion, *J. Am. Chem. Soc.* **1988**, *110*, 1299-1301.
159. Piton N, Mu Y, Stock G, Prisner TF, Schiemann O and Engels JW, Base-specific spin-labeling of RNA for structure determination, *Nucleic Acids Res.* **2007**, *35*, 3128-3143.
160. Cekan P, Smith AL, Barhate N, Robinson BH and Sigurdsson ST, Rigid spin-labeled nucleoside C: a nonperturbing EPR probe of nucleic acid conformation, *Nucleic Acids Res.* **2008**, *36*, 5946-5954.
161. Hara H, Horiuchi T, Saneyoshi M and Nishimura S, 4-Thiouridine-specific spin-labeling of E-coli transfer RNA, *Biochem. Biophys. Res. Commun.* **1970**, *38*, 305-311.
162. Qin PZ, Butcher SE, Feigon J and Hubbell WL, Quantitative analysis of the isolated GAAA tetraloop/receptor interaction in solution: A site-directed spin labeling study, *Biochemistry* **2001**, *40*, 6929-6936.
163. Edwards TE, Okonogi TM, Robinson BH and Sigurdsson ST, Site-specific incorporation of nitroxide spin-labels into internal sites of the TAR RNA; structure-dependent dynamics of RNA by EPR spectroscopy, *J. Am. Chem. Soc.* **2001**, *123*, 1527-1528.
164. Ding P, Wunnicke D, Steinhoff HJ and Seela F, Site-directed spin-labeling of DNA by the azide-alkyne 'Click' reaction: Nanometer distance measurements on 7-Deaza-2'-deoxyadenosine and 2'-deoxyuridine nitroxide conjugates spatially separated or linked to a 'dA-dT' base pair, *Chem. Eur. J.* **2010**, *16*, 14385-14396.
165. Jakobsen U, Shelke SA, Vogel S and Sigurdsson ST, Site-directed spin-labeling of nucleic acids by Click chemistry: detection of abasic sites in duplex DNA by EPR spectroscopy, *J. Am. Chem. Soc.* **2010**, *132*, 10424-10428.

166. Kim NK, Murali A and Deroose VJ, A distance ruler for RNA using EPR and site-directed spin labeling, *Chem. Biol.* **2004**, *11*, 939-948.
167. Edwards TE and Sigurdsson ST, Site-specific incorporation of nitroxide spin-labels into 2'-positions of nucleic acids, *Nat. Protoc.* **2007**, *2*, 1954-1962.
168. Aurup H, Tuschl T, Benseler F, Ludwig J and Eckstein F, Oligonucleotide duplexes containing 2'-amino-2'-deoxycytidines: thermal-stability and chemical-reactivity *Nucleic Acids Res.* **1994**, *22*, 20-24.
169. Sigurdsson ST, Tuschl T and Eckstein F, Probing RNA tertiary structure: interhelical crosslinking of the hammerhead ribozyme, *RNA* **1995**, *1*, 575-583.
170. Saha S, Jagtap AP and Sigurdsson ST, Site-directed spin labeling of 2'-amino groups in RNA with isoindoline nitroxides that are resistant to reduction, *Chem. Commun.* **2015**, *51*, 13142-13145.
171. Mileo E, Etienne E, Martinho M, Lebrun R, Roubaud V, Tordo P, Gontero B, Guigliarelli B, Marque SRA and Belle V, Enlarging the panoply of site-directed spin labeling electron paramagnetic resonance (SDSL-EPR): sensitive and selective spin-labeling of tyrosine using an isoindoline-based nitroxide, *Bioconjugate Chem.* **2013**, *24*, 1110-1117.

Publications

- I. Jagtap AP, Krstic I, Kunjir NC, Hänsel R, Prisner TF and Sigurdsson ST, Sterically shielded spin labels for in-cell EPR spectroscopy: Analysis of stability in reducing environment, *Free Radical Res.* **2015**, 49, 78-85.
- II. Saha S†, Jagtap AP† and Sigurdsson ST, Site-directed spin labeling of 2'-amino groups in RNA with isoindoline nitroxides that are resistant to reduction, *Chem. Commun.* **2015**, 51, 13142-13145.
(† These two authors contributed equally)
- III. Jagtap AP, Geiger M-A, Stöppler D, Oschkinat H and Sigurdsson ST, bcTol: A highly water-soluble biradical for efficient dynamic nuclear polarization of biomolecules, *Chem. Commun.* **2016**, manuscript submitted.
- IV. Saha S, Jagtap AP and Sigurdsson ST, In: Peter Z. Qin and Kurt Warncke, Editor(s), Chapter fifteen - Site-directed spin labeling of RNA by post-synthetic modification of 2'-amino groups, *Methods in Enzymol.*, Academic Press **2015**, 563, 397-414.

Article I. In-cell stability studies of spin labels

Sterically shielded spin labels for in-cell EPR spectroscopy: Analysis of stability in reducing environment

Free Radical Res. **2015**, *49*, 78-85.

Free Radical Research, January 2015; 49(1): 78–85
 © 2014 Informa UK, Ltd.
 ISSN 1071-5762 print/ISSN 1029-2470 online
 DOI: 10.3109/10715762.2014.979409

informa
healthcare

ORIGINAL ARTICLE

Sterically shielded spin labels for in-cell EPR spectroscopy: Analysis of stability in reducing environment

A. P. Jagtap¹, I. Krstic², N. C. Kunjir¹, R. Hänsel³, T. F. Prisner² & S. Th. Sigurdsson¹

¹University of Iceland, Department of Chemistry, Science Institute, Reykjavik, Iceland, ²Institute of Physical and Theoretical Chemistry, Goethe University Frankfurt, Frankfurt, Germany, and ³Institute of Biophysical Chemistry and Center for Biomolecular Magnetic Resonance, Goethe University, Frankfurt, Germany

Abstract

Electron paramagnetic resonance (EPR) spectroscopy is a powerful and widely used technique for studying structure and dynamics of biomolecules under bio-orthogonal conditions. In-cell EPR is an emerging area in this field; however, it is hampered by the reducing environment present in cells, which reduces most nitroxide spin labels to their corresponding diamagnetic *N*-hydroxyl derivatives. To determine which radicals are best suited for in-cell EPR studies, we systematically studied the effects of substitution on radical stability using five different classes of radicals, specifically piperidine-, imidazolidine-, pyrrolidine-, and isoindoline-based nitroxides as well as the Finland trityl radical. Thermodynamic parameters of nitroxide reduction were determined by cyclic voltammetry; the rate of reduction in the presence of ascorbate, cellular extracts, and after injection into oocytes was measured by continuous-wave EPR spectroscopy. Our study revealed that tetraethyl-substituted nitroxides are good candidates for in-cell EPR studies, in particular pyrrolidine derivatives, which are slightly more stable than the trityl radical.

Keywords: nitroxide reduction, aminoxyl radical, radical stability, spin labeling, trityl radical

Introduction

RNA molecules have a central role in cellular processes and gene regulation. Their three-dimensional structures and conformational dynamics are essential for their functions as biological catalysts, structural scaffolds, and regulators of gene expression [1]. Thus, information about structure and motion can give insights into RNA function and how it might be modulated. Besides X-ray crystallography [2], nuclear magnetic resonance (NMR) [3], and fluorescence spectroscopy [4], pulsed electron–electron double resonance (PELDOR or DEER) spectroscopy [5] has, over the past few years, demonstrated its applicability to map the global structure of nucleic acids [6,7] and other macromolecules [8,9] through distance measurements in the range of 1.5–8 nm, utilizing distance-dependent magnetic dipole–dipole interaction between two covalently attached aminoxyl (nitroxide) radicals. EPR spectroscopy also holds promise for in-cell measurements because there is no background interference, as can be the case with fluorescence spectroscopy. In fact, PELDOR was recently used to study structural aspects of nucleic acids [10,11] and proteins [12] inside intact *Xenopus laevis* oocytes. However, the short lifetimes of nitroxide spin labels under cellular conditions is a severe limitation to the general applicability of PELDOR for in-cell measurements [13].

In addition to the use as labels for EPR spectroscopy, cyclic nitroxide radicals are an important class of

compounds for biological and medical applications [14–16], such as contrast agents for magnetic resonance imaging (MRI) [17], as antioxidants, and as superoxide dismutase mimics [18], where the nitroxide is involved in redox reactions by a one-electron exchange between its reduced and oxidized state [19]. Additionally, nitroxide radicals have been used to determine the partial pressure of oxygen [20] and pH [21] values in living tissues via EPR spectroscopy. The aforementioned applications of nitroxides in biological fluids are adversely affected when the paramagnetic center is readily reduced to the EPR-silent hydroxylamine [22].

Since the application of nitroxides inside living cells is of growing interest, extensive efforts have been taken for the design and synthesis of nitroxide radicals that are more resistant toward reduction [23,24]. Several factors affect the stability of nitroxides, such as ring size (piperidine, pyrrolidine, and isoindoline), the presence of heteroatoms within the ring (imidazolidine), substituents (neutral or charged), and the identity of the alkyl substituents in the positions adjacent to the nitroxide functional group. Although the stability of a variety of nitroxides in the presence of ascorbate has been reported [22,25–36], the biostability of radicals has invariably been investigated under different conditions [26–30,37–41]. Furthermore, each of these biostability studies has focused on a small number of radicals. The study of Kinoshita et al. is similar to the work described here in terms of the techniques and

Correspondence: Prof. Snorri Th. Sigurdsson, PhD, University of Iceland, Department of Chemistry, Science Institute, Dunhagi 3, 107 Reykjavik, Iceland. Tel: +354 525 4800. Fax: +354 552 8911. E-mail: snorrisi@hi.is

(Received date: 20 September 2014; Accepted date: 19 October 2014; Published online: 19 November 2014)



conditions used for evaluation of radical stability. They also compared tetramethyl and tetraethyl piperidine nitroxides; however, our work additionally includes imidazolidine and isoindoline nitroxides as well as a triphenylmethyl (trityl) radical [37].

In this paper, we compare redox properties of a series of nitroxides varying with ring type, substituents, and charge, using several approaches with the aim of identifying radicals that are suitable for in-cell studies. A trityl radical, which has been shown to be relatively stable under reductive conditions [42], was chosen for comparison. We also determined the hyperfine coupling constants (A_{iso}) of all the nitroxides that are sensitive to the polarity around the nitroxide moiety, by continuous-wave (CW) EPR. With regard to the nitroxides, we focused on tetraethyl-substituted radicals with pyrrolidine-, piperidine-, isoindoline-, and imidazolidine-based structures and compared them with the more reactive tetramethyl-substituted analogs. The effect of electronegative and charged substituents on the nitroxide rings was also evaluated. In addition to determination of the kinetic and thermodynamic stability of the radicals in the presence of ascorbic acid, their stability was tested in a cytosolic extract from *X. laevis* oocytes and inside living oocyte cells.

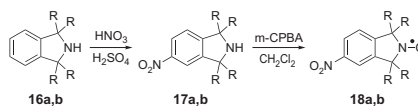
Material and methods

Preparation of radicals

Chemicals were purchased primarily from Sigma-Aldrich Chemical Company and Acros, Belgium, and were used without further purification. Thin-layer chromatography (TLC) was performed on glass-backed TLC plates with extra hard layer (Kieselgel 60 F₂₅₄, 250 μm , Silicycle) and compounds were visualized using UV light at 254 nm. Silica gel (230–400 mesh, 60 \AA) was purchased from Silicycle, and used for flash chromatography. Molecular masses of organic compounds were determined by high-resolution electrospray ionization mass spectrometry (HR-ESI-MS) (Bruker, MicroTof-Q).

Tetramethyl-derived spin labels **1**, **2**, **3** and pyrrolidine spin label **12** were purchased, while tetraethyl piperidine derivative **4** was prepared according to the reported procedure [37] and used for the synthesis of compounds **5** and **6** [37,43]. Compounds **11** and **13–15** were synthesized as previously described [44–47].

Compounds **8** and **10** were prepared using a modification of previously reported method [48]. In the reported procedure for the synthesis of **8**, compound **16a** was oxidized and then nitrated to obtain **18a**. However, nitration gave multiple spots in our hands; therefore, compound **16a** was first nitrated to obtain compound **17a** (Scheme 1) [49]. Subsequent oxidation with meta-chloroperoxybenzoic acid (*m*-CPBA) yielded compound **18a** in moderate yields, which was converted to compound **8** using the previously published protocol [48]. This modified procedure was also used for the synthesis of the corresponding tetraethyl derivative **10**. Preparation of compound **8** using



Scheme 1. Syntheses of isoindoline-derived radicals **18a** and **b**, used for synthesis of **8** and **10**; R is either methyl (**a**) or ethyl (**b**).

this strategy has recently been reported by Mileo et al. [50].

1,1,3,3-Tetramethyl-5-nitroisoindoline 18a

To a solution of compound **17a** (0.9 g, 4 mmol) in CH_2Cl_2 (5 mL) at 0°C , a solution of *m*-CPBA (1.4 g, 8.17 mmol) in CH_2Cl_2 (6 mL) was added. The resulting solution was stirred at 0°C for 1 h and then at 24°C for 2 h. The reaction mixture was diluted with CH_2Cl_2 (10 mL) and the organic layer was washed successively with an aqueous NaOH solution (2.5 N, 2×10 mL) and brine (10 mL). The organic layer was dried over anhydrous Na_2SO_4 , filtered, and then concentrated *in vacuo*. The crude reaction mixture was purified by column chromatography (5% MeOH in CH_2Cl_2) to yield **18a** as a yellow solid (0.9 g, 94% yield). HR-ESI-MS: 258.0975 ($\text{M} + \text{Na}$), calcd. 235.0953 for $\text{C}_{12}\text{H}_{15}\text{N}_2\text{O}_3$.

Tetraethyl-5-nitroisoindoline 18b

To a solution of compound **17b** (0.120 g, 0.43 mmol) in CH_2Cl_2 (2 mL) at 0°C , a solution of *m*-CPBA (0.089 g, 0.5 mmol) in CH_2Cl_2 (1 mL) was added. The resulting solution was stirred at 0°C for 1 h and then at 24°C for 3 h. The reaction mixture was diluted with CH_2Cl_2 (5 mL) and the organic layer was washed successively with an aqueous NaOH solution (2.5 N, 2×10 mL) and brine (10 mL). The organic layer was dried over anhydrous Na_2SO_4 , filtered, and then concentrated *in vacuo*. The crude reaction mixture was purified by column chromatography (30% ethyl acetate in petroleum ether) to yield **18b** as a yellow solid (0.1 g, 79% yield). HR-ESI-MS: 314.1602 ($\text{M} + \text{Na}$), calcd. 291.1601 for $\text{C}_{16}\text{H}_{23}\text{N}_2\text{O}_3$.

Cyclic voltammetry

Cyclic voltammetry experiments were performed in a 4 mM phosphate buffer solution (PBS; pH: 7.2) containing 1 mM radical concentration. A three-electrode cell arrangement was used encompassing glassy carbon working electrode, which was polished before each measurement, a reference electrode Ag/AgCl/KCl(3 M), and a double-wire platinum counter electrode. The following parameters were used: scan rate, 0.1 V/s; starting potential, 0.0 V; upper vertex potential, 1.0 V; lower vertex potential, -1.5 ; cathodic step potential, -0.00244 V; and anodic step potential, 0.00244 V. In case of compound **6**, the starting potential was -0.2 V, because of similar anodic and cathodic peak potentials.

Monitoring reduction of radicals in ascorbic acid and in cell extract using CW-EPR

Preparation of the crude cytoplasmic extracts from *X. laevis* oocytes was as previously described [10]; 19 μL of 5 mM ascorbic acid solution in 4 mM PBS (pH = 7.4), or 19 μL of cell extract were mixed with 1 μL of a 4 mM radical solution (final radical concentration, 200 μM). The solution was transferred into an EPR tube (1 mm inner diameter, Wilmad, USA) and the EPR signal intensity was measured as a function of time using a Bruker E500 CW-EPR spectrometer at X-band (9.43 GHz), using the following settings: modulation frequency, 9.43 GHz; time constant, 40.96 ms; microwave power, 1.0 mW; conversion time, 40.96 ms; modulation amplitude, 1.0 G; number of points, 1024; field sweep, 70 G; and sweeps, 160–170.

Monitoring reduction of radicals inside cells by CW-EPR

Oocytes from *X. laevis* trapped in stage VI, characterized by ca. 1 mm diameter and ca. 1 μL volume were used [10]. Samples were prepared by microinjection of ca. 40 nL of 4 mM spin label stock solution into 50 oocytes and subsequent incubation at room temperature for a variable time (0, 15, 30, 60, and 120 min) before freezing the cells in liquid nitrogen, until the radical concentration was determined by CW-EPR: microwave power, 0.2 mW; modulation amplitude, 2.0 G; number of scans, 10; and temperature, 125 K.

Results and discussion

Selection of radicals

Five classes of spin labels were investigated, each of which was based on a specific cyclic nitroxide, that is, piperidine (Figure 1A), isoindoline (Figure 1B), imidazolidine (Figure 1C), and pyrrolidine derivatives (Figure 1C) or a trityl radical (Figure 1C). The piperidine series served to investigate the effects of the substituents on the ring, all of which were electron withdrawing, except for the alkyl groups flanking the nitroxide. The isoindolines (Figure 1B) had ionizable groups to facilitate solubility in aqueous solutions—a sulfonate in compounds **7** [51,52] and **9** [51,52], and a tetraalkylammonium ion in compounds **8** and **10**. Each type of nitroxide was prepared as tetramethyl and tetraethyl derivatives. The trityl radical **15** was the only carbon-based radical in this study.

Thermodynamic parameters for reduction in the presence of ascorbic acid

Ascorbic acid, a reducing agent present to some extent in biological systems [53–55], is commonly used for evaluation of radical stability [29] and was used to investigate the thermodynamic parameters of the radicals. To determine the Gibbs free energy (ΔG) and the reaction equilibrium con-

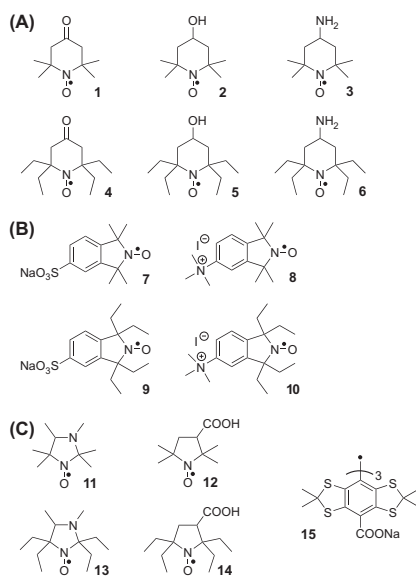


Figure 1. Radicals for evaluation of reductive stability. (A) Piperidine-based nitroxides. (B) Isoindoline-based nitroxides. (C) Imidazolidine- and pyrrolidine-based nitroxides and a trityl radical.

stant (K) for the reduction, the redox potential of each radical was measured by cyclic voltammetry. The half-wave potentials correspond to standard redox potentials as long as the diffusion coefficients of the reduced and oxidized state are equal, which is generally the case.

A typical voltammogram of a nitroxide, recorded by sweeping the potential of a glassy carbon electrode between -1.5 and 1 V (vs Ag/AgCl/KCl) in both the anodic and the cathodic direction, respectively, contains two peak couples (Supplementary Figure 4A to be found online at <http://informahealthcare.com/doi/abs/10.3109/10715762.2014.979409>). The first peak couple appears at the anodic potential of the voltammogram and originates from the reversible oxidation of the nitroxide to an oxoammonium cation (Supplementary Figure 4B to be found online at <http://informahealthcare.com/doi/abs/10.3109/10715762.2014.979409>). The peak separation is close to the theoretical value of 59 mV for a one-electron transfer. This reaction is not important in a biological context, where nitroxide radicals are reduced. The second peak couple represents the reduction of the nitroxide (Supplementary Figure 4C to be found online at <http://informahealthcare.com/doi/abs/10.3109/10715762.2014.979409>) and the corresponding oxidation of hydroxylamine. In this case, the electron transfer to the nitroxide is coupled to a chemical reaction, making the peak separation larger. Since the redox behavior of trityl radicals differs significantly from

nitroxides, compound **15** was not studied by cyclic voltammetry.

The half-wave potentials ($E_{1/2}$) were determined from the cyclic voltammograms as the midpoint between the oxidation and the reduction peak potentials for the second peak couple: $E_{1/2} = (E_p^{ox} + E_p^{red})/2$ (Table I). The tetramethyl-substituted piperidines had the highest $E_{1/2}$ value (*ca.* -0.07 V), while the tetraethyl-substituted isoindoline- and pyrrolidine-derived nitroxides displayed the lowest redox potential (-0.32 V), making them the most resistant to reduction. The differences between the standard redox potential of ascorbic acid ($E_0 = -0.15$ V vs Ag/AgCl/KCl) and the measured $E_{1/2}$ of each nitroxide were used to determine ΔG and K for the reduction of the nitroxide with ascorbate [56] (Table I). The ΔG values for the reduction were negative for the tetramethyl-derived piperidines, thus making the nitroxide reduction energetically favorable. In contrast, the tetraethyl-substituted nitroxides yielded ΔG values of about 6–16 kJ/mol and small equilibrium constants, showing that their equilibrium lies toward the educts.

Using the equilibrium constants determined from the cyclic voltammetry measurements and known starting concentrations of educts, the equilibrium concentrations of the nitroxide radicals were calculated, normalized to the starting concentration ($[N]_{eq}/[N]_0$), and expressed in Table I as percentages. The equilibrium concentrations of the nitroxides in reaction with ascorbic acid were also determined experimentally by following the intensity of the low-field nitroxide line of the EPR spectra as a function of time (Figure 2A). The decaying EPR signal was fitted with the pseudo-first-order reaction kinetic implicitly including the equilibrium signal as a fit parameter (see Kinetics of the reduction of radicals in ascorbic acid solution). This signal originates from radicals present at equilibrium and was compared with the equilibrium

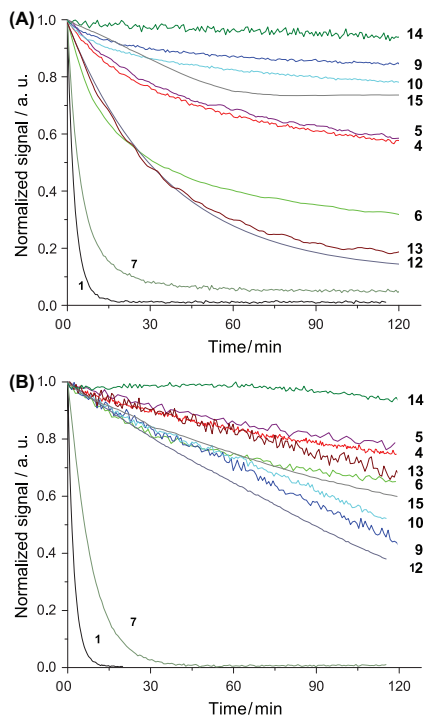


Figure 2. (A) Reduction of selected radicals with ascorbic acid (200 μ M conc. of radical and 5 mM ascorbic acid in PBS buffer, pH: 7.2, except for compounds **1**–**3**, when ascorbate conc. was 1 mM). The EPR signal intensity is plotted as a function of time. (B) Decay curves for the radicals in a cytosolic extract.

Table I. Half-wave potentials ($E_{1/2}$) of nitroxide radicals, Gibbs free energy (ΔG) and equilibrium constants (K) for reduction of nitroxides with ascorbic acid, and equilibrium concentrations of the nitroxides (calculated and measured).

Rad.*	$E_{1/2}^{\dagger}$ [V]	ΔG^{\ddagger} [kJ/mol]	$K = e^{-(\Delta G/RT)}$	$[N]_{eq}/[N]_0$ (%)	
				Calculated	Measured
1	-0.08	-7 ± 2	16 ± 5	1.4 ± 0.5	1.2 ± 0.1
4	-0.27	12 ± 1	0.009 ± 0.003	59 ± 6	53 ± 3
2	-0.08	-7 ± 2	16 ± 5	1.4 ± 0.5	1.4 ± 0.1
5	-0.27	12 ± 1	0.009 ± 0.003	59 ± 6	55 ± 2
3	-0.07	-7 ± 2	16 ± 5	0.9 ± 0.5	1.5 ± 0.3
6	-0.23	8 ± 1	0.04 ± 0.02	33 ± 6	31 ± 2
7	-0.16	1 ± 1	0.7 ± 0.3	4.5 ± 2.0	5.0 ± 0.5
9	-0.32	16 ± 1	0.0012 ± 0.0005	82 ± 4	84 ± 2
8	-0.16	0.5 ± 1	0.8 ± 0.3	3.8 ± 1.2	4.8 ± 0.5
10	-0.32	16 ± 1	0.0012 ± 0.0005	82 ± 4	76 ± 2
11	-0.16	1 ± 1	0.7 ± 0.3	4.5 ± 2.0	5 ± 2
13	-0.21	6 ± 1	0.09 ± 0.04	22 ± 5	16 ± 1
12	-0.18	3 ± 1	0.3 ± 0.1	9 ± 3	11 ± 1
14	-0.32	16 ± 1	0.0012 ± 0.0005	86 ± 4	91 ± 7

*Radicals.

[†]For the half-wave potential ($E_{1/2}$) the error is ± 0.01 .

[‡] $\Delta G = -nF \Delta E^{\circ} = -RT \ln(K)$.

concentrations of nitroxides that were calculated from the redox potentials. Comparison of the last two columns in Table I shows an excellent agreement between the equilibrium concentrations of the nitroxide radicals as measured by EPR spectroscopy and those calculated from the thermodynamic parameters. Thus, knowledge of the redox properties of radicals can be used to predict the equilibrium concentration with high precision, for their reduction with ascorbate anion.

Kinetics of the reduction of radicals in ascorbic acid solution

The large excess of ascorbate that was used for reduction of radicals ensured (pseudo) first-order kinetics and allowed fitting of the decay curve with a first-order exponential function: $[N] = [N]_{eq} + [N]_0 \times e^{-k't}$, where $[N]$ is the concentration of the radical at time t , $[N]_0$ is the initial concentration, and k' is the pseudo-first-order rate constant. $[N]_{eq}$ is a constant offset given by the thermodynamic equilibrium of nitroxide radicals under steady-state conditions. Dividing k' by the concentration of ascorbic acid yielded the bimolecular rate constants (Table II).

The calculated bimolecular rate constants confirmed that the rate of reduction depends on several factors: the size of the nitroxide ring system, the nature of the substituents, and shielding of the nitroxide moiety (Figure 2A and Supplementary Figure 1 to be found online at <http://informahealthcare.com/doi/abs/10.3109/10715762.2014.979409>). Replacing the methyl groups adjacent to the nitroxides with ethyl groups had the largest impact on radical stability, presumably by sterically restricting access

of reductants to the nitroxide [22,25]. The hyperfine coupling constants (A_{iso}) of the radicals were determined from their CW-EPR spectra (Supplementary Table I to be found online at <http://informahealthcare.com/doi/abs/10.3109/10715762.2014.979409>) and confirmed that the ethyl-derivatized nitroxides had a lower A_{iso} value than their corresponding methyl derivatives, as expected for a more hydrophobic environment. The steric effect was most pronounced in the case of the piperidine derivatives, where the tetraethyl-substituted nitroxides **4**, **5**, and **6** were found to be ca. 100 times more stable against reduction than the tetramethyl derivatives **1**, **2**, and **3**. These data are in agreement with the recently published study of Kajer et al. [57]. It has been shown that cyclohexyl or pyran groups do not further increase radical stability [22,58], making tetraethyl-derived nitroxide radicals good candidates for *in vivo* EPR.

Other substituents also affected stability of the radicals, although to a lesser extent than the alkyl groups adjacent to the nitroxides. Positively charged substituents decreased the stability of the radicals, presumably by attracting the ascorbate anion. For example, compound **3**, where the amino group is protonated at pH: 7, is threefold more reactive than compound **2**. The imidazolidine **13** was considerably less stable than the other tetraethyl derivatives, presumably due to protonation [44]. For the isoindoline derivatives, the effect of charge was not as pronounced, presumably because the charge is farther from the nitroxide functional group; the positively charged compound **8** is less than twofold more reactive than the negatively charged **7**, while no difference was observed for the tetraethyl-substituted compounds **9** and **10**.

Table II. Half-life of the radicals and their corresponding second-order reaction rate constant for reduction with ascorbic acid, and EPR signal intensities after incubation (2 h) with ascorbic acid in the cell extracts and inside oocyte cells.

Rad.*	Lifetime [s] [†]	2nd order rate const [(M·s) ⁻¹]	Extent of reduction [‡]		
			Asc. [§]	Cell extract	Oocyte cells
1	158 ± 1	5.75 ± 0.04	1	0	—
4	2600 ± 50	0.066 ± 0.001	57	75	34
2	165 ± 2	5.51 ± 0.005	1	0	—
5	2640 ± 60	0.058 ± 0.002	58	78	15
3	54 ± 2	16.8 ± 0.7	1	0	—
6	1480 ± 40	0.115 ± 0.003	31	65	66
7	365 ± 5	0.44 ± 0.01	5	0	—
9	1980 ± 50	0.079 ± 0.003	84	45	51
8	220 ± 3	0.74 ± 0.01	5	0	—
10	2350 ± 60	0.081 ± 0.001	78	52	55
11	100 ± 2	1.62 ± 0.04	5	0	—
13	1940 ± 30	0.084 ± 0.002	19	66	25
12	2160 ± 20	0.079 ± 0.001	14	38	—
14	85000 ± 30000	0.002 ± 0.001	94	94	88
15	10500 ± 1000	0.016 ± 0.002	74	60	70

*Radicals. The starting concentration of radicals was 200 mM and concentration of ascorbic acid was 5 mM, except for spin label **1–3** where it was 1 mM.

[†]Calculated as $t_{1/2} = 1/k'$.

[‡]listed as a percentage, after reaction time of 2 h.

[§]Ascorbic acid.

The largest effect on the nitroxide stability of the tetramethyl-substituted nitroxides was caused by the structure of the nitroxide-bearing ring. The five-membered pyrrolidine, imidazolidine, and isoindoline derivatives were three- to ten-fold more stable toward reduction than the six-membered piperidine derivatives [32]. Similar rates of reduction for compounds **7** and **12** indicate that the pyrrolidine and isoindoline rings have similar stability. The slowest reduction rate was found to be that for the negatively charged tetraethyl pyrrolidine derivative **14**.

Radical stability in cell extract

The rate of radical reduction was also investigated in cytoplasmic extracts of oocytes and as in the case of ascorbate reduction, all tetramethyl-substituted radicals were rapidly reduced in the cellular extract (Figure 2B and Supplementary Figure 2 to be found online at <http://informahealthcare.com/doi/abs/10.3109/10715762.2014.979409>). The EPR time traces (Figure 2B) did not follow a single exponential decay, presumably due to the presence of various reducing agents (ascorbate, glutathione, cysteine, nicotinamide adenine dinucleotide [NAD] hydrogen, and NAD phosphate hydrogen) and a significant amount of dissolved oxygen in the cell extract. Therefore, signal intensities after reaction time of 2 h were used for comparing the stability of the radicals in the cytosolic fluid. As seen from Figure 2B and Table II, the most resistant radical is the pyrrolidine derivative **14**, which was 95% intact after 2 h, followed by the tetraethyl piperidines **4** and **5** (75%), tetraethyl imidazolidine and tetraethyl piperidine **6** (65%), trityl (60%), and tetraethyl-isoindoline (50%). The different relative stabilities of isoindoline *versus* piperidine nitroxides in the cell extract, compared with ascorbate reduction, are presumably due to the presence of different reducing agents in the cell. In addition, different rates of re-oxidation of the corresponding hydroxylamines to nitroxides by oxidants in the cell extract, including molecular oxygen, could also be a contributing factor [59].

Radical stability inside cells

As stated above, the primary aim of this study was to compare, under identical experimental conditions, the stability of potential spin labels for investigation of biomolecules in living cells by pulsed EPR spectroscopy. Therefore, the ultimate test was their persistence in oocyte cells. Charged radicals **6**, **9**, **10**, **14**, and **15** gave reduction profiles that are very similar to those recorded in cell extracts (Table II), presumably because they were distributed in the cytosol which should yield reduction kinetics similar to that of cell extracts (see Supplementary Figures 2 and 3 to be found online at <http://informahealthcare.com/doi/abs/10.3109/10715762.2014.979409> for decay curves for all radicals in cytosolic extract and inside cells). In contrast, the reduction kinetics for non-charged radicals **4**, **5**, and **13** inside cells were much faster than in the cell extracts, e.g., only about 15% of **5** remained after 2 h. Radical **6**, containing the same ring size but

carrying a protonated amino group, retained 65% of the signal. A possible explanation for this discrepancy is that the non-charged radicals could have entered intracellular membranes and been reduced rapidly by the electron transport chain components in the mitochondrial membrane [60]. Pyrrolidine **14** was the most persistent radical, retaining more than 85% of the signal, with the trityl radical **15** following closely behind (70%).

Conclusions

In conclusion, introduction of bulky ethyl groups next to a nitroxide group leads to significant stabilization against reduction by both ascorbic acid and the reductants present in living cells, yielding radicals that are more stable in cells than trityl radical **15**. The tetraethyl-substituted pyrrolidine-based nitroxide carrying a carboxylic group (**14**) demonstrated superior stability against reduction due to combination of sterical shielding, ring size, and charge, all of which are factors that should be taken into account for the design of spin labels for *in vivo* studies. Charged and neutral radicals showed different relative stabilities in cell extracts than in cells, indicating that conjugation to biomolecules could have a large effect on the stability of these radicals. The trityl radical exhibited considerable stability toward reduction, especially in cells.

Acknowledgements

We thank Dr. S. Jonsdottir for assistance in collecting analytical data for structural characterization of compounds.

Declaration of interest

The authors report no conflicts of interest. The authors alone are responsible for the content and writing of the paper.

This work was supported by the Icelandic Research Fund (120001021), the Deutsche Forschungsgemeinschaft (SFB 902, Molecular principles of RNA-based regulation) and by a doctoral fellowship to A. P. Jagtap from the University of Iceland Research Fund.

References

- [1] Gesteland RF, Cech TR, Atkins JF. The RNA World: The Nature of Modern RNA Suggests a Prebiotic RNA, 3rd ed Cold Spring Harbor Laboratory Press, New York; 2006.
- [2] Holbrook SR. Structural principles from large RNAs. *Annu Rev Biophys* 2008;37:445–464.
- [3] Scott LG, Hennig M. RNA structure determination by NMR. *Methods Mol Biol* 2008;452:29–61.
- [4] Blanchard SC. Single-molecule observations of ribosome function. *Curr Opin Struc Biol* 2009;19:103–109.
- [5] Milov AD, Ponomarev AB, Tsvetkov YD. Electron Electron Double-Resonance in electron-spin echo-Model biradical systems and the sensitized photolysis of decalin. *Chem Phys Lett* 1984;110:67–72.

- [6] Schiemann O. Mapping global folds of oligonucleotides by Pulsed Electron-Electron Double Resonance. *Method Enzymol* 2009;469:329–351.
- [7] Sowa GZ, Qin PZ. Site-directed spin labeling studies on nucleic acid structure and dynamics. *Prog Nucleic Acid Res* 2008;82:147–197.
- [8] Schiemann O, Prisner TF. Long-range distance determinations in biomacromolecules by EPR spectroscopy. *Q Rev Biophys* 2007;40:1–53.
- [9] Jeschke G, Polyhach Y. Distance measurements on spin-labelled biomacromolecules by pulsed electron paramagnetic resonance. *Phys Chem Chem Phys* 2007;9:1895–1910.
- [10] Krstic I, Hansel R, Romainczyk O, Engels JW, Dotsch V, Prisner TF. Long-range distance measurements on nucleic acids in cells by pulsed EPR spectroscopy. *Angew Chem Int Ed Engl* 2011;50:5070–5074.
- [11] Azarkh M, Okle O, Singh V, Seemann IT, Hartig JS, Dietrich DR, Drescher M. Long-range distance determination in a DNA model system inside *Xenopus laevis* oocytes by in-cell spin-label EPR. *ChemBiochem* 2011;12:1992–1995.
- [12] Igarashi R, Sakai T, Hara H, Tenno T, Tanaka T, Tochio H, Shirakawa M. Distance determination in proteins inside *xenopus laevis* oocytes by double electron-electron resonance experiments. *J Am Chem Soc* 2010;132:8228–9229.
- [13] Azarkh M, Singh V, Okle O, Seemann IT, Dietrich DR, Hartig JS, Drescher M. Site-directed spin-labeling of nucleotides and the use of in-cell EPR to determine long-range distances in a biologically relevant environment. *Nat Protoc* 2013;8:131–147.
- [14] Zhelev Z, Bakalova R, Aoki I, Matsumoto KI, Gadjeva V, Anzai K, Kanno I. Nitroxyl radicals as low toxic spin-labels for non-invasive magnetic resonance imaging of blood-brain barrier permeability for conventional therapeutics. *Chem Commun* 2009;53–55.
- [15] Soule BP, Hyodo F, Matsumoto K-I, Simone NL, Cook JA, Krishna MC, Mitchell JB. The chemistry and biology of nitroxide compounds. *Free Radical Biol Med* 2007;42:1632–1650.
- [16] Zhelev Z, Matsumoto KI, Gadjeva V, Bakalova R, Aoki I, Zhelev A, Anzai K. EPR signal reduction kinetic of several nitroxyl derivatives in blood in vitro and in vivo. *Gen Physiol Biophys* 2009;28:356–362.
- [17] Rajca A, Wang Y, Boska M, Paletta JT, Olankitwanit A, Swanson MA, et al. Organic radical contrast agents for magnetic resonance imaging. *J Am Chem Soc* 2012;134:15724–15727.
- [18] Samuni A, Goldstein S, Russo A, Mitchell JB, Krishna MC, Neta P. Kinetics and mechanism of hydroxyl radical and OH-adduct radical reactions with nitroxides and with their hydroxylamines. *J Am Chem Soc* 2002;124:8719–8724.
- [19] Israeli A, Patt M, Oron M, Samuni A, Kohen R, Goldstein S. Kinetics and mechanism of the comproportionation reaction between oxoammonium cation and hydroxylamine derived from cyclic nitroxides. *Free Radical Biol Med* 2005;38:317–324.
- [20] Swartz HM, Clarkson RB. The measurement of oxygen in vivo using EPR techniques. *Phys Med Biol* 1998;43:1957–1975.
- [21] Khramtsov VV, Grigor'ev IA, Foster MA, Lurie DJ, Nicholson I. Biological applications of spin pH probes. *Cell Mol Biol* 2000;46:1361–1374.
- [22] Bobko AA, Kirilyuk IA, Grigor'ev IA, Zweier JL, Khramtsov VV. Reversible reduction of nitroxides to hydroxylamines: roles for ascorbate and glutathione. *Free Radical Biol Med* 2007;42:404–412.
- [23] Sakai K, Yamada K, Yamasaki T, Kinoshita Y, Mito F, Utsumi H. Effective 2,6-substitution of piperidine nitroxyl radical by carbonyl compound. *Tetrahedron* 2010;66:2311–2315.
- [24] Ma ZK, Huang QT, Bobbitt JM. Oxoammonium salts .5¹ A new synthesis of hindered piperidines leading to unsymmetrical tempo-type nitroxides - synthesis and enantioselective oxidations with chiral nitroxides and chiral oxoammonium salts. *J Org Chem* 1993;58:4837–4843.
- [25] Marx L, Chiarelli R, Guiberteau T, Rassat A. A comparative study of the reduction by ascorbate of 1,1,3,3-tetraethylisoin-dolin-2-yloxy and of 1,1,3,3-tetramethylisoin-dolin-2-yloxy. *J Chem Soc Perk Trans* 12000;(8):1181–1182.
- [26] Belkin S, Mehlhorn RJ, Hideg K, Hankovsky O, Packer L. Reduction and destruction rates of nitroxide spin probes. *Arch Biochem Biophys* 1987;256:232–243.
- [27] Couet WR, Eriksson UG, Tozer TN, Tuck LD, Wesbey GE, Nitecki D, Brasch RC. Pharmacokinetics and metabolic-fate of two nitroxides potentially useful as contrast agents for magnetic-resonance imaging. *Pharm Res* 1984;1:203–209.
- [28] Yelinova V, Krainev A, Savelov A, Grigor'ev I. Comparative-study of the reduction rates of various types of imidazoline radicals in tissues. *J Chem Soc Perk Trans* 2 1993;(11):2053–2055.
- [29] Sentjurs M, Pecar S, Chen K, Wu M, Swartz H. Cellular-metabolism of proxyl nitroxides and hydroxylamines. *Biochim Biophys Acta* 1991;1073:329–335.
- [30] Eriksson UG, Tozer TN, Sosnovsky G, Lukszó J, Brasch RC. Human-erythrocyte membrane-permeability and nitroxyl spin-label reduction. *J Pharm Sci* 1986;75:334–337.
- [31] Couet WR, Brasch RC, Sosnovsky G, Lukszó J, Prakash I, Gnewuch CT, Tozer TN. Influence of chemical-structure of nitroxyl spin labels on their reduction by ascorbic-acid. *Tetrahedron* 1985;41:1165–1172.
- [32] Morris S, Sosnovsky G, Hui B, Huber CO, Rao NUM, Swartz HM. Chemical and electrochemical reduction rates of cyclic nitroxides (nitroxyls). *J Pharm Sci* 1991;80:149–152.
- [33] Brasch RC, McNamara MT, Ehman RL, Couet WR, Tozer TN, Sosnovsky G, et al. Influence of chemical-structure on nitroxyl spin label magnetic-relaxation characteristics. *Eur J Med Chem* 1989;24:335–340.
- [34] Nothiglaslo V, Bobst AM. Reinvestigation of the oxidation properties of nitroxides. *Croat Chem Acta* 1991;64:1–8.
- [35] Blinco JP, Hodgson JL, Morrow BJ, Walker JR, Will GD, Coote ML, Bottle SE. Experimental and theoretical studies of the redox potentials of cyclic nitroxides. *J Org Chem* 2008;73:6763–6771.
- [36] Kavala M, Boca R, Dihan L, Brezova V, Breza M, Kozisek J, et al. Preparation and spectroscopic, magnetic and electrochemical studies of mono-/biradical TEMPO derivatives. *J Org Chem* 2013;78:6558–6569.
- [37] Kinoshita Y, Yamada K, Yamasaki T, Mito F, Yamato M, Kosem N, et al. In vivo evaluation of novel nitroxyl radicals with reduction stability. *Free Radical Biol Med* 2010;49:1703–1709.
- [38] Fuchs J, Freisleben HJ, Podda M, Zimmer G, Milbradt R, Packer L. Nitroxide radical biostability in skin. *Free Radical Biol Med* 1993;15:415–423.
- [39] Quintanilha AT, Packer L. Surface localization of sites of reduction of nitroxide spin-labeled molecules in mitochondria. *Proc Natl Acad Sci USA* 1977;74:570–574.
- [40] Okazaki S, Mannan MA, Sawai K, Masumizu T, Miura Y, Takeshita K. Enzymatic reduction-resistant nitroxyl spin probes with spirocyclohexyl rings. *Free Radical Res* 2007;41:1069–1077.
- [41] Azarkh M, Okle O, Eyring P, Dietrich DR, Drescher M. Evaluation of spin labels for in-cell EPR by analysis of nitroxide reduction in cell extract of *Xenopus laevis* oocytes. *J Magn Reson* 2011;212:450–454.
- [42] Bobko AA, Dhimitruka I, Zweier JL, Khramtsov VV. Trityl radicals as persistent dual function pH and oxygen probes for in vivo electron paramagnetic resonance spectroscopy and imaging: concept and experiment. *J Am Chem Soc* 2007;129:7240–7241.

- [43] Siegenthaler KO, Schafer A, Studer A. Chemical surface modification via radical C-C bond-forming reactions. *J Am Chem Soc* 2007;129:5826–5827.
- [44] Kirilyuk IA, Bobko AA, Grigor'ev IA, Khramtsov VV. Synthesis of the tetraethyl substituted pH-sensitive nitroxides of imidazole series with enhanced stability towards reduction. *Org Biomol Chem* 2004;2:1025–1030.
- [45] Volodarsky LB, Reznikov VA, Grigor'ev IA. Chemical properties of heterocyclic nitroxides. In: Volodarsky LB (ed.). *Imidazoline Nitroxides, Volume 1*. Boca Raton, Florida: CRC Press; 1988. pp. 5–23.
- [46] Paletta JT, Pink M, Foley B, Rajca S, Rajca A. Synthesis and reduction kinetics of sterically shielded pyrrolidine nitroxides. *Org Lett* 2012;14:5322–5325.
- [47] Liu Y, Villamena FA, Sun J, Xu Y, Dhimitruka I, Zweier JL. Synthesis and characterization of ester-derivatized tetrathiatri-arylmethyl radicals as intracellular oxygen probes. *J Org Chem* 2008;73:1490–1497.
- [48] Reid DA, Bottle SE, Micallef AS. The synthesis of water soluble isoindoline nitroxides and a pronitroxide hydroxylamine hydrochloride UV-VIS probe for free radicals. *Chem Commun* 1998:1907–1908.
- [49] Miller TR, Hopkins PB. Toward the synthesis of a 2nd-generation nitroxide spin-probe for DNA dynamics studies. *Bioorg Med Chem Lett* 1994;4:981–986.
- [50] Mileo E, Etienne E, Martinho M, Lebrun R, Roubaud V, Tordo P, et al. Enlarging the panoply of site-directed spin labeling electron paramagnetic resonance (SDSL-EPR): sensitive and selective spin-labeling of tyrosine using an isoindoline-based nitroxide. *Bioconjugate Chem* 2013;24:1110–1117.
- [51] Huang WL, Charleux B, Chiarelli R, Marx L, Rassat A, Vairon JP. Synthesis of water-soluble nitroxides and their use as mediators in aqueous-phase controlled radical polymerization. *Macromol Chem Phys* 2002;203:1715–1723.
- [52] Belton PS, Sutcliffe LH, Gillies DG, Wu XP, Smirnov AI. A new water-soluble and lipid-insoluble spin probe: application to the study of aqueous sucrose solutions. *Magn Reson Chem* 1999;37:36–42.
- [53] Vianello F, Momo F, Scarpa M, Rigo A. Kinetics of nitroxide spin-label removal in biological-systems - an in-vitro and in-vivo ESR study. *Magn Reson Imaging* 1995;13:219–226.
- [54] Keana JFW, Pou S, Rosen GM. Nitroxides as potential contrast enhancing agents for MRI application: influence of structure on the rate of reduction by rat hepatocytes, whole liver homogenate, subcellular-fractions, and ascorbate. *Magnet Reson Med* 1987;5:525–536.
- [55] Levine M, Padayatty SJ, Espey MG. Vitamin C: a concentration-function approach yields pharmacology and therapeutic discoveries. *Adv Nutr* 2011;2:78–88.
- [56] Loach PA. *Handbook of Biochemistry and Molecular Biology*. CRC Press Inc, Cleveland, Ohio; 1976. pp. 122–130.
- [57] Kajer TB, Fairfull-Smith KE, Yamasaki T, Yamada K, Fu SL, Bottle SE, et al. Inhibition of myeloperoxidase- and neutrophil-mediated oxidant production by tetraethyl and tetramethyl nitroxides. *Free Radical Biol Med* 2014;70:96–105.
- [58] Kinoshita Y, Yamada KI, Yamasaki T, Sadasue H, Sakai K, Utsumi H. Development of novel nitroxyl radicals for controlling reactivity with ascorbic acid. *Free Radical Res* 2009;43:565–571.
- [59] Morrow BJ, Keddie DJ, Gueven N, Lavin MF, Bottle SE. A novel profluorescent nitroxide as a sensitive probe for the cellular redox environment. *Free Radical Biol Med* 2010;49:67–76.
- [60] Quintanilha AT, Packer L. Surface localization of sites of reduction of nitroxide spin-labeled molecules in mitochondria. *Proc Natl Acad Sci USA* 1977;74:570–574.

Supplementary material available online

Supplementary Figures 1–4 and Table I.

Sterically shielded spin labels for in-cell EPR spectroscopy: Analysis of stability in reducing environment

Anil P. Jagtap¹, Ivan Krstic², Nitin C. Kunjir¹, Robert Hänsel³, Thomas F. Prisner², Snorri Th. Sigurdsson^{*1}

¹University of Iceland, Department of Chemistry, Science Institute, Dunhagi 3, 107 Reykjavik, Iceland.

²Institute of Physical and Theoretical Chemistry, Goethe University Frankfurt, Max-von-Laue-Str. 7, Frankfurt, Germany.

³Institute of Biophysical Chemistry and Center for Biomolecular Magnetic Resonance, Goethe University, Frankfurt/Main, Germany.

Supporting information

Table of contents

1. Reduction of spin labels under different conditions.....	S2
1.1. Figure S1 : Decay of EPR signal for radicals in ascorbic acid	S2
1.2. Figure S2 : Decay of EPR signal for radicals in cell extract.....	S3
1.2. Figure S3 : Decay of EPR signal for radicals inside oocyte cells.....	S4
2. Figure S4 : Cyclic voltammetry of spin labels.....	S5
3. Table S1 : Hyperfine coupling constants of spin labels.....	S6

1. Reduction of spin labels under different conditions

1.1 Decay of EPR signal intensities in ascorbic acid

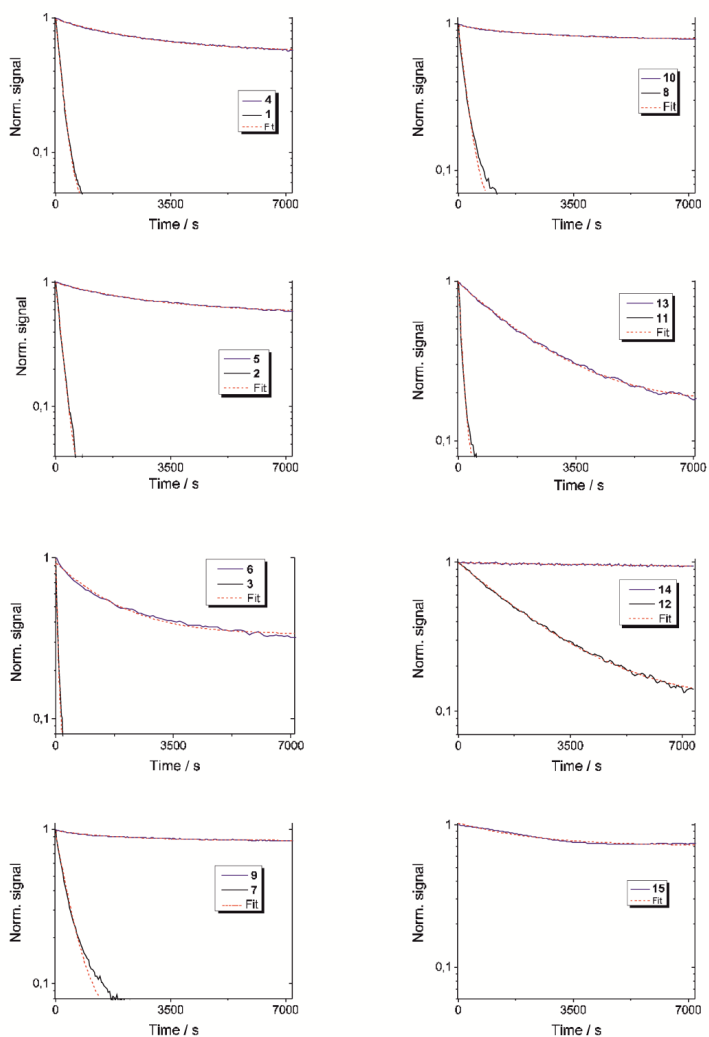


Fig. S1. Decay of EPR signal for radicals in 5 mM ascorbic acid solution, for compounds 1-3 the concentration of ascorbic acid was 1 mM. The fits are shown as a red dotted line.

1.2 Decay of EPR signal in cell extract

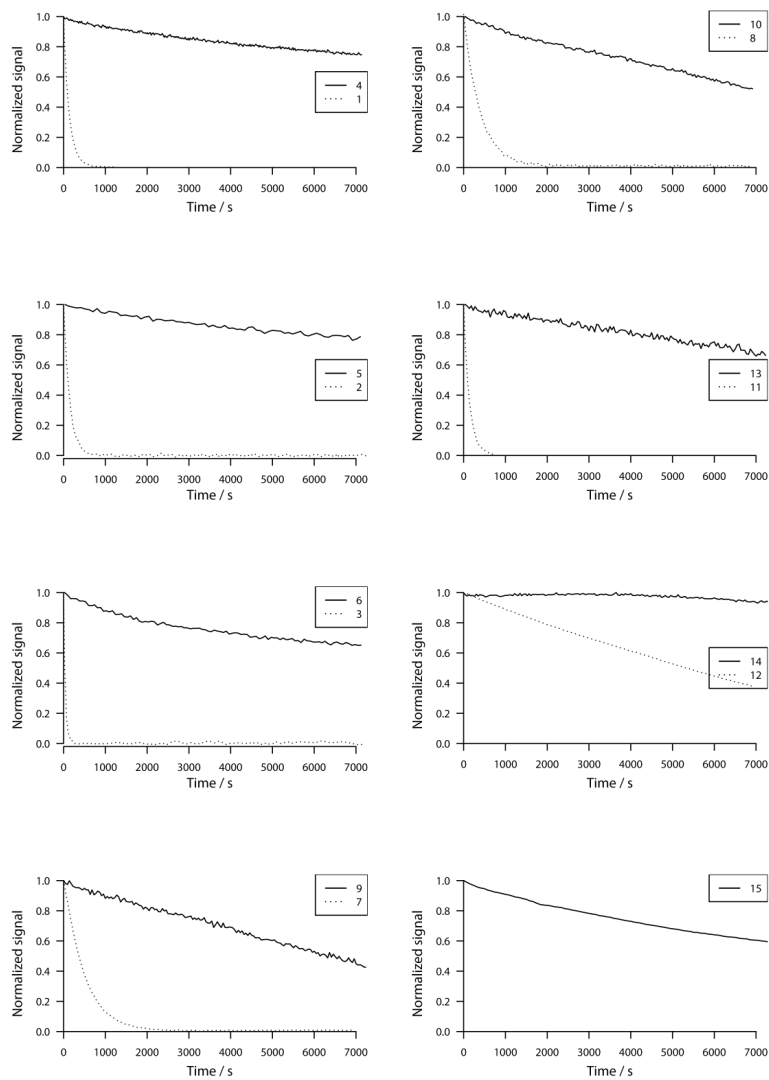
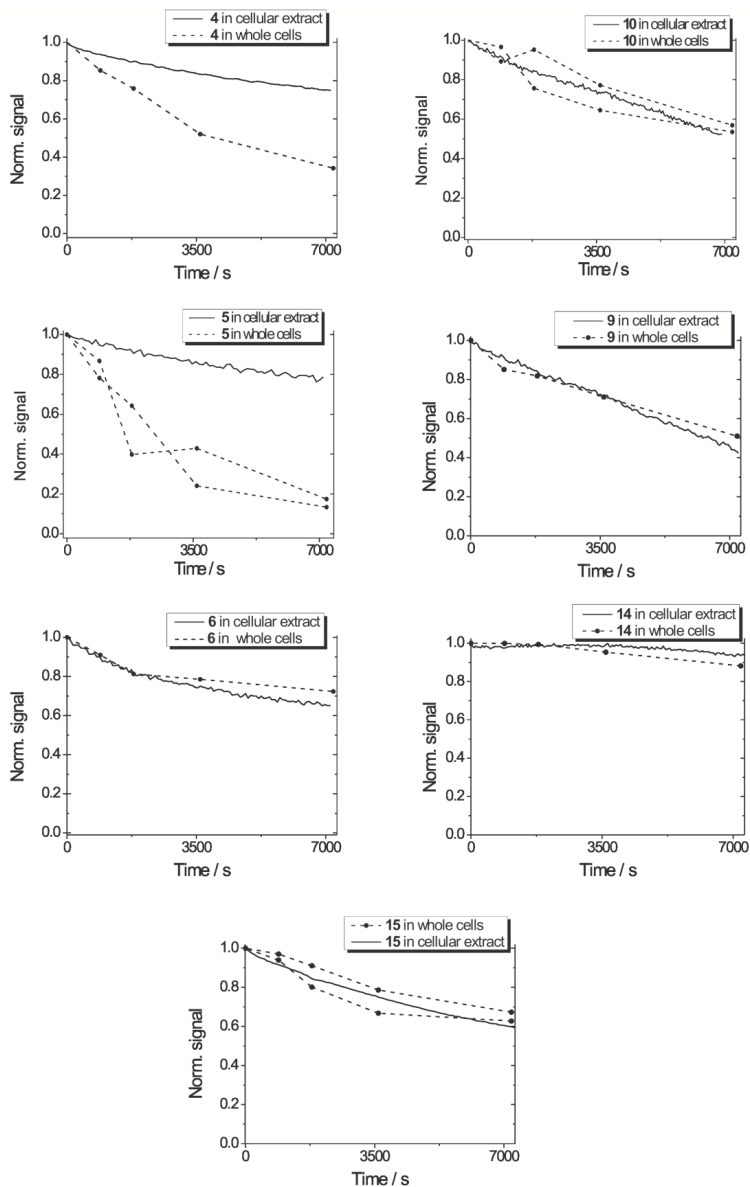


Fig. S2. Decay of EPR signal intensities for radicals in cell extract.

1.3 Decay of EPR signal intensities for radicals inside oocyte cells**Fig. S3.** Decay of EPR signal intensities for radicals inside oocyte cells.

2. Cyclic voltammetry of spin labels

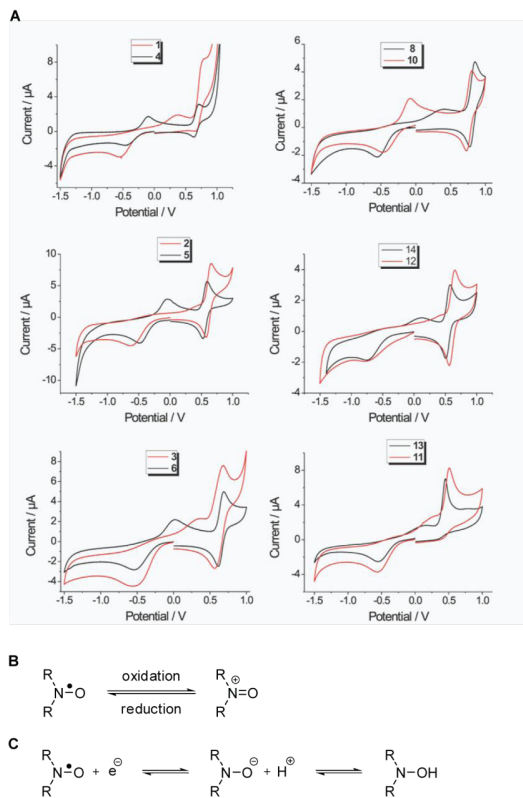


Fig. S4. (A) Cyclic voltammograms for nitroxide radicals. (B) Oxidation of the nitroxide to an oxoammonium cation. (C) Reduction of a nitroxide to a hydroxylamine *via* formation of a hydroxylamine anion.

3. Measurements of hyperfine coupling constants

Table S1. Hyperfine coupling constants of spin labels

Nitroxide	A_{iso}^* [mT]	Nitroxide	A_{iso}^* [mT]
2	1.71	7	1.60
5	1.62	9	1.55
1	1.61	11	1.60
4	1.55	13	1.54
3	1.70	12	1.63
6	1.60	14	1.57
8	1.59		
10	1.54		

*Error is 0.01 mT

**Article II. SDSL of 2'-amino groups in RNA
with isoindoline nitroxides...**

**Site-directed spin labeling of 2'-amino groups in
RNA with isoindoline nitroxides that are resistant
to reduction**

Chem. Commun. **2015**, *51*, 13142-13145.



ChemComm

COMMUNICATION

View Article Online
View Journal | View IssueCite this: *Chem. Commun.*, 2015, 51, 13142Received 17th June 2015,
Accepted 8th July 2015

DOI: 10.1039/c5cc05014f

www.rsc.org/chemcomm

Site-directed spin labeling of 2'-amino groups in RNA with isoindoline nitroxides that are resistant to reduction†

Subham Saha,‡ Anil P. Jagtap‡ and Snorri Th. Sigurdsson*

Two aromatic isothiocyanates, derived from isoindoline nitroxides, were synthesized and selectively reacted with 2'-amino groups in RNA. The spin labels displayed limited mobility in RNA, making them promising candidates for distance measurements by pulsed EPR. After conjugation to RNA, a tetraethyl isoindoline derivative showed significant stability under reducing conditions.

Electron paramagnetic resonance (EPR) spectroscopy is a biophysical technique that is routinely applied for the study of the structure and dynamics of nucleic acids in order to gain insights into their mechanism of action.¹ Structural information is usually derived from distance measurements, in particular using pulsed techniques, such as pulsed electron-electron double resonance (PELDOR),² also known as double electron-electron resonance (DEER). Information about dynamics can be derived from line-shape analysis of continuous wave (CW) EPR spectra,³ from the width of distance distributions⁴ and by analysis of orientation-dependent PELDOR measurements.^{1d,5}

Most EPR studies of nucleic acids require incorporation of paramagnetic reporter groups at specific sites, a technique referred to as site-directed spin labeling (SDSL).^{1a,e,6} Aminoxy radicals, usually called nitroxides, are common spin labels that can be attached to the desired site in the nucleic acid of interest with a covalent bond, although there are examples of noncovalent labeling.⁷ Two main approaches have been used for covalent spin-labeling of nucleic acids.⁸ The phosphoramidite method utilizes spin-labeled phosphoramidites as building blocks for automated chemical synthesis of the spin-labeled oligonucleotide.⁹ This strategy usually involves significant synthetic effort¹⁰ and the spin label is exposed to reagents used in nucleic acid synthesis that can partially reduce the nitroxide.¹¹ The other covalent SDSL approach involves a post-synthetic modification of the nucleic acid, wherein

a spin-labeling reagent reacts with a specific reactive functional group within the nucleic acid.¹² Post-synthetic spin-labeling usually requires less effort than the classical phosphoramidite approach and can often be performed with commercially available reagents.

Post-synthetic modification of 2'-amino groups in RNA is an efficient method for site-directed spin labeling of oligonucleotides.¹³ 2'-Amino-modified RNAs are commercially available or can alternately be prepared using commercially available phosphoramidites. This 2'-labeling method has been used to incorporate the paramagnetic 2'-ureido-TEMPO [(2,2,6,6-tetramethylpiperidin-1-yl)oxyl] at specific sites by reaction of 2'-amino groups with 4-isocyanato-TEMPO.^{12c} However, isocyanates are relatively reactive and, therefore, prone to hydrolysis and can react with other functional groups of the nucleic acid.¹⁴ Thus, special care is required while handling this reagent and when carrying out the spin-labeling reaction.^{13b} In addition, incomplete labeling has been observed for some long RNAs, presumably due to the formation of secondary structures under the spin-labeling conditions (−8 °C), which may slow down the spin-labeling reaction relative to the competing hydrolysis of the isocyanate. Therefore, it is of interest to find more suitable reagents to react with 2'-amino groups in oligonucleotides, which would make this spin-labeling strategy even more useful.

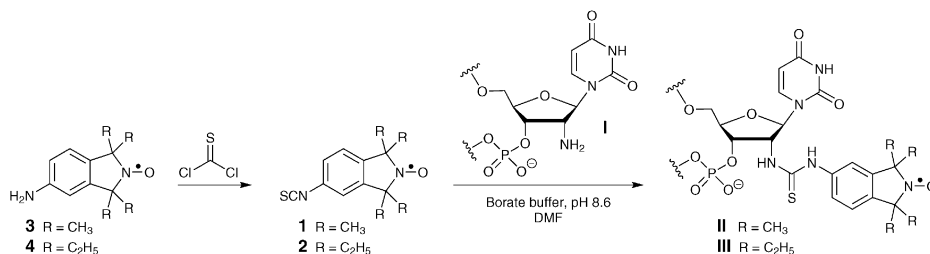
This report describes the spin-labeling of 2'-amino groups in RNA using isoindoline-derived aromatic isothiocyanates. Aromatic isothiocyanates are more stable than isocyanates and yet reactive enough to modify 2'-amino groups in RNA.¹⁵ We show here that the isothiocyanate spin labels react very efficiently with 2'-amino uridine in RNA, forming a stable thiourea linkage. Moreover, the spin-labeling reactions were carried out at 37 °C in the presence of a denaturing agent (DMF), which minimizes the formation of secondary structures that might reduce the efficiency of 2'-amino labeling.

Two spin-labeling reagents were prepared, isothiocyanates **1** and **2** (Scheme 1), in a single step using readily accessible starting materials. When isoindolines are utilized for spin-labeling, tetramethyl derivatives are normally used,^{10b,c,16} but isoindoline **2** was included because tetraethyl derivatives have

University of Iceland, Department of Chemistry, Science Institute, Dunhaga 3, 107 Reykjavik, Iceland. E-mail: snorrissi@hi.is

† Electronic supplementary information (ESI) available. See DOI: 10.1039/c5cc05014f

‡ These authors contributed equally to this work.



Scheme 1 Preparation of spin-labeling reagents **1** and **2** and their reaction with the 2'-amino modified RNA oligonucleotide **I** [5'-GAC CUC G(2'-NH₂U)A UCG UG] to yield spin-labeled oligonucleotides **II** and **III**.

been shown to be more resistant towards reduction.¹⁷ 1,1,3,3-Tetramethylisoidolin-5-amine-2-oxyl (**3**)^{17b,18} and its corresponding tetraethyl derivative (**4**)^{17b} were treated with thiophosgene to obtain the isothiocyanate spin-labeling reagents **1** and **2** in 82% and 57% yields, respectively (Scheme 1). Unlike 4-isocyanato-TEMPO, aromatic isothiocyanates **1** and **2** were found to be stable solids and did not require special precautions when prepared or handled.

Spin-labeling reagents **1** and **2** were reacted with the 2'-amino-modified RNA oligonucleotide 5'-GAC CUC G(2'-NH₂U)A UCG UG (**I**) at 37 °C, in borate buffer (pH 8.6) containing 50% DMF. Samples were removed at specific intervals of time and analyzed by denaturing polyacrylamide gel electrophoresis (DPAGE) analysis (Fig. 1). A new product was formed in each reaction that migrated slower than the parent oligonucleotide, thus indicating successful covalent attachment of the spin labels to the RNA. Tetramethyl-derivative **1** reacted faster than **2**; the former fully converted RNA **I** within 4 h and the latter in 8 h, to the corresponding spin-labeled derivatives. Selective reaction at the 2'-amino group was verified by the lack of reaction between **1** and an unmodified RNA, even after heating at 60 °C for 48 h (Fig. S3, ESI†).

The spin-labeled oligonucleotides **II** and **III** were purified by DPAGE to give **II** and **III** in ca. 75–80% yields. It is noteworthy that ethanol precipitation of RNA **II** gave material of the same purity, as judged by EPR and DPAGE, (Page S7, ESI†), making it a very rapid spin-labeling method. MALDI-TOF analysis of the oligonucleotides showed the mass expected for the spin-labeled oligomers (Fig. S4, ESI†). Circular dichroism (CD) spectroscopy

of the corresponding spin-labeled RNA duplexes **IV** and **V** showed negative and positive molar ellipticities at ca. 210 nm and 262–264 nm, respectively (Fig. S5, ESI†), values that are characteristic of A-form RNA duplexes.¹⁹ The thermodynamic stabilities of the spin-labeled RNA duplexes were determined by thermal denaturation (*T*_M) experiments (Table S3 and Fig. S6, ESI†). Only minor destabilization of 1.2 °C and 2.0 °C were observed for the tetramethyl- and the tetraethyl-derivative, respectively, relative to an unmodified duplex. The corresponding TEMPO-labeled RNA duplex **VII**, prepared by reaction of 4-isocyanato-TEMPO with oligonucleotide **I**,^{13b} was considerably less stable ($\Delta T_M = -5.3$ °C).

The EPR spectra of **II** and **III** (Fig. 2) show broadening of the EPR spectral lines relative to spin labels **1** and **2** (Fig. S1 and S2, ESI†), which is consistent with their covalent attachment to the RNA. The EPR spectra of single stranded oligonucleotides **II** and **III** were also compared with the corresponding TEMPO-derived oligonucleotide **VI**, which had a noticeably narrower spectrum. The narrow spectrum of **VI** presumably reflects in part the inherent flexibility of TEMPO, in which the six-membered ring can sample different conformations. The EPR spectra of the corresponding RNA duplexes (Fig. 2, **IV**, **V**, **VII**) were considerably broader than for

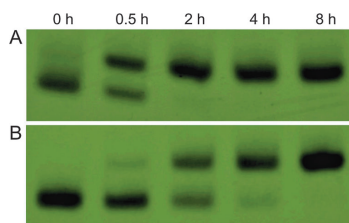


Fig. 1 A time-course of the spin-labeling reactions between the 2'-amino oligonucleotide **I** and the aromatic isothiocyanates **1** (A) and **2** (B). Reaction conditions: 1 mM RNA, 50 mM **1**, 50 mM borate buffer (pH 8.6), 50% DMF.

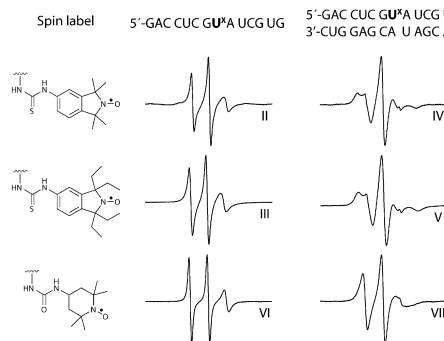


Fig. 2 EPR spectra of the spin-labeled oligonucleotides at 10 °C (10 mM phosphate, 100 mM NaCl, 0.1 mM Na₂EDTA, pH 7.0). U* indicates the position of the spin-labeled uridine and roman numerals under the spectra identify the oligonucleotides (see Table S1, ESI†).

ChemComm

View Article Online

Communication

the single strand and again, the EPR spectra of the isoindoline-derived duplexes (**IV** and **V**) were broader than that of the TEMPO-modified duplex (**VII**). It was somewhat surprising to see how broad the spectra for isoindoline nitroxide-labeled duplexes **IV** and **V** were, with both the high- and low-field peaks splitting at 10 °C (see Fig. S7, ESI† for other temperatures), given the fact that rotation is possible around bonds in the linker. Since the thiourea can be regarded as a stiff tether, flexibility is restricted to rotation between two single bonds, namely the one connecting the 2'-C and the 2'-N as well as the bond between the urea and the isoindoline. Molecular modeling (Fig. 3) showed that there is only one low-energy rotamer for the C-N bond, in which the large sulfur atom is lodged between two oxygen atoms on the spin-labeled nucleotide: the 3'-oxygen and the oxygen of the tetrahydrofuran ring, resulting in a snug fit for the sulfur atom. Otherwise, the label is projected away from the nucleic acid; the limited mobility indicates that there is restricted rotation around the bond connecting the isoindoline to the urea, as might be expected because of conjugation.

In-cell EPR spectroscopy has emerged as a promising technique to study nucleic acids *in vivo*.²⁰ Pyrrolidine- and piperidine-based nitroxides have very limited stabilities in reductive environments²¹ and are thus considered to be ineffective spin labels for in-cell EPR studies. On the other hand, isoindolines have shown higher stability towards reduction, especially tetraethyl derivatives.¹⁷ The stabilities of the spin-labeled duplexes **IV**, **V** and **VII** were tested in the presence of ascorbic acid, which is a known cellular reducing agent and often used to evaluate the stability of nitroxides.^{17b,21a,22} Fig. 4 shows a normalized EPR signal as a function of time. There was a striking difference in the stability of the different spin labels: the TEMPO label was fully reduced within 10 min and the tetraethyl isoindoline within an hour, while ca. 90% of the tetraethyl isoindoline label still remained intact after 10 h (Fig. 4, inset). It is

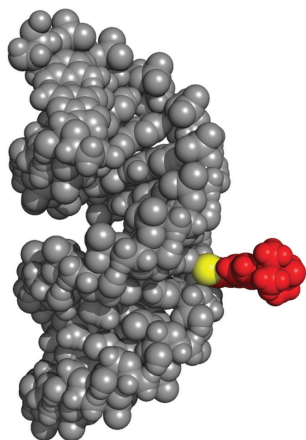


Fig. 3 A space-filling molecular model of spin-labeled oligonucleotide duplex **IV**. The RNA constituents are shown in grey and covalently attached spin label **1** in red, except for the sulfur (yellow) in the thiourea linker.

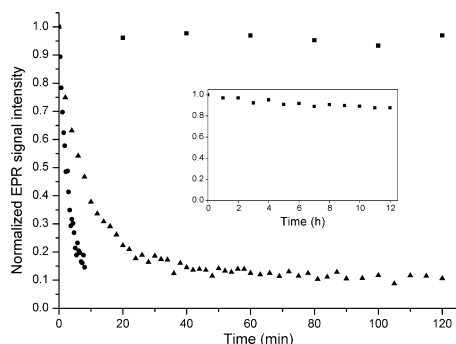


Fig. 4 Stabilities of the spin-labeled RNA duplexes **IV** (triangle), **V** (square) and **VII** (circle) towards reduction (5 mM ascorbic acid, 10 mM phosphate, 100 mM NaCl, 0.1 mM Na₂EDTA, pH 7.0). Inset shows a longer time course (12 h) for duplex **V**.

also noteworthy that the stabilities of the nitroxide radicals were slightly higher after being conjugated to the RNA oligonucleotides. For example, under identical conditions, 5% of simple tetraethyl isoindoline derivatives remained after 2 h,^{17b} while 12% of RNA duplex **IV** (Fig. S9, ESI†) still had an intact spin label. Taken together, these ascorbate experiments indicate that the tetraethyl derivative is a promising spin label for in-cell EPR studies. However, a more detailed study of spin-label stability under cellular conditions, where other reducing agents (e.g. glutathione) are present, will be conducted and reported in due course.

In summary, we have described an efficient method for post-synthetic spin-labeling of 2'-amino groups with aromatic isothiocyanates using two new isoindoline-derived spin labels. This divergent synthetic approach can be used for a variety of isoindoline spin labels and has three major advantages over the previously described 2'-TEMPO derivative. First, the new spin labels have only a minor effect on the thermal stability of RNA duplexes. Second, the isoindoline labels have limited mobility independent of the nucleic acid duplex to which they are attached, which should make them useful for distance measurements. Third, the tetraethyl isoindoline conjugated to RNA exhibits high stability towards reduction, making it a promising candidate for in-cell EPR studies. This spin-labeling strategy should also be useful for spin-labeling long RNAs, either through direct derivatization of 2'-amino groups or by ligation of oligonucleotides containing the tetraethyl spin label, which is carried out in the presence of a reducing agent.

This work was supported by the Icelandic Research Fund (141062-051). S. S. and A. P. J. gratefully acknowledge doctoral fellowships provided by the University of Iceland. The authors thank Dr S. Jonsdottir for assistance with collecting analytical data for structural characterization of compounds prepared and members of the Sigurdsson research group for critical reading of the manuscript.

References

- (a) G. Z. Sowa and P. Z. Qin, *Prog. Nucleic Acid Res. Mol. Biol.*, 2008, **82**, 147–197; (b) O. Schiemann, *Methods Enzymol.*, 2009, **469**,

- 329–351; (c) P. Nguyen and P. Z. Qin, *Wiley Interdiscip. Rev.: RNA*, 2012, **3**, 62–72; (d) T. F. Prisner, A. Marko and S. T. Sigurdsson, *J. Magn. Reson.*, 2015, **252**, 187–198; (e) Y. Ding, P. Nguyen, N. S. Tangprasertchai, C. V. Reyes, X. Zhang and P. Z. Qin, *Electron Paramagnetic Resonance*, The Royal Society of Chemistry, 2015, vol. 24, pp. 122–147.
- 2 (a) A. Milov, K. Salikhov and M. Shirov, *Sov. Phys. Solid State*, 1981, **23**, 565–569; (b) O. Schiemann, A. Weber, T. E. Edwards, T. F. Prisner and S. T. Sigurdsson, *J. Am. Chem. Soc.*, 2003, **125**, 3434–3435; (c) O. Schiemann and T. F. Prisner, *Q. Rev. Biophys.*, 2007, **40**, 1–53.
- 3 X. J. Zhang, P. Cekan, S. T. Sigurdsson and P. Z. Qin, *Methods Enzymol.*, 2009, **469**, 303–328.
- 4 (a) A. D. Milov, Y. D. Tsvetkov, F. Formaggio, S. Oancea, C. Toniolo and J. Raap, *J. Phys. Chem. B*, 2003, **107**, 13719–13727; (b) N. A. Kuznetsov, A. D. Milov, V. V. Koval, R. I. Samoilova, Y. A. Grishin, D. G. Khorre, Y. D. Tsvetkov, O. S. Fedorova and S. A. Dzuba, *Phys. Chem. Chem. Phys.*, 2009, **11**, 6826–6832; (c) G. Y. Shevlev, O. A. Krumkacheva, A. A. Lomzov, A. A. Kuzhelev, D. V. Trukhin, O. Y. Rogozhnikova, V. M. Tormyshev, D. V. Pyshnyi, M. V. Fedin and E. G. Bagryanskaya, *J. Phys. Chem. B*, 2015, DOI: 10.1021/acs.jpcc.5b03026, ahead of print.
- 5 A. Marko, V. Denysenkov, D. Margraft, P. Cekan, O. Schiemann, S. T. Sigurdsson and T. F. Prisner, *J. Am. Chem. Soc.*, 2011, **133**, 13375–13379.
- 6 (a) S. Shelke and S. T. Sigurdsson, in *Structural Information from Spin-Labels and Intrinsic Paramagnetic Centres in the Biosciences*, ed. C. R. Timmel and J. R. Harmer, Springer, Berlin, Heidelberg, 2013, vol. 152, ch. 62, pp. 121–162; (b) G. W. Reginsson and O. Schiemann, *Encyclopedia of Biophysics*, Springer, 2013, pp. 2429–2431.
- 7 (a) P. Belmont, C. Chapelle, M. Demeunynck, J. Michon, P. Michon and J. Lhomme, *Bioorg. Med. Chem. Lett.*, 1998, **8**, 669–674; (b) K. Maekawa, S. Nakazawa, H. Atsumi, D. Shiomi, K. Sato, M. Kitagawa, T. Takui and K. Nakatani, *Chem. Commun.*, 2010, **46**, 1247–1249; (c) S. A. Shelke and S. T. Sigurdsson, *Angew. Chem., Int. Ed.*, 2010, **49**, 7984–7986; (d) S. A. Shelke, G. B. Sandholt and S. T. Sigurdsson, *Org. Biomol. Chem.*, 2014, **12**, 7366–7374; (e) B. A. Chalmers, S. Saha, T. Nguyen, J. McMurtrie, S. T. Sigurdsson, S. E. Bottle and K. S. Masters, *Org. Lett.*, 2014, **16**, 5528–5531.
- 8 S. A. Shelke and S. T. Sigurdsson, *Eur. J. Org. Chem.*, 2012, 2291–2301.
- 9 A. Spaltenstein, B. H. Robinson and P. B. Hopkins, *J. Am. Chem. Soc.*, 1988, **110**, 1299–1301.
- 10 (a) T. R. Miller, S. C. Alley, A. W. Reese, M. S. Solomon, W. V. McCallister, C. Mailer, B. H. Robinson and P. B. Hopkins, *J. Am. Chem. Soc.*, 1995, **117**, 9377–9378; (b) N. Barhate, P. Cekan, A. P. Massey and S. T. Sigurdsson, *Angew. Chem., Int. Ed.*, 2007, **46**, 2655–2658; (c) D. B. Gophane and S. T. Sigurdsson, *Chem. Commun.*, 2013, **49**, 999–1001.
- 11 (a) N. Piton, Y. Mu, G. Stock, T. F. Prisner, O. Schiemann and J. W. Engels, *Nucleic Acids Res.*, 2007, **35**, 3128–3143; (b) P. Cekan, A. L. Smith, N. Barhate, B. H. Robinson and S. T. Sigurdsson, *Nucleic Acids Res.*, 2008, **36**, 5946–5954.
- 12 (a) H. Hara, T. Horiuchi, M. Saneyoshi and S. Nishimura, *Biochem. Biophys. Res. Commun.*, 1970, **38**, 305–311; (b) P. Z. Qin, S. E. Butcher, J. Feigon and W. L. Hubbell, *Biochemistry*, 2001, **40**, 6929–6936; (c) T. E. Edwards, T. M. Okonogi, B. H. Robinson and S. T. Sigurdsson, *J. Am. Chem. Soc.*, 2001, **123**, 1527–1528; (d) P. Z. Qin, K. Hideg, J. Feigon and W. L. Hubbell, *Biochemistry*, 2003, **42**, 6772–6783; (e) P. Z. Qin, I. S. Haworth, Q. Cai, A. K. Kusnetzow, G. P. G. Grant, E. A. Price, G. Z. Sowa, A. Popova, B. Herreros and H. He, *Nat. Protoc.*, 2007, **2**, 2354–2365; (f) G. P. G. Grant and P. Z. Qin, *Nucleic Acids Res.*, 2007, **35**, e77; (g) P. Ding, D. Wunnicke, H. J. Steinhoff and F. Seela, *Chem. – Eur. J.*, 2010, **16**, 14385–14396; (h) U. Jakobsen, S. A. Shelke, S. Vogel and S. T. Sigurdsson, *J. Am. Chem. Soc.*, 2010, **132**, 10424–10428.
- 13 (a) N. K. Kim, A. Murali and V. J. DeRose, *Chem. Biol.*, 2004, **11**, 939–948; (b) T. E. Edwards and S. T. Sigurdsson, *Nat. Protoc.*, 2007, **2**, 1954–1962.
- 14 S. T. Sigurdsson and F. Eckstein, *Nucleic Acids Res.*, 1996, **24**, 3129–3133.
- 15 (a) H. Aurrup, T. Tuschl, F. Benseler, J. Ludwig and F. Eckstein, *Nucleic Acids Res.*, 1994, **22**, 20–24; (b) S. T. Sigurdsson, T. Tuschl and F. Eckstein, *RNA*, 1995, **1**, 575–583.
- 16 D. B. Gophane, B. Endeward, T. F. Prisner and S. T. Sigurdsson, *Chem. – Eur. J.*, 2014, **20**, 15913–15919.
- 17 (a) L. Marx, R. Chiarelli, T. Guiberteau and A. Rassat, *J. Chem. Soc., Perkin Trans. 1*, 2000, 1181–1182; (b) A. P. Jagtap, I. Krstić, N. C. Kunjir, R. Hänsel, T. F. Prisner and S. T. Sigurdsson, *Free Radical Res.*, 2015, **49**, 78–85.
- 18 (a) D. A. Reid, S. E. Bottle and A. S. Micallef, *Chem. Commun.*, 1998, 1907–1908; (b) E. Mileo, E. Etienne, M. Martinho, R. Lebrun, V. Roubaud, P. Tordo, B. Gontero, B. Guigliarelli, S. R. A. Marque and V. Belle, *Bioconjugate Chem.*, 2013, **24**, 1110–1117.
- 19 H. T. Steely, D. M. Gray, D. Lang and M. F. Maestre, *Biopolymers*, 1986, **25**, 91–117.
- 20 (a) I. Krstić, R. Hänsel, O. Romainczyk, J. W. Engels, V. Dötsch and T. F. Prisner, *Angew. Chem., Int. Ed.*, 2011, **50**, 5070–5074; (b) M. Azarkh, O. Okle, V. Singh, I. T. Seemann, J. S. Hartig, D. R. Dietrich and M. Drescher, *ChemBioChem*, 2011, **12**, 1992–1995; (c) I. T. Holder, M. Drescher and J. S. Hartig, *Bioorg. Med. Chem.*, 2013, **21**, 6156–6161; (d) M. Azarkh, V. Singh, O. Okle, I. T. Seemann, D. R. Dietrich, J. S. Hartig and M. Drescher, *Nat. Protoc.*, 2013, **8**, 131–147; (e) M. Qi, A. Groß, G. Jeschke, A. Godt and M. Drescher, *J. Am. Chem. Soc.*, 2014, **136**, 15366–15378; (f) R. Hänsel, L. M. Luh, I. Corbeski, L. Trantirek and V. Dötsch, *Angew. Chem., Int. Ed.*, 2014, **53**, 10300–10314.
- 21 (a) W. R. Couet, R. C. Brasch, G. Sosnovsky, J. Lukszo, I. Prakash, C. T. Gnewuch and T. N. Tozer, *Tetrahedron*, 1985, **41**, 1165–1172; (b) J. P. Blinco, J. L. Hodgson, B. J. Morrow, J. R. Walker, G. D. Will, M. L. Coote and S. E. Bottle, *J. Org. Chem.*, 2008, **73**, 6763–6771; (c) M. Azarkh, O. Okle, P. Eyring, D. R. Dietrich and M. Drescher, *J. Magn. Reson.*, 2011, **212**, 450–454; (d) T. B. Kajer, K. E. Fairfull-Smith, T. Yamasaki, K. Yamada, S. Fu, S. E. Bottle, C. L. Hawkins and M. J. Davies, *Free Radical Biol. Med.*, 2014, **70**, 96–105.
- 22 (a) Y. Kinoshita, K. Yamada, T. Yamasaki, H. Sadasue, K. Sakai and H. Utsumi, *Free Radical Res.*, 2009, **43**, 565–571; (b) Y. Kinoshita, K. Yamada, T. Yamasaki, F. Mito, M. Yamato, N. Kosem, H. Deguchi, C. Shirahama, Y. Ito, K. Kitagawa, N. Okukado, K. Sakai and H. Utsumi, *Free Radical Biol. Med.*, 2010, **49**, 1703–1709.

Site-directed spin-labeling of 2'-amino groups in RNA with isoindoline nitroxides that are resistant to reduction

Subham Saha[†], Anil P. Jagtap[†] and Snorri Th. Sigurdsson*

University of Iceland, Department of Chemistry, Science Institute, Dunhaga 3, 107 Reykjavik, Iceland. E-mail: snorrisi@hi.is

[†] These authors contributed equally to this work

Table of contents

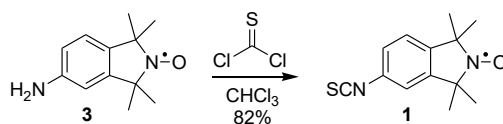
List of abbreviations	S2
Synthetic procedures	S2
General materials and methods	S2
1,1,3,3-Tetramethylisoindolin-5-isothiocyanate-2-oxyl (1).....	S3
1,1,3,3-Tetraethylisoindolin-5-isothiocyanate-2-oxyl (2).....	S4
RNA synthesis and purification	S5
General procedure for RNA spin-labeling with 1 and 2	S7
Investigating if reaction of 1 with RNA results in non-specific labeling.....	S8
Analyses of spin-labeled oligonucleotides.....	S9
Instruments and methods.....	S9
MALDI-TOF analyses	S10
Circular dichroism (CD) spectra	S11
Thermal denaturation experiments.....	S12
Electron paramagnetic resonance (EPR) spectra	S13
Molecular modeling.....	S14
Stability of spin-labeled RNAs towards ascorbate reduction	S15
References.....	S16

List of abbreviations

DPAGE	Denaturing polyacrylamide gel electrophoresis
EPR	Electron paramagnetic resonance
DMF	<i>N,N</i> -Dimethylformamide
MALDI-TOF	Matrix-assisted laser desorption/ionization - time of flight
HR-ESI-MS	High-resolution electrospray ionization mass spectrometry
TLC	Thin layer chromatography
IR	Infrared spectroscopy
CD	Circular dichroism
TBDMS	<i>tert</i> -butyldimethylsilyl
UV	Ultraviolet
CW	Continuous wave
MMFF	Merck Molecular Force Field

Synthetic procedures**General materials and methods**

All reagents and CHCl_3 , used as a solvent for reactions, were purchased from Sigma Aldrich and used without further purification. Water was purified on a MILLI-Q water purification system. TLC was carried out using glass plates pre-coated with silica gel (0.25 mm, F-254) from Silicycle, Canada. All synthesized compounds were visualized by UV light. Flash column chromatography was performed using ultra pure flash silica gel (Silicycle, 230-400 mesh size, 60 Å). All moisture and air-sensitive reactions were carried out in oven-dried glassware under an inert argon atmosphere. Nitroxide radicals show broadening and loss of NMR signals due to their paramagnetic nature,^{1, 2} and therefore, the NMR data for the isoindoline spin labels have not been shown. Mass spectrometric analyses of all organic compounds were performed on an HR-ESI-MS (Bruker, MicrOTOF-Q) in a positive ion mode.

**1,1,3,3-Tetramethylisoindolin-5-isothiocyanate-2-oxyl (1)**

A solution of thiophosgene (0.041 mL, 0.54 mmol) in CHCl_3 (1 mL) was added dropwise to a solution of 1,1,3,3-tetramethylisoindolin-5-amine-2-oxyl³ (**3**) (0.100 g, 0.49 mmol) in CHCl_3 (3.5 mL). The reaction mixture was stirred at 24 °C for 2 h, diluted with CH_2Cl_2 (5 mL) and the organic layer was washed successively with NaOH solution (4 mL, 1 M), water (2 x 5 mL) and brine (5 mL). The organic layer was dried over anhydrous Na_2SO_4 , filtered and concentrated *in vacuo* to obtain the crude product, which was purified by flash column chromatography (silica) using a gradient elution (EtOAc:pet. ether; 0:100 to 5:95) to give **1** (0.098 g, 82%) as a yellowish solid.

TLC: (Silica gel, 20% EtOAc in pet. ether), R_f (**3**) = 0.2, R_f (**1**) = 0.5.

EPR: Compound **1** shows characteristic EPR triplet of a nitroxide radical (**Fig. S1**).

HRMS: Calculated for $\text{C}_{13}\text{H}_{15}\text{N}_2\text{OS}$: 247.09, found 270.0802 ($\text{M}+\text{Na}^+$).

IR: Shows the characteristic isothiocyanato (-NCS) stretching frequency at 2120 cm^{-1} .

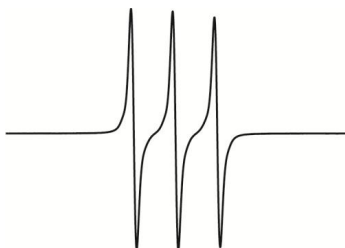
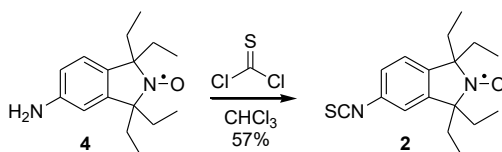


Fig. S1. EPR spectrum of 1,1,3,3-tetramethylisoindolin-5-isothiocyanate-2-oxyl (**1**) recorded in EtOH at 25 °C.

**1,1,3,3-Tetraethylisindolin-5-isothiocyanate-2-oxyl (2)**

A solution of thiophosgene (0.032 mL, 0.42 mmol) in CHCl₃ (1 mL) was added dropwise to a solution of 1,1,3,3-tetraethylisindolin-5-amine-2-oxyl³ (**4**) (0.100 g, 0.38 mmol) in CHCl₃ (3.5 mL). The reaction mixture was stirred at 24 °C for 2 h, diluted with CH₂Cl₂ (5 mL) and the organic layer was washed successively with NaOH solution (4 mL, 1 M), water (2 x 5 mL) and brine (5 mL). The organic layer was dried over anhydrous Na₂SO₄, filtered and concentrated *in vacuo* to obtain the crude product, which was purified by flash column chromatography (silica) using a gradient elution (EtOAc:pet. ether; 0:100 to 5:95) to give 1,1,3,3-tetraethylisindolin-5-isothiocyanate-2-oxyl (**2**) (0.066 g, 57%) as a yellowish solid.

TLC: (Silica gel, 20% EtOAc in pet. ether), R_f (**4**) = 0.2, R_f (**2**) = 0.8.

EPR: Compound **2** shows characteristic EPR triplet of a nitroxide radical (**Fig. S2**).

HRMS: Calculated for C₁₇H₂₃N₂OS: 303.15, found 326.1426 (M+Na⁺).

IR: Shows the characteristic isothiocyanato (-NCS) stretching frequency at 2120 cm⁻¹.

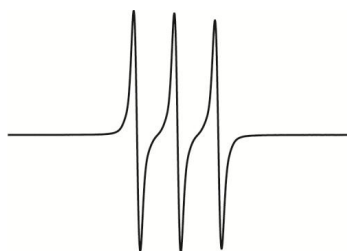
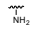
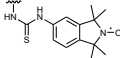
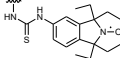
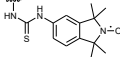
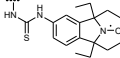
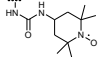
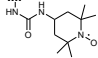
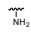


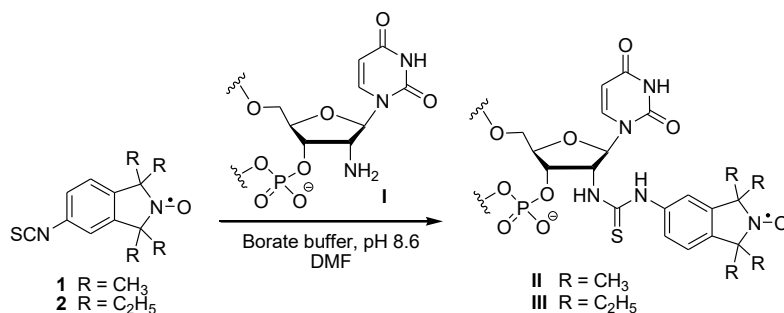
Fig. S2. EPR spectrum of 1,1,3,3-tetraethylisindolin-5-isothiocyanate-2-oxyl (**2**) recorded in EtOH at 25 °C.

RNA synthesis and purification

All unmodified RNA oligonucleotides and 2'-amino uridine-modified oligonucleotide **I** were synthesized in-house on an automated ASM800 DNA synthesizer (BIOSSET Ltd., Russia) using phosphoramidite chemistry. All phosphoramidites, the activator 5-benzylthiotetrazole, acetonitrile for oligomer synthesis and controlled pore glass (CPG) columns (1000 Å) were purchased from ChemGenes Corp., USA. All other reagents and solvents were purchased from Sigma-Aldrich Co. Syntheses were performed on a 1 µmol scale by trityl-off synthesis. After completion of RNA synthesis, the oligonucleotides were deprotected and cleaved from the resin by adding a 1:1 solution (2 mL) of CH₃NH₂ (8 M in EtOH) and NH₃ (33% w/w in H₂O) and heating for 40 min at 65 °C. The solvent was removed *in vacuo* and the TBDMS-protection groups were removed by incubation in NEt₃:3HF (600 µL) for 90 min at 55 °C in DMF (200 µL), followed by addition of water (200 µL). The resulting solution was transferred into a 50 mL Falcon tube and the RNA was precipitated by adding 1-butanol (20 mL, 12 h at -80 °C). All oligonucleotides were subsequently purified by 20% DPAGE and extracted from the gel slices using the “crush and soak method” with Tris buffer containing 250 mM NaCl, 10 mM Tris, 1 mM Na₂EDTA, pH 7.5. The solutions were filtered through 0.45 µm, 25 mm diameter GD/X syringe filters (Whatman, USA) and were subsequently desalted using Sep-Pak cartridges (Waters, USA), following the instructions provided by the manufacturer. Dried oligonucleotides were dissolved in sterilized and deionized water (200 µL for each oligonucleotide). Concentrations of the oligonucleotides were determined by UV absorbance at 260 nm using a Perkin Elmer Inc. Lambda 25 UV/Vis spectrometer and calculated by Beer's law. Isocyanato-TEMPO-modified RNA oligonucleotide **VI** was prepared following a previously reported procedure.⁴ **Table S1** shows the complete list of all the modified and unmodified RNA oligonucleotides along with the structure of the modifications.

Table S1. List of all RNA oligonucleotides.

Modification (U ^X)	RNA	Sequence
	I	5'-GAC CUC G (2'-NH ₂ U) A UCG UG-3'
	II	5'-GAC CUC GU ^X A UCG UG-3'
	III	5'-GAC CUC GU ^X A UCG UG-3'
	IV	5'-GAC CUC GU ^X A UCG UG-3' 3'-CUG GAG CA U AGC AC-5'
	V	5'-GAC CUC GU ^X A UCG UG-3' 3'-CUG GAG CA U AGC AC-5'
	VI	5'-GAC CUC GU ^X A UCG UG-3'
	VII	5'-GAC CUC GU ^X A UCG UG-3' 3'-CUG GAG CA U AGC AC-5'
	VIII	5'-GAC CUC G (2'-NH ₂ U) A UCG UG-3' 3'-CUG GAG C A U AGC AC-5'
-	IX	5'-GAC CUC GUA UCG UG-3'
-	X	5'-GAC CUC GUA UCG UG-3' 3'-CUG GAG CAU AGC AC-5'



General procedure for RNA spin-labeling with **1** and **2**

A solution of RNA oligonucleotide **I** (40 nmol) in 100 mM borate buffer, pH 8.6 (20 μ L) was added to a solution of **1** or **2** (2 μ mol) in DMF (20 μ L). The reaction mixture was heated at 37 $^{\circ}$ C for 8 h, followed by addition of sterile water (200 μ L) and extraction with EtOAc (6 x 500 μ L) to remove any unreacted spin label. For RNA **II**, an EtOH precipitation was performed [5 μ L of 3M sodium acetate (pH 4.6), 300 μ L of cold (-20 $^{\circ}$ C) absolute ethanol and storing at -80 $^{\circ}$ C for 4 h] to remove the rest of the free-spin contaminant. RNA **II** obtained by precipitation was of similar purity (as judged by EPR and DPAGE), as observed for **II** that was purified further by 20% DPAGE, to obtain 32 nmol of RNA oligonucleotide **II** (76%). DPAGE purification of RNA oligonucleotide **III** yielded 34 nmol (80%) after the EtOAc extraction.

Investigating if reaction of **1 with RNA results in non-specific labeling**

To test the selectivity of the spin labeling strategy, a solution of RNA oligonucleotide **IX** (40 nmol) in borate buffer (20 μ L, 100 mM, pH 8.6) was added to a solution of **1** (2 μ mol) in DMF (20 μ L) and heated at 60 $^{\circ}$ C. Aliquots were collected at specific time points (described in **Table S2**) and analyzed by DPAGE (**Fig. S3**). No change was observed in the mobility of the unmodified oligonucleotide, even after heating for 48 h (**Fig. S3**, lane D), proving that the spin labeling procedure is highly specific to 2'-amino groups in RNA. Spin-labeled RNA **II** was used as a marker for modified RNA.

Table S2. Table describing the control reactions (showed in **Fig. S7**).

Lane	RNA	Temperature	Duration
A	5' -GAC CUC GUA UCG UG	---	0 h
B	5' -GAC CUC GUA UCG UG	60 $^{\circ}$ C	12 h
C	5' -GAC CUC GUA UCG UG	60 $^{\circ}$ C	24 h
D	5' -GAC CUC GUA UCG UG	60 $^{\circ}$ C	48 h

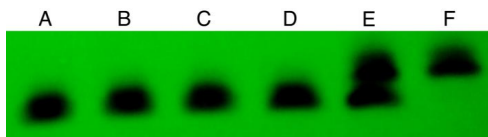


Fig. S3. DPAGE analysis of reaction of **1** and **I**. Lanes A-D are described in **Table S2**, Lane F contains spin-labeled RNA **II** and lane E is an equimolar mixture of lanes D and F.

Analyses of spin-labeled oligonucleotides

Instruments and methods

MALDI-TOF analyses of the RNA oligonucleotides were performed on a Bruker Daltonics Autoflex III. The instrument was calibrated with external standards prior to measuring the mass of the spin-labeled oligonucleotides and 3-hydroxypicolinic acid was used as the matrix. Prior to analysis by CD, thermal denaturation and EPR, an appropriate quantity of each RNA stock solution was dried on a Thermo Scientific ISS 110 Speedvac and dissolved in phosphate buffer (10 mM phosphate, 100 mM NaCl, 0.1 mM Na₂EDTA, pH 7.0). RNA duplexes were formed by annealing in an MJ Research PTC 200 Thermal Cycler using the following protocol: 90 °C for 2 min, 60 °C for 5 min, 50 °C for 5 min, 40 °C for 5 min and 22 °C for 15 min. CD spectra of RNA duplexes were recorded in a Jasco J-810 spectropolarimeter. Cuvettes with 1 mm path length were used and the CD data were recorded from 350 nm to 200 nm at 25 °C. Thermal denaturation curves of the oligonucleotides were obtained using a Perkin Elmer PTP-1 and PCB 150 Water Peltier System. Prior to recording T_M data, the samples were diluted to 1.0 mL with phosphate buffer, making the final concentration 3 µM and degassed using argon. The samples were heated up from 10 °C to 90 °C (1.0 °C/min) while recording the absorbance at 260 nm. EPR spectroscopy was performed to judge the mobilities of the spin-labeled oligonucleotides and measured over a range of temperatures from 30 °C to -10 °C, with intervals of 10 °C on an X-band EPR spectrometer (Miniscope MS 200, Magnettech, Germany) with 100 kHz modulation frequency, 1.0 G modulation amplitude and 2.0 mW microwave power and using 60 to 100 scans for each sample after placing them into a quartz capillary tube (BLAUBRAND®-intraMARK). The temperature was regulated by a Magnettech temperature controller M01.

MALDI-TOF analyses

To verify incorporation of the spin labels into the oligonucleotides, they were analyzed by MALDI-TOF experiments. **Fig. S4** shows the MALDI-TOF spectra of spin-labeled oligonucleotides **II** (5'-GAC CUC GU¹A UCG UG-3') (4667.121, calcd. 4666.711) and **III** (5'-GAC CUC GU²A UCG UG-3') (4722.435, calcd. 4722.771).

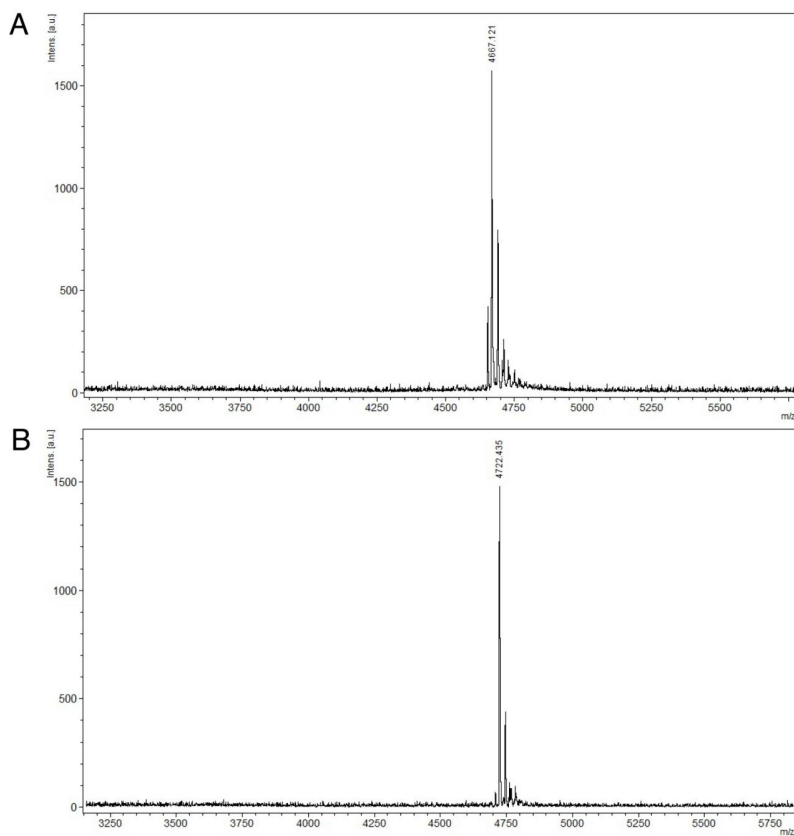


Fig. S4. MALDI-TOF spectra of spin-labeled oligonucleotides **II** (A) and **III** (B).

Circular dichroism (CD) spectra

CD spectra were recorded to determine if modifications on the oligonucleotides altered the RNA duplex conformation. **Fig. S5** shows the CD spectra of RNA duplexes **IV**, **V**, **VIII** and **X**. All the RNA duplexes showed negative and positive molar ellipticities at ca. 210 nm and 262-264 nm, respectively.

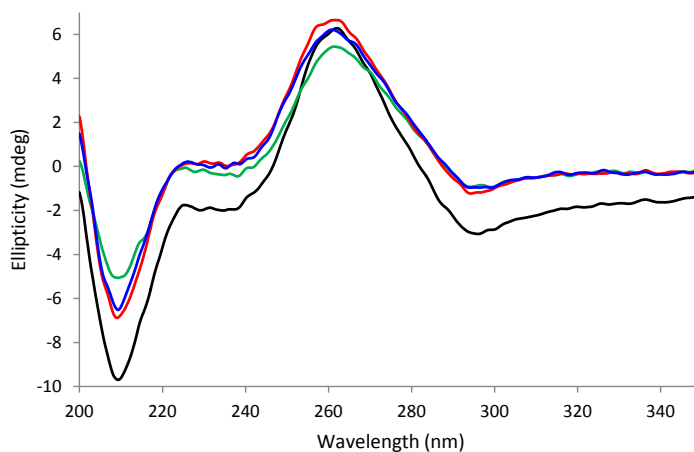


Fig. S5. CD spectra of 14-mer RNA duplex **IV** (red), **V** (blue), **VIII** (green) and **X** (black) (12.5 μ M each) recorded at 25 $^{\circ}$ C in phosphate buffer (10 mM phosphate, 100 mM NaCl, 0.1 mM Na₂EDTA, pH 7.0).

Thermal denaturation experiments

To investigate if the spin labels affect RNA duplex stability, thermal denaturation experiments were performed. **Fig. S6** shows representative melting curves for RNA duplexes, showing cooperative melting transitions. The T_M values were determined from the first derivatives of the melting curves and summarized in **Table S3**.

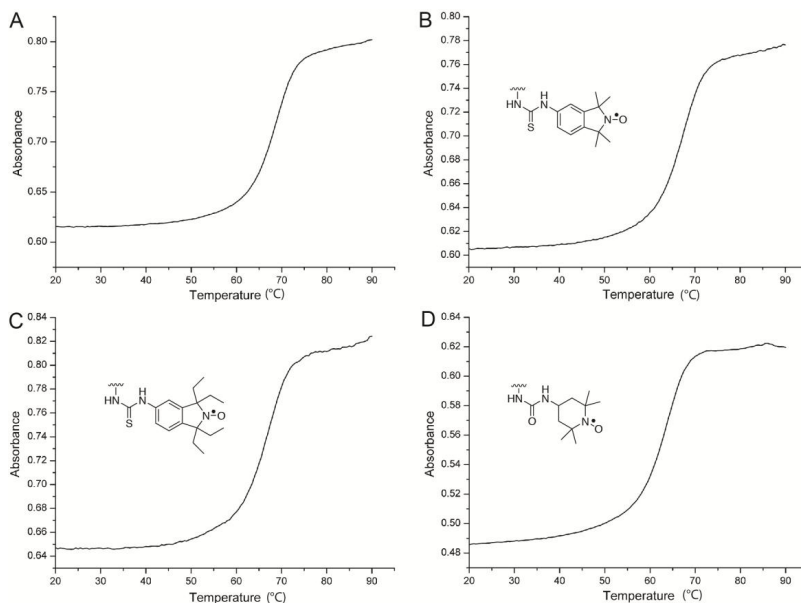


Fig. S6. Thermal denaturation curves of unmodified duplex X (A), as well as spin-labeled duplexes IV (B), V (C) and VII (D).

Table S3. Melting temperatures (T_M) of the RNA duplexes.

Modification	RNA	Duplex sequences	T_M (°C)	ΔT_M (°C)
–	X	5'–GAC CUC GUA UCG UG–3' 3'–CUG GAG CAU AGC AC–5'	68.5 ± 0.5	–
	VIII	5'–GAC CUC G(2'–NH ₂ U)A UCG UG–3' 3'–CUG GAG C A U AGC AC–5'	66.3 ± 0.5	–2.2
	IV	5'–GAC CUC GU ^X A UCG UG–3' 3'–CUG GAG CA U AGC AC–5'	67.3 ± 0.7	–1.2
	V	5'–GAC CUC GU ^X A UCG UG–3' 3'–CUG GAG CA U AGC AC–5'	66.5 ± 0.9	–2.0
	VII	5'–GAC CUC GU ^X A UCG UG–3' 3'–CUG GAG CA U AGC AC–5'	63.2 ± 0.5	–5.3

Electron paramagnetic resonance (EPR) spectra

Fig. S7 shows EPR spectra of single strands (A) and duplexes (B) at different temperatures. As expected, the spectra become broader upon cooling. Furthermore, the spectral width for duplexes **IV** and **V** were significantly wider than for the single-stranded counterparts, indicating that duplex formation severely restricted the mobility of the spin labels. Therefore, molecular modeling was performed on the spin-labeled duplexes (See **Page S14**).

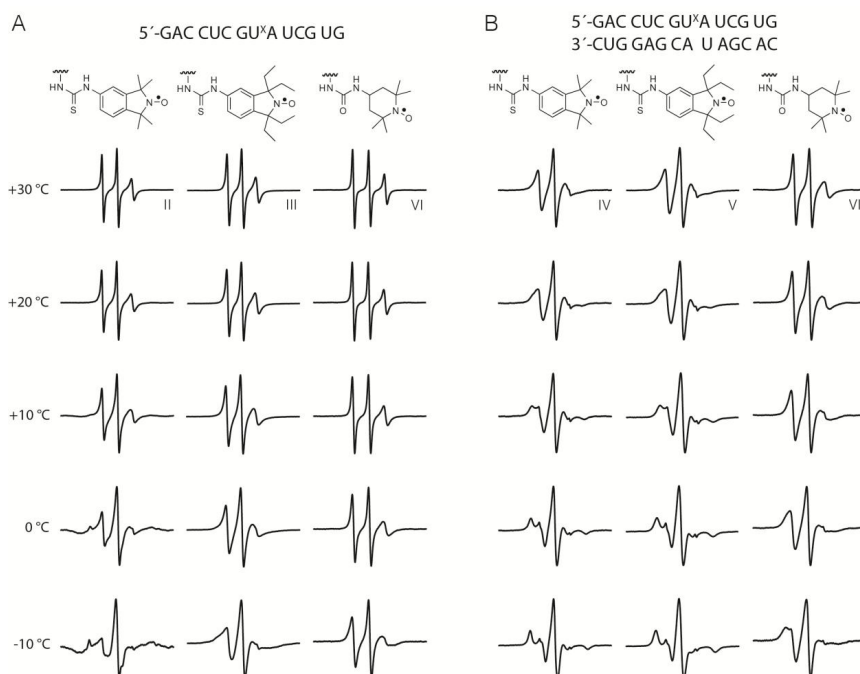


Fig. S7. CW EPR data of spin-labeled RNA single strands **II**, **III**, **VI** (A) and duplexes **IV**, **V** and **VII** (B) plotted as a function of decreased temperature. All spectra were phase corrected and aligned with respect to the central peak.

Molecular modeling

A molecular model for an RNA duplex was generated in Spartan'10 using the “nucleotide” constructing feature and the spin label was constructed using the “organic” construction tool. Energy of the spin label was minimized using the minimizer built into Spartan, which is based on the MMFF force field. The spin label was then connected to the desired position in the RNA using the “make bond” tool. **Fig. S8A** shows the resulting structure as obtained from PyMOL, in a space-filling display. The sulfur atom (yellow) nestled snugly between two oxygen atoms of the spin-labeled nucleotide, the 3'-oxygen and the oxygen within the corresponding ribose sugar ring (**Fig. S8B-C**), restricting its motion.

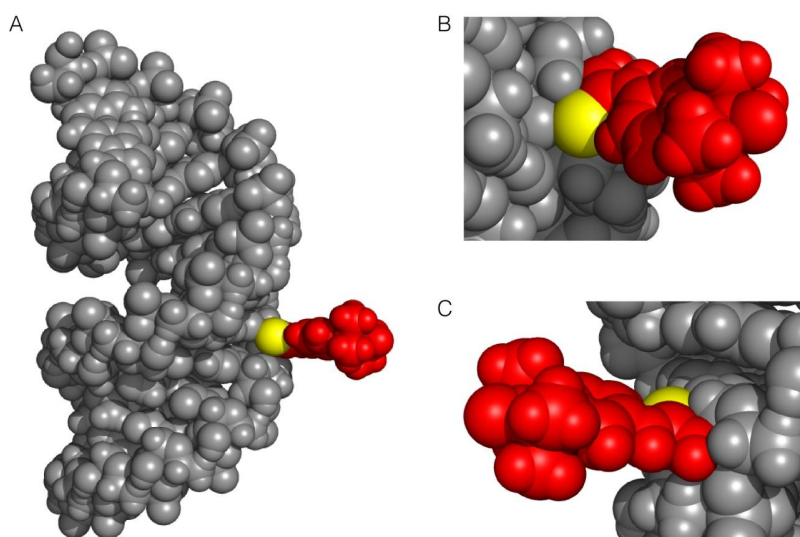


Fig. S8. Molecular model of the RNA duplex **IV** (grey) shown in entirety (A) and as close-ups from two different dimensions (B) and (C). Conjugated spin label **I** has been shown in red except for the sulfur atom that has been coloured yellow.

Stability of spin-labeled RNAs towards ascorbate reduction

To check the stability of the spin labels in RNA under reducing conditions, the spin-labeled RNAs were reacted with ascorbic acid (5 mM ascorbic acid, 200 μ M spin-labeled RNA, 10 mM phosphate, 100 mM NaCl, 0.1 mM Na₂EDTA, pH 7.0) and the EPR signal decay was plotted as a function of time (**Fig. S9**). Ethyl isoindoline-derived oligonucleotides **III** and **V** were found to be highly stable and thus, their decay curves have been plotted up to 12 h. Methyl isoindoline-derived RNAs **II** and **IV** were moderately stable (2 h plots) whereas isocyanato-TEMPO-labeled oligonucleotides **VI** and **VII** were found to be rapidly reduced.

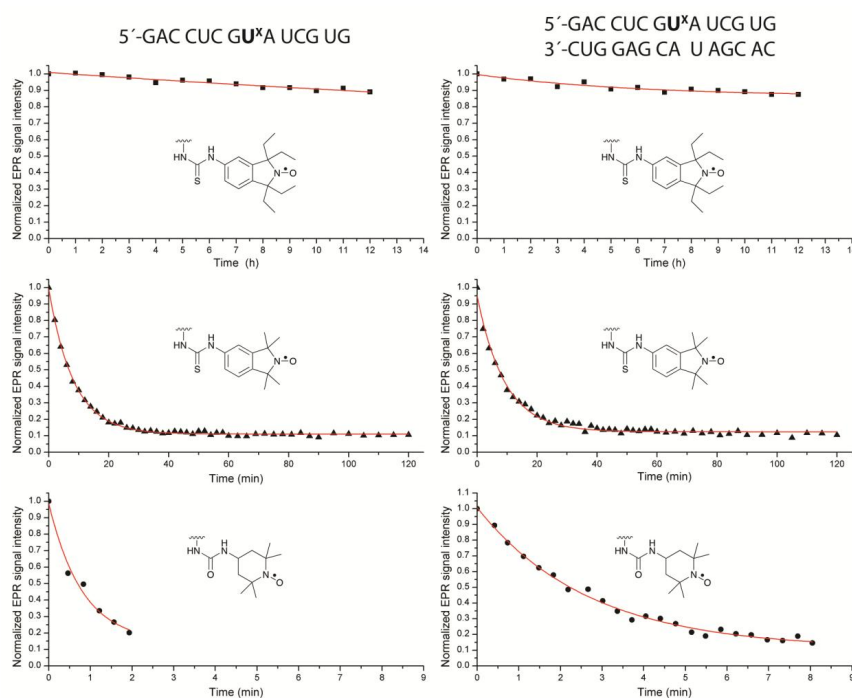
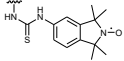
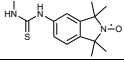
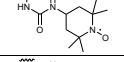
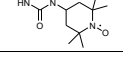


Fig. S9. Ascorbic acid reduction curves for single-stranded RNA oligonucleotides **III**, **II**, **VI** (left column) and their corresponding duplexes **V**, **IV** and **VII** (right column). All curves were fitted with their exponential functions (red line).

Due to the large excess of ascorbic acid, reduction of the radicals followed (pseudo) first order kinetics. The EPR signal decay curves were fitted with a first order exponential function and their half-lives ($t_{1/2}$) were calculated accordingly. **Table S4** shows the half-lives of the tetramethyl isoindoline- and 4-isocyanato TEMPO-labeled oligonucleotides. Single-

stranded tetramethyl isoindoline-labeled RNA **II** showed a $t_{1/2}$ of 6.7 min whereas it increased slightly to 7.2 min as duplex **IV**. The TEMPO label was the least stable one with the single strand **VI** and duplex **VII** showing half-lives of 0.7 min and 2.2 min, respectively. Reduction kinetics of the tetraethyl isoindoline-labeled RNAs **III** and **V** did not follow exponential decay, but ca. 90% was still intact after 12 h.

Table S4. Half-lives ($t_{1/2}$) of select RNA sequences.

Modification	RNA	Sequence	$t_{1/2}$
	II	5'-GAC CUC GU ^X A UCG UG-3'	6.7 min
	IV	5'-GAC CUC GU ^X A UCG UG-3' 3'-CUG GAG CA U AGC AC-5'	7.2 min
	VI	5'-GAC CUC GU ^X A UCG UG-3'	0.7 min
	VII	5'-GAC CUC GU ^X A UCG UG-3' 3'-CUG GAG CA U AGC AC-5'	2.2 min

References

1. T. D. Lee and J. F. Keana, *J. Org. Chem.*, 1975, **40**, 3145-3147.
2. Y. Li, X. Lei, X. Li, R. G. Lawler, Y. Murata, K. Komatsu and N. J. Turro, *Chem. Commun.*, 2011, **47**, 12527-12529.
3. A. P. Jagtap, I. Krstić, N. C. Kunjir, R. Hänsel, T. F. Prisner and S. T. Sigurdsson, *Free Radical Res.*, 2014, **49**, 1-25.
4. T. E. Edwards and S. T. Sigurdsson, *Nat. Protoc.*, 2007, **2**, 1954-1962.

**Article III. bcTol: A highly water-soluble
biradical for efficient DNP...**

**bcTol: A highly water-soluble biradical for
efficient dynamic nuclear polarization of
biomolecules**

Chem. Commun. **2016**, Manuscript submitted.

bcTol: A highly water-soluble biradical for efficient dynamic nuclear polarization of biomolecules

Anil P. Jagtap,¹ Michel-Andreas Geiger,² Daniel Stöppler,² Marcella Orwick-Rydmark,²⁺ Hartmut Oschkinat,^{2*} Snorri Th. Sigurdsson^{1*}

¹University of Iceland, Department of Chemistry, Science Institute, Dunhaga 3, 107 Reykjavik, Iceland. ²Leibniz-Institut für Molekulare Pharmakologie im Forschungsverbund Berlin e.V. (FMP), Campus Berlin-Buch, Robert-Rössle-Str. 10, 13125 Berlin, Germany.

*Corresponding authors: email: snorrisi@hi.is, oschkinat@fmp-berlin.de

⁺Current address: University of Oslo, Department of BioSciences P.O box 1066 Blindern 0316, Oslo, Norway

Dynamic nuclear polarization (DNP) is an efficient method to overcome the inherent low sensitivity of magic-angle spinning (MAS) solid-state NMR. We report a new polarizing agent (bcTol), designed for biological applications, that yielded an enhancement value of 244 in a microcrystalline SH3 domain sample at 110 K and displayed minimal PRE effect.

Keywords: Dynamic nuclear polarization (DNP), solid-state NMR, nitroxide biradicals, water-soluble polarizing agents, SH3 protein, channelrhodopsin

Magic-angle spinning (MAS) NMR is now routinely applied to study structure and dynamics of biological systems, with a focus on membrane proteins,¹ protofibrils,² and microcrystalline protein preparations.³ A limiting factor in exploiting the full power of MAS NMR in structural biology is its low sensitivity. This shortcoming has been addressed by the application of dynamic nuclear polarization (DNP), which involves the transfer of electron spin polarization to the spin states of nuclei in the investigated biological macromolecule.⁴ The theoretical maximum NMR signal enhancement (ϵ) of DNP is γ_e/γ_n , where γ_e and γ_n are the gyromagnetic ratios of the electron and nucleus ($\gamma_e/\gamma_H = 658$, $\gamma_e/\gamma_{13C} = 2618$ and $\gamma_e/\gamma_{15N} = 6494$). Among the mechanisms that contribute to DNP, the cross-effect (CE) has yielded so far the highest nuclear polarization at magnetic fields in the range of 4.7-14.1 T.⁵ The CE arises from the interaction of three spins, namely two electrons and one nucleus, and is most efficient when the Larmor frequencies of the two electrons are separated by the nuclear Larmor frequency.⁶

Nitroxide biradicals, in which two 2,2,6,6-tetramethyl-1-piperidinyloxy (TEMPO) units are connected by a linker, have been shown to be particularly useful polarizing agents for CE DNP,⁷ such as bTurea⁸ (Fig. 1). The DNP enhancement not only depends on the electron-electron distance, but also on the relative orientations of the TEMPO units.^{7c} The electron relaxation properties of the biradicals also effect the DNP process; for this reason, low

temperatures (< 200 K) and glass-forming solvents such as mixtures of 60% glycerol- d_8 , 30% D_2O and 10% H_2O (GDH) are applied to avoid relaxation enhancement through interactions with ice crystals that may form upon freezing.^{5, 9} Chemical fine-tuning of the structures of biradicals by replacement of the methyl groups on the TEMPO moieties with spirocyclohexyl¹⁰ or CD_3 groups,^{7d, 11} has also yielded significantly higher DNP efficiency by increasing electron and nuclear relaxation times.

A drawback of many biradicals is their hydrophobic nature, making them less suited for studies of biological systems, primarily due to low solubility in glycerol/water mixtures. Furthermore, it is more likely that such biradicals show high affinity to hydrophobic surface areas of proteins or to membranes¹² and the concomitant paramagnetic relaxation enhancement (PRE) effects can reduce signal intensities and broaden the signals of nuclei in their vicinity.¹³ Polarizing agents that are most suitable for biological applications should thus show minimal binding to the proteins or associated membranes. For these reasons, considerable efforts have been devoted to making biradicals more soluble in aqueous media and glycerol/water mixtures, for example by noncovalent complexation of hydrophobic radicals with cyclodextrin¹⁴ and micelles.¹⁵ Another approach involves covalent addition of solubility-supporting tags. One example is **AMUPol**,¹⁶ a pentaethylene glycol derivative of bTurea (Fig. 1), that is soluble in water or GDH in concentrations of up to 30 mM. Despite these successes, biradicals that have high solubility in aqueous solutions and GDH and minimized protein binding properties, while maintaining large DNP enhancements, are still in high demand.

Here we report the synthesis of a new water-soluble biradical using a novel synthetic strategy for its preparation and its application to NMR studies of biological samples. The synthesis approach replaces the methyl groups of TEMPO with spirocyclohexanolyl groups, forming the bTurea-derivative **bcTol** [bis-(spirocyclohexyl-TEMPO-alcohol)-urea] (Fig. 1), leading to substantially enhanced solubility (> 100 mM in water and GDH), while minimizing the binding to hydrophobic surfaces of proteins.

Synthesis of **bcTol** started with the condensation of acetone (1) with 4-hydroxycyclohexanone, followed by oxidation to yield the dihydroxy biradical **2**¹⁷ (Scheme 1). The hydroxyl groups of **2** were protected as silyl ethers and the ketone was subjected to reductive amination to yield amine **3**. Compound **3** was reacted with carbonyldiimidazole, followed by deprotection of the hydroxyl groups to give **bcTol**, which showed excellent solubility in GDH (150 mM) and water (100 mM). Furthermore, **bcTol** dissolves immediately in these solvents without the need for sonication.¹⁶ The crystallinity and high solubility of

bcTol in GDH, and even in glycerol alone, simplifies handling and preparation of stock solutions.

The DNP performance of **bcTol** was investigated using samples of proline, of a water-soluble protein, and of a membrane protein contained in zirconium rotors. The signal enhancements and apparent proton T_1 values of proline were determined as a function of temperature (Fig. 2A). All enhancements for the proline sample were determined using $1.3 \times T_1$ (^1H) as the recycle delay and 8000 Hz MAS-frequency, which represents the best compromise between undesired sample heating and spectral resolution. At 110 K, an enhancement of 221 ± 8 was obtained for proline. The enhancement decreased nearly linearly with temperature to around 21 ± 5 at 181 K. The apparent proton T_1 values also decreased strongly with temperature, by more than a factor of five.

To investigate the potential of **bcTol** as a polarizing agent in a biological context, we used samples containing a microcrystalline preparation of ^2H , ^{13}C , and ^{15}N -labeled (80% ^1H -backexchanged) α -spectrin Src homology 3 (SH3) domain in GDH.^{3a} A maximum enhancement of 244 ± 5 was observed at 110 K and 8889 Hz MAS at a concentration of 20 mM (Fig. 2A). The enhancement factor decreased to 40 ± 4 at 181 K, while at 200 K the enhancement was still 12 ± 2 . All enhancements for the SH3 domain samples were determined by scaling the signal intensities of the carbonyl resonances between spectra with and without microwave irradiation. The apparent proton T_1 (Fig. 2A) dropped from 14.5 s at 110 K to 5.1 s at 181 K and further to 2.7 s at 200 K.

Since radical- or temperature-dependent changes in apparent proton T_1 -values, thermal noise, heterogeneous line width and depolarisation effects¹⁸ - together with the different Boltzmann distributions - are as relevant for the overall sensitivity as the enhancement, we determined the signal-to-noise-ratio per unit measurement-time of 10 min ($^{10\text{m}}\text{SNR}$) at 110 K, 181 K and 200 K (Table 1), with the relaxation delay adjusted to $1.3 \times T_1$ for maximizing the sensitivity. Since the samples were prepared in a reproducible manner, the radical performance can be compared to that of other radicals by normalizing the $^{10\text{m}}\text{SNR}$ values to the amount of protein. At 110 K, the sample containing 20 mM **bcTol** yielded a $^{10\text{m}}\text{SNR}$ of 9473 ± 474 with 7.0 mg of protein and thus a $^{10\text{m}}\text{SNR}/\text{mg}$ of 1353 ± 68 , whereby a sample prepared with 20 mM **AMUPol** containing 7.2 mg of SH3 yielded a comparable $^{10\text{m}}\text{SNR}/\text{mg}$ of 1319 ± 26 . At 181 K, the situation was more in favour of **bcTol**, with $^{10\text{m}}\text{SNR}/\text{mg}$ values of 238 ± 11 and 147 ± 7 for **bcTol** and **AMUPol**, respectively. Surprisingly, the drop in $^{10\text{m}}\text{SNR}/\text{mg}$ between the two temperatures is only a factor of 6 for **bcTol** but 9 for **AMUPol**. A comparison of the values

obtained for the radicals at 200 K are less reliable since this temperature is too close to the phase transition temperature, causing unexpectedly large variations in the values between samples. Comparison of $^{10\text{m}}\text{SNR}_{\text{off}}/\text{mg}$ values from the **AMUPol** (6.8) and **bcTol** (6.4) samples with that of a sample without radical (12.5) at 110 K highlights the depolarisation effects¹⁸ of the radicals, pointing to the significantly higher SNR when no radical is present. However, DNP always yields SNR that is orders of magnitude larger.

The performance of **bcTol** was tested further with a sample of the membrane protein channelrhodopsin¹⁹ in liposomes at 110 K (Fig. 2A). Protein and lipid signals showed enhancements of 36 ± 6 , which is an improvement by a factor of more than three compared to polarisation by the biradical TOTAPOL^{7b} ($\epsilon \approx 10$). An apparent proton T_1 of 2.3 s was observed.

Measurements at higher temperatures result in a reduction in heterogeneous broadening that may become too severe in biological studies at temperatures around 110 K.²⁰ Therefore, we exploited the increase in enhancement by **bcTol** for improving resolution in two-dimensional ^{13}C - ^{13}C dipolar-assisted-rotational-resonance (DARR) correlations of the SH3 sample by measuring at 181 K (Fig. 3A).²¹ 768 t_1 -increments were recorded in 5.8 h at an enhancement of 40 ± 4 using a DARR mixing time of 25 ms. The cross sections shown in Fig. 3B indicate ample signal-to-noise, even without the application of a window function in F_2 , enabled by the choice of a sufficiently long acquisition time. Overall, the spectrum strongly resembles the corresponding room temperature spectra,^{3a} with a somewhat increased line width as indicated by the analysis of the cross sections taken through the cross peaks Ala55 C β -C α , Leu10 C β -C α and Ala55 C α -C β , yielding values of 135, 137, and 177 Hz in F_2 , respectively (Fig. 3B). We estimate that the spectral resolution observed at 181 K is sufficient for obtaining sequence-specific resonance assignments on the basis of a set of three-dimensional spectra in case of our SH3 domain sample.

Compared with other known biradicals, **bcTol** has structural features that may reduce non-specific or even specific binding to proteins. In comparison to **AMUPol**, the spirotetrahydropyran rings adjacent to the nitroxides have been replaced by the more hydrophilic spirocyclohexanolyl rings. Furthermore, **bcTol** does not have a flexible pentaethylene glycol tag, as present in **AMUPol**, that may adapt to surface features in a productive manner for binding through hydrophobic interactions or by hydrogen bonding. Worthy of note is that the potential hydrogen bond-donating hydroxyl groups in **bcTol** remain more or less in the same orientation relative to each other, and require matching geometries for

multivalent binding to a protein surface. These structural features of **bcTol** should contribute to a reduction of PRE effects in comparison to other radicals.

In conclusion, we have described the preparation of the new biradical **bcTol** that facilitates high DNP enhancements and displays unparalleled solubility in water, GDH and glycerol. Measurements of signal-to-noise per unit time suggest a comparable DNP performance of **bcTol** at 110 K to that of **AMUPol**, but remarkably a less severe drop in DNP enhancement when measuring at 181 K (factors of 6 and 9 for **bcTol** and **AMUPol**, respectively). 2D spectra of the SH3 domain sample recorded at 181 K and with an enhancement of 40 ± 4 show acceptable resolution for structural studies. Therefore, this biradical is particularly well-suited for investigation of biomolecules by MAS DNP NMR spectroscopy. The incorporation of spirocyclohexanoly groups may represent a general strategy for preparation of efficient and water-soluble radicals for DNP.

Acknowledgment

This work was financially supported by the Icelandic Research Fund (141062051), the Deutsche Forschungsgemeinschaft (SFB 1078, 740 and 765) and by a doctoral fellowship to A. P. J. from the University of Icelandic Research Fund. We thank A. Diehl, K. Rehbein, N. Erdmann and D. Michl for the preparation of microcrystalline SH3 and channelrhodopsin samples, Dr. S. Jonsdottir for assistance in collecting analytical data for structural characterization of the radicals, as well as P. Hegemann and K. Stehfest for helpful discussions concerning expression and purification of channelrhodopsin.

List of Figures/ Schemes

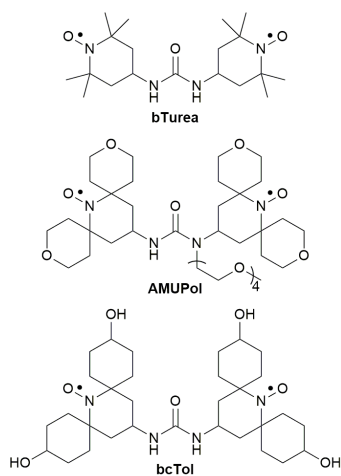
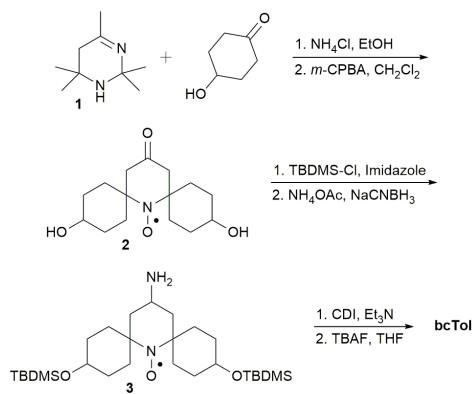


Fig. 1 Structures of **bTurea**, **AMUPol** and **bcTol**.



Scheme 1 Synthesis of **bcTol**. TBDMS-Cl *tert*-butyldimethylsilyl chloride; CDI, carbonyldiimidazole.

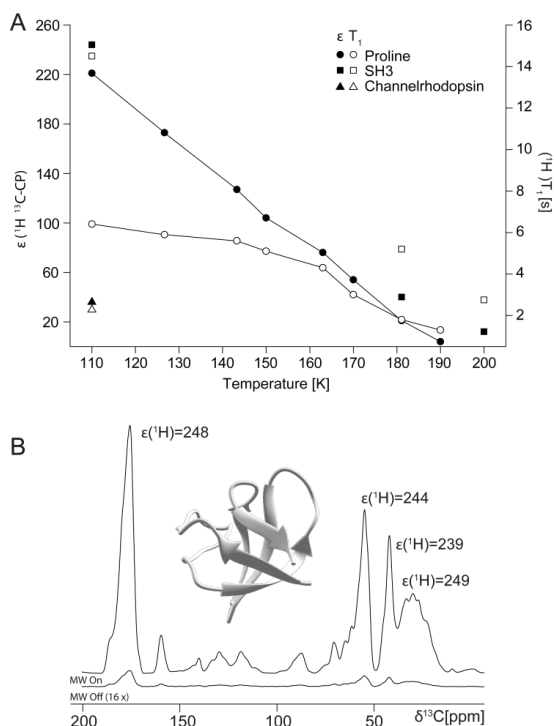


Fig.2 (A) ^1H -DNP-signal enhancement (ϵ , filled symbols) and T_1 open symbols) for proline, microcrystalline SH3 and channelrhodopsin as a function of temperature using **bcTol** as a polarizing agent. The proline (0.25 M) was uniformly ^{13}C -, ^{15}N - labeled. Spectra were recorded in glycerol- d_8 /D $_2$ O/H $_2$ O (60/30/10 v/v/v) containing **bcTol** (10 mM), measured at 9.4 T in a 3.2 mm zirconia rotor at 8 kHz MAS. T_1 was measured via an inversion recovery experiment with ^1H - ^{13}C -CP. (B) A sample of SH3 (7.0 mg) containing **bcTol** (20 mM) (18.78 s recycle delay) measured with and without microwave irradiation at 9.4 T (110 K, 16 scans, 4 dummy scans, 5 W microwave power at end of probe waveguide). Insert shows a ribbon representation of the three-dimensional structure of the SH3 protein (PDB entry 1U06).

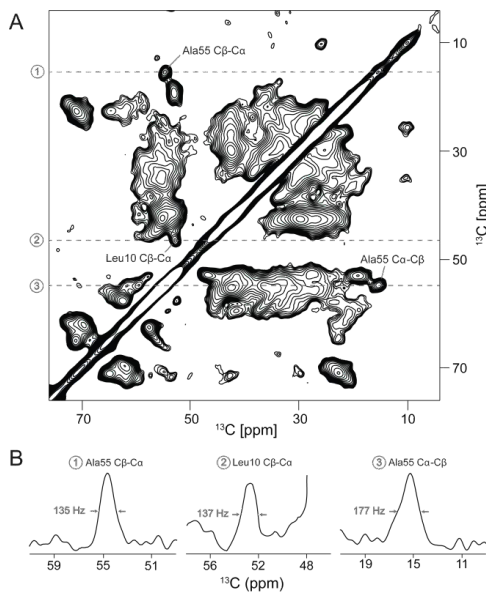


Fig.3 DNP enhanced ^{13}C - ^{13}C correlation spectrum of microcrystalline SH3 at 100 MHz carbon frequency, recorded at 181 K. (A) 2D ^{13}C - ^{13}C DARR spectrum recorded with 25 ms mixing time. The dashed lines indicate positions of cross sections for evaluation of line widths. (B) Cross sections for selected cross peaks as indicated in (A), along with their line widths. To enable the evaluation of line width, the spectrum was recorded with a sufficiently long acquisition time and processed without application of a window function in F_2 .

Table 1: Values of signal-to-noise-ratio per unit time (10 min, ^{10m}SNR) measured by ^{13}C -CP-MAS experiments with and without microwave irradiation (ON and OFF, respectively) for a microcrystalline SH3 sample with 20 mM **bcTol** and 20 mM **AMUPol**. NH protons were initially back exchanged to 80% and 1.5 times v/v d_8 -glycerol was added, relative to all water, including crystal water. Measurements were taken in 3.2 mm zirconia rotors containing 7.2 mg SH3 for the AMUPol sample and 7 mg for the bcTol sample at 8.8 kHz MAS.

T [K]	$^{10m}\text{SNR}_{\text{ON}}$		$^{10m}\text{SNR}_{\text{OFF}}$	
	bcTol	AMUPol	bcTol	AMUPol
110	9473 \pm 474	9497 \pm 188	45 \pm 3	49 \pm 2
181	1667 \pm 74	1056 \pm 51	40 \pm 2	36 \pm 2
200	180 \pm 16	656 \pm 21	13 \pm 1	35 \pm 2

References

- (a) Q. Z. Ni, E. Daviso, T. V. Can, E. Markhasin, S. K. Jawla, T. M. Swager, R. J. Temkin, J. Herzfeld and R. G. Griffin, *Acc. Chem. Res.*, 2013, **46**, 1933-1941; (b) Y. C. Su, L. Andreas and R. G. Griffin, *Annu. Rev. Biochem.*, 2015, **84**, 465-497.
- (a) A. T. Petkova, Y. Ishii, J. J. Balbach, O. N. Antzutkin, R. D. Leapman, F. Delaglio and R. Tycko, *Proc. Natl. Acad. Sci. USA*, 2002, **99**, 16742-16747; (b) C. Wasmer, A. Lange, H. V. Melckebeke, A. B. Siemer, R. Riek and B. H. Meier, *Science*, 2008, **319**, 1523-1526; (c) H. Heise, W. Hoyer, S. Becker, O. C. Andronesi, D. Riedel and M. Baldus, *Proc. Natl. Acad. Sci. USA*, 2005, **102**, 15871-15876.
- (a) F. Castellani, B. van Rossum, A. Diehl, M. Schubert, K. Rehbein and H. Oschkinat, *Nature*, 2002, **420**, 98-102; (b) W. T. Franks, B. J. Wylie, H. L. F. Schmidt, A. J. Nieuwkoop, R. M. Mayrhofer, G. J. Shah, D. T. Graesser and C. M. Rienstra, *Proc. Natl. Acad. Sci. USA*, 2008, **105**, 4621-4626; (c) S. G. Zech, A. J. Wand and A. E. McDermott, *J. Am. Chem. Soc.*, 2005, **127**, 8618-8626.
- (a) A. W. Overhauser, *Phys. Rev.*, 1953, **92**, 411-415; (b) T. R. Carver and C. P. Slichter, *Phys. Rev.*, 1953, **92**, 212-213.
- A. B. Barnes, G. De Paëpe, P. C. A. van der Wel, K.-N. Hu, C.-G. Joo, V. S. Bajaj, M. L. Mak-Jurkauskas, J. R. Sirigiri, J. Herzfeld, R. J. Temkin and R. G. Griffin, *Appl. Magn. Reson.*, 2008, **34**, 237-263.
- (a) T. Maly, G. T. Debelouchina, V. S. Bajaj, K.-N. Hu, C.-G. Joo, M. L. Mak-Jurkauskas, J. R. Sirigiri, P. C. A. van der Wel, J. Herzfeld, R. J. Temkin and R. G. Griffin, *J. Chem. Phys.*, 2008, **128**, 052211-052219; (b) Y. Hovav, A. Feintuch and S. Vega, *J. Magn. Reson.*, 2012, **214**, 29-41.
- (a) K.-N. Hu, H.-H. Yu, T. M. Swager and R. G. Griffin, *J. Am. Chem. Soc.*, 2004, **126**, 10844-10845; (b) C. Song, K.-N. Hu, C.-G. Joo, T. M. Swager and R. G. Griffin, *J. Am. Chem. Soc.*, 2006, **128**, 11385-11390; (c) Y. Matsuki, T. Maly, O. Ouari, H. Karoui, F. Le Moigne, E. Rizzato, S. Lyubenova, J. Herzfeld, T. Prisner, P. Tordo and R. G. Griffin, *Angew. Chem. Int. Ed.*, 2009, **48**, 4996-5000; (d) D. J. Kubicki, G. Casano, M. Schwarzwald, S. Abel, C. Sauvee, K. Ganesan, M. Yulikov, A. J. Rossini, G. Jeschke, C. Coperet, A. Lesage, P. Tordo, O. Ouari and L. Emsley, *Chem. Sci.*, 2016, **7**, 550-558.
- K.-N. Hu, C. Song, H.-H. Yu, T. M. Swager and R. G. Griffin, *J. Chem. Phys.*, 2008, **128**, 052302.
- K. L. Ngai, S. Capaccioli and N. Shinyashiki, *J. Phys. Chem. B*, 2008, **112**, 3826-3832.
- (a) A. Zagdoun, G. Casano, O. Ouari, G. Lapadula, A. J. Rossini, M. Lelli, M. Baffert, D. Gajan, L. Veyre, W. E. Maas, M. Rosay, R. T. Weber, C. Thieuleux, C. Coperet, A. Lesage, P. Tordo and L. Emsley, *J. Am. Chem. Soc.*, 2012, **134**, 2284-2291; (b) A. Zagdoun, G. Casano, O. Ouari, M. Schwarzwald, A. J. Rossini, F. Aussenac, M. Yulikov, G. Jeschke, C. Coperet, A. Lesage, P. Tordo and L. Emsley, *J. Am. Chem. Soc.*, 2013, **135**, 12790-12797; (c) A. Rajca, Y. Wang, M. Boska, J. T. Paletta, A. Olankitwanit, M. A. Swanson, D. G. Mitchell, S. S. Eaton, G. R. Eaton and S. Rajca, *J. Am. Chem. Soc.*, 2012, **134**, 15724-15727.
- F. A. Perras, R. R. Reinig, I. I. Slowing, A. D. Sadow and M. Pruski, *Phys. Chem. Chem. Phys.*, 2016, **18**, 65-69.
- (a) A. H. Linden, S. Lange, W. T. Franks, Ü. Akbey, E. Specker, B. J. van Rossum and H. Oschkinat, *J. Am. Chem. Soc.*, 2011, **133**, 19266-19269; (b) E. Ravera, B. Corzilius, V. K. Michaelis, C. Rosa, R. G. Griffin, C. Luchinat and I. Bertini, *J. Am. Chem. Soc.*, 2013, **135**, 1641-1644.

13. I. Bertini, C. Luchinat and G. Parigi, *Solution NMR of paramagnetic molecules: applications to metallobiomolecules and models*, Elsevier, 2001.
14. (a) J. Mao, D. Akhmetzyanov, O. Ouari, V. Denysenkov, B. Corzilius, J. Plackmeyer, P. Tordo, T. F. Prisner and C. Glaubitz, *J. Am. Chem. Soc.*, 2013, **135**, 19275-19281; (b) X. Tan, Y. Song, H. Liu, Q. Zhong, A. Rockenbauer, F. A. Villamena, J. L. Zweier and Y. Liu, *Org. Biomol. Chem.*, 2016, **14**, 1694-1701.
15. (a) M. K. Kieseewetter, V. K. Michaelis, J. J. Walish, R. G. Griffin and T. M. Swager, *J. Phys. Chem. B*, 2014, **118**, 1825-1830; (b) M. Lelli, A. J. Rossini, G. Casano, O. Ouari, P. Tordo, A. Lesage and L. Emsley, *Chem. Commun.*, 2014, **50**, 10198-10201.
16. C. Sauvée, M. Rosay, G. Casano, F. Aussenac, R. T. Weber, O. Ouari and P. Tordo, *Angew. Chem. Int. Ed.*, 2013, **52**, 10858-10861.
17. S. Okazaki, M. A. Mannan, K. Sawai, T. Masumizu, Y. Miura and K. Takeshita, *Free Radical Res.*, 2007, **41**, 1069-1077.
18. (a) K. R. Thurber and R. Tycko, *J. Chem. Phys.*, 2014, **140**, 184201; (b) F. Mentink-Vigier, S. Paul, D. Lee, A. Feintuch, S. Hediger, S. Vega and G. De Paëpe, *Phys. Chem. Chem. Phys.*, 2015, **17**, 21824-21836.
19. S. Bruun, D. Stoeppler, A. Keidel, U. Kuhlmann, M. Luck, A. Diehl, M.-A. Geiger, D. Woodmansee, D. Trauner, P. Hegemann, H. Oschkinat, P. Hildebrandt and K. Stehfest, *Biochemistry*, 2015, **54**, 5389-5400.
20. A. H. Linden, W. T. Franks, Ü. Akbey, S. Lange, B. J. van Rossum and H. Oschkinat, *J. Biomol. NMR*, 2011, **51**, 283-292.
21. (a) K. Takegoshi, S. Nakamura and T. Terao, *J. Chem. Phys.*, 2003, **118**, 2325-2341; (b) K. Takegoshi, S. Nakamura and T. Terao, *Chem. Phys. Lett.*, 2001, **344**, 631-637.

bcTol: A highly water-soluble biradical for efficient dynamic nuclear polarization of biomolecules

Anil P. Jagtap,¹ Michel-Andreas Geiger,² Daniel Stöppler,² Marcella Orwick-Rydmak,² Hartmut Oschkinat,^{2*} Snorri Th. Sigurdsson^{1*}

¹University of Iceland, Department of Chemistry, Science Institute, Dunhaga 3, 107 Reykjavik, Iceland. ²Leibniz-Institut für Molekulare Pharmakologie im Forschungsverbund Berlin e.V. (FMP), Campus Berlin-Buch, Robert-Rössle-Str. 10, 13125 Berlin, Germany.

*Corresponding authors: email: snorrisi@hi.is, oschkinat@fmp-berlin.de

Table of contents

Abbreviations	2
Synthetic procedures	2
General materials and methods	2
Synthetic protocols	3
Compound 4	3
Compound 3	4
Compound 5	5
bcTol	6
DNP measurements	7
General Information	7
Sample preparation	7
Determination of Signal-to-noise per unit time (SNR)	8
Dependence of MAS frequency of the enhancement for bcTol	9
References	10

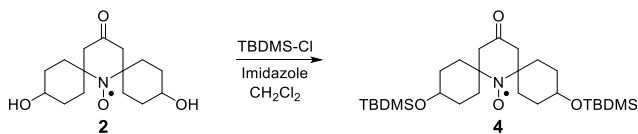
Abbreviations

HRMS	high-resolution mass spectrometry
TLC	thin layer chromatography
TBDMS-Cl	<i>tert</i> -butyldimethylsilyl chloride
<i>m</i> -CPBA	<i>meta</i> -chloroperbenzoic acid
PMA	phosphomolybdic acid
THF	tetrahydrofuran
CDI	carbonyldiimidazole
Et ₃ N	triethylamine
TBAF	tetra- <i>n</i> -butylammonium fluoride
DNP	dynamic nuclear polarization
MAS	magic angle spinning
GDH	glycerol- <i>d</i> ₈ , D ₂ O, H ₂ O (60/30/10 v/v/v)
TPPM	two pulse phase modulation
EPR	electron paramagnetic resonance
SNR	Signal-to-noise ratio per unit time
ssNMR	solid-state nuclear magnetic resonance

Synthetic procedures**General materials and methods**

All reagents were purchased from Sigma-Aldrich and used without further purification. TLC was carried out using glass plates pre-coated with silica gel (0.25 mm, F-254) from Silicycle, Canada. All compounds were visualized by UV light and by staining with PMA. Flash column chromatography was performed using ultra-pure flash silica gel (Silicycle, 230-400 mesh, size 60 Å). All moisture and air-sensitive reactions were carried out in oven-dried glassware under an inert argon atmosphere. Nitroxide radicals show broadening and loss of NMR signals due to their paramagnetic nature,¹ and therefore, integration of the NMR peaks was not done. HRMS analyses of all organic compounds were performed on Bruker, MicroTOF-Q, equipped with an electron spray ionization module, in a positive ion mode.

Synthetic protocols



Compound 4

A solution of **2** (0.020 g, 0.07 mmol) in CH_2Cl_2 (3 mL) was treated with imidazole (0.019 g, 0.28 mmol) and TBDMS-Cl (0.026 g, 0.177 mmol) and the resulting solution was stirred at 24 °C for 12 h. After addition of CH_2Cl_2 (15 mL), the organic layer was washed successively with water (10 mL) and brine (10 mL). The organic layer was dried over anhydrous sodium sulfate, filtered and concentrated *in vacuo* to obtain the crude product, which was purified by flash column chromatography (silica) using a gradient elution (EtOAc:pet. ether; 0:100 to 2:98) to give **4** (0.034 g, 94% yield) as a yellow solid.

TLC (Silica gel, 10% MeOH in CH_2Cl_2), $R_f(\mathbf{2}) = 0.2$, $R_f(\mathbf{4}) = 1$, PMA active.

(Silica gel, 20% EtOAc in pet. ether), $R_f(\mathbf{4}) = 0.6$, PMA active.

HRMS: calculated for $\text{C}_{27}\text{H}_{52}\text{NO}_4\text{Si}_2$: 510.3435, found 533.3374 ($\text{M}+\text{Na}$)⁺.

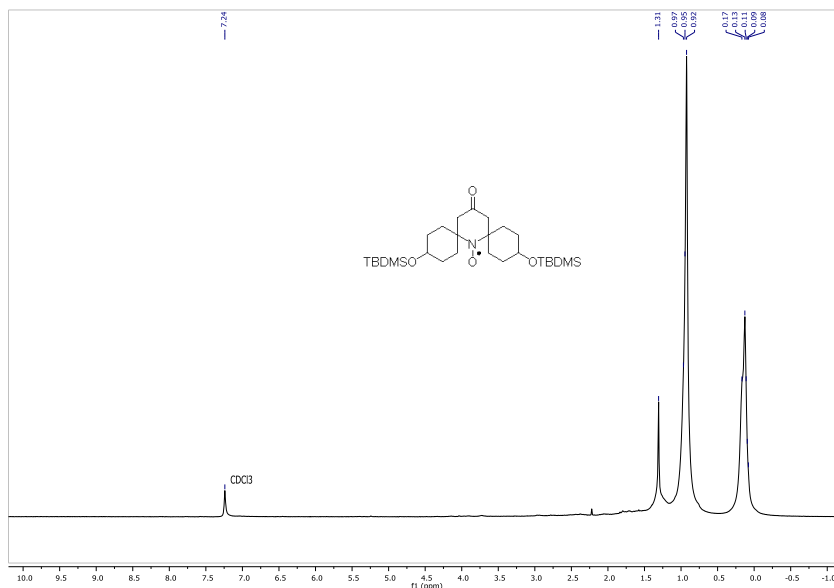
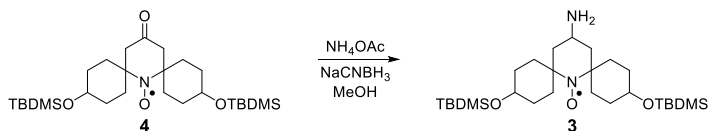


Figure S1. ^1H NMR spectrum of compound **4** in CDCl_3 .



Compound 3

Ammonium acetate (0.150 g, 1.95 mmol) was added to a solution of **4** (0.1 g, 0.195 mmol) in MeOH (4 mL) and stirred for 2 h, followed by portion-wise addition of NaCNBH₃ (0.016 g, 0.254 mmol). The reaction mixture was stirred at 24 °C for 12 h, the solvent was removed *in vacuo* and a saturated solution of NaHCO₃ (5 mL) added. The aqueous layer was extracted with CH₂Cl₂ (3 x 15 mL), the combined organic layer dried over anhydrous sodium sulfate, filtered and concentrated to obtain the crude product. Purification was performed by flash column chromatography (silica) using a gradient elution (MeOH:CH₂Cl₂; 0:100 to 4:96) to give **3** (0.057 g, 57% yield) as a yellow solid.

TLC (Silica gel, 20% EtOAc in pet. ether), R_f(**4**) = 0.6, R_f(**3**) = 0.0, PMA active.

(Silica gel, 10% MeOH in CH₂Cl₂), R_f(**3**) = 0.2, PMA active.

HRMS: calculated for C₂₇H₅₅N₂O₃Si₂: 511.3751, found 512.3831 (M+H)⁺.

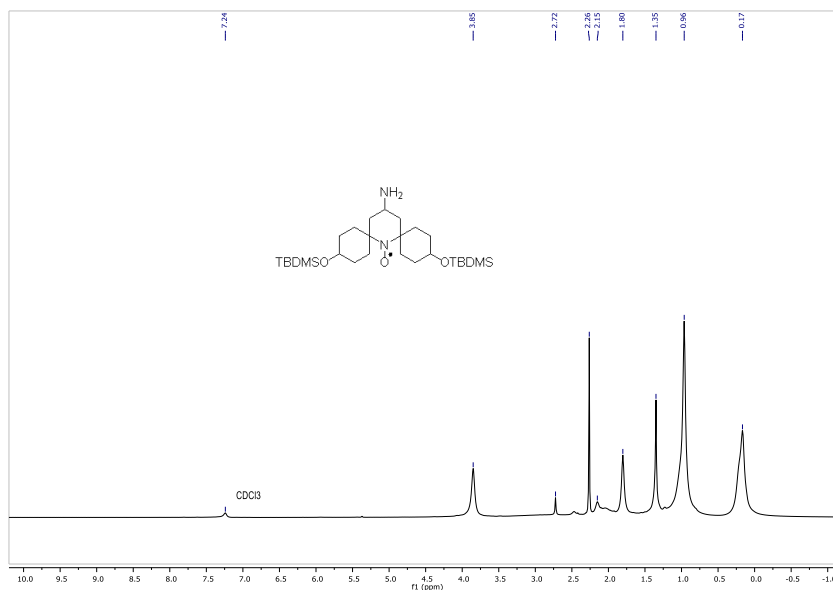
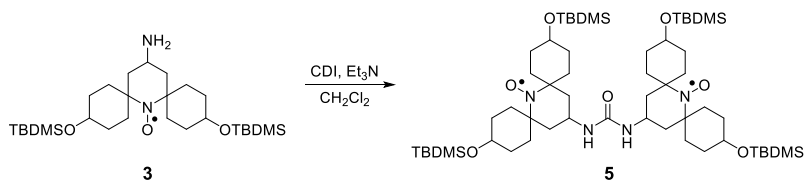


Figure S2. ¹H NMR spectrum of compound **3** in CDCl₃.



Compound 5

Carbonyldiimidazole (0.021 g, 0.13 mmol) and triethylamine (0.071 mL, 0.52 mmol) were added to a solution of **3** (0.132 g, 0.26 mmol) in CH_2Cl_2 (6 mL) and stirred at 24 °C for 12 h. The reaction mixture was diluted with CH_2Cl_2 (10 mL) and washed consecutively with H_2O (10 mL) and brine (15 mL). The organic layer was dried over anhydrous sodium sulfate, filtered and concentrated to obtain the crude product, which was purified by flash column chromatography (silica) using a gradient elution (EtOAc:Pet. ether; 0:100 to 15:85) to afford **5** as an orange solid (0.043 g, 70% yield based on recovery of starting material).

TLC (Silica gel, 10% MeOH in CH_2Cl_2), $R_f(\mathbf{3}) = 0.2$, $R_f(\mathbf{5}) = 0.8$, PMA active.

HRMS: calculated for $\text{C}_{55}\text{H}_{108}\text{N}_4\text{O}_7\text{Si}_4$: 1048.7295, found 1071.7159 ($\text{M}+\text{Na}$)⁺.

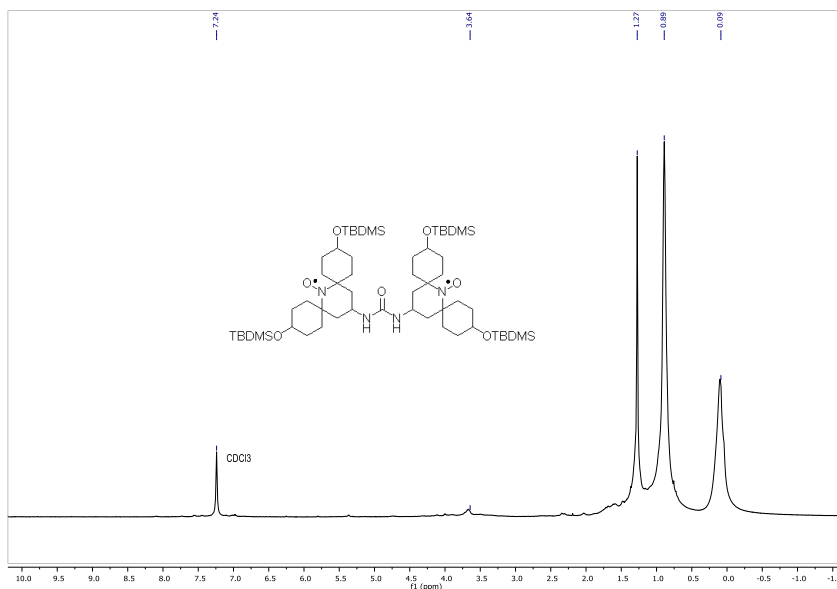
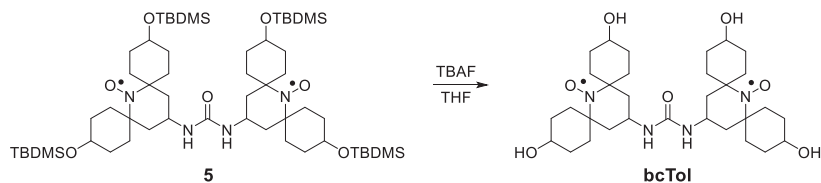


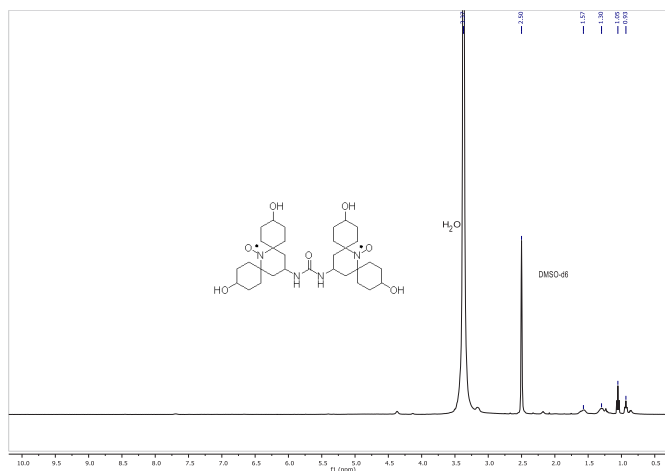
Figure S3. ^1H NMR spectrum of compound **5** in CDCl_3 .

**bcTol**

A solution of **5** (0.105 g, 0.1 mmol) in THF (7 mL) was treated dropwise with TBAF (2.6 mL, 2.6 mmol, 1M in THF) and stirred for 48 h at 24 °C. The solvent was removed *in vacuo* and the crude material was purified by flash column chromatography (silica) using a gradient elution (MeOH:CH₂Cl₂; 0:100 to 20:80) to give **bcTol** (0.051 g, 89% yield) as a pale yellow solid.

TLC (Silica gel, 20% MeOH in CH₂Cl₂), $R_f(\mathbf{5}) = 1$, $R_f(\mathbf{bcTol}) = 0.2$, PMA active.

HRMS: calculated for C₃₁H₅₂N₄O₇: 592.3836, found 615.3730 (M+Na)⁺.



DNP measurements

General Information

All samples were measured on a 400 MHz (9.4 T) wide-bore spectrometer (Bruker Avance III console) combined with a Bruker 263 GHz gyrotron (~5 W at the end of the waveguide). The variable temperature was adjusted with a Bruker Cryo-NMR cooling cabinet. All samples were measured in the triple resonance mode of the Cryo-MAS probe. Standard 3.2 mm zirconium rotors from Bruker were used for all measurements, at magic angle spinning frequencies of 8000 Hz for proline (25 μ l Volume), 8889 Hz for SH3 and channelrhodopsin respectively. Between on/off comparisons with and without microwaves, the temperature was equilibrated for 10 minutes before data acquisition. All on/off comparisons were recorded with 16 scans and 4 dummy scans (for the channelrhodopsin sample 128 scans and 16 dummy scans) and processed with Topspin version 2.1. ^1H -DNP signals were recorded via a cross polarization (^1H - ^{13}C) MAS experiment with TPPM decoupling.² Spectra for enhancement determination were recorded under the same conditions with and without microwave irradiation. At each temperature, the proton 90° pulse and proton T_1 were evaluated and the recycle delay set to $1.3 \times T_1$. The T_1 times were measured with an inversion recovery experiment with 2 scans and 1 dummy scans (for channelrhodopsin 8 scans and 2 dummy scans) and fit in the Topspin relaxation module. The Sample temperature was calibrated using KBr^3 , T_1 and chemical shift value measurements. The reported sample temperatures correspond to the calibrated temperature with microwave irradiation.

Sample preparation

The SH3 samples were crystallized and prepared for DNP experiments according to previously published procedures.⁴ The channelrhodopsin samples were prepared as described in Bruun & Stoeppler et al.⁵ Instead of using TOTAPOL, 20 mM **bcTol** in GDH was added to the pellet containing C1C2 reconstituted with C(12)-C(15)-C(20)- ^{13}C -labeled retinal in lipid vesicles.

Determination of Signal-to-noise per unit time (SNR)

In order to evaluate the performance of **bcTol** in more detail, we conducted signal-to-noise per 10 min measurement time (^{10m}SNR) determinations. We used 7.0 mg microcrystalline SH3 in GDH with 20 mM **bcTol** and, as a comparison, a sample of 7.2 mg microcrystalline SH3 in GDH with 20 mM **AMUPol**. At 110 K, 181 K and 200 K, the ^{10m}SNR of both samples for both with and without microwave irradiation was determined. The reported values are averages of five measurements. One-dimensional ^1H - ^{13}C -CP spectra were recorded at 8889 Hz MAS with an acquisition time of 30 ms. The recycle delay was set to $1.3 \times T_1 (^1\text{H})$ and the number of scans adjusted to complete each measurement within 10 min., whereas all other conditions were kept identical to the measurements described under General Information.

For data evaluation, we used Bruker TopSpin 3.2 software. All spectra for SNR determinations were processed without window function and recorded with a spectral width of 1380 ppm with the transmitter frequency offset at 102 ppm. Two baseline corrections with a polynomial degree of five were applied, the first between 750 ppm and -550 ppm and the second from -300 ppm to -550 ppm. The SNR was determined for the carbonyl resonances (194 ppm to 164 ppm) using the region ranging from -350 ppm to -450 ppm as noise. To normalize the ^{10m}SNR according to the amount of protein, the ^{10m}SNR value was divided by 7 for **bcTol** (7.0 mg protein in the sample containing 20 mM **bcTol**) and 7.2 for **AMUPol** (7.2 mg protein in the sample containing 20 mM **AMUPol**).

Dependence of MAS frequency of the enhancement for bcTol

The MAS frequency dependence of the DNP ^1H - ^{13}C -CP signal was recorded at 110 K. No significant changes of the enhancement values were observed between 2 and 12 kHz. This differs from the results obtained for TOTAPOL where a significant loss was observed.⁶ The shown results are consistent with the observation reported for **AMUPol** where the authors suggest that the spinning independency might be due to a lower temperature dependence and to stronger electron-electron dipolar coupling.⁷

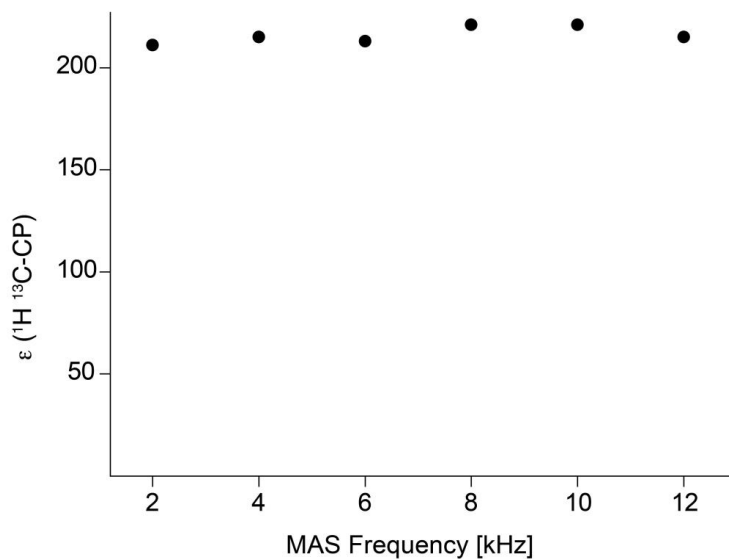


Figure S7. DNP signal enhancement ^1H - ^{13}C -CP as a function of MAS frequency (kHz) at 263 GHz (400 MHz). The sample contains 0.25 M U^{13}C - ^{15}N proline (25 μL in GDH). For each data point 16 scans and 4 dummy scans were recorded with and without microwave irradiation.

References

1. (a) T. D. Lee and F. W. Keana, *J. Org. Chem.*, 1975, **40**, 3145-3147; (b) Y. J. Li, X. G. Lei, X. Li, R. G. Lawler, Y. Murata, K. Komatsu and N. J. Turro, *Chem. Commun.*, 2011, **47**, 12527-12529.
2. A. E. Bennett, C. M. Rienstra, M. Auger, K. V. Lakshmi and R. G. Griffin, *J. Chem. Phys.*, 1995, **103**, 6951-6958.
3. K. R. Thurber and R. Tycko, *J. Magn. Reson.*, 2009, **196**, 84-87.
4. (a) Ü. Akbey, H. Oschkinat and B. J. van Rossum, *J. Am. Chem. Soc.*, 2009, **131**, 17054-17055; (b) Ü. Akbey, S. Lange, W. T. Franks, R. Linser, K. Rehbein, A. Diehl, B. J. van Rossum, B. Reif and H. Oschkinat, *J. Biomol. NMR*, 2010, **46**, 67-73.
5. S. Bruun, D. Stoeppler, A. Keidel, U. Kuhlmann, M. Luck, A. Diehl, M.-A. Geiger, D. Woodmansee, D. Trauner, P. Hegemann, H. Oschkinat, P. Hildebrandt and K. Stehfest, *Biochemistry*, 2015, **54**, 5389-5400.
6. (a) M. Rosay, L. Tometich, S. Pawsey, R. Bader, R. Schauwecker, M. Blank, P. M. Borchard, S. R. Cauffman, K. L. Felch, R. T. Weber, R. J. Temkin, R. G. Griffin and W. E. Maas, *Phys. Chem. Chem. Phys.*, 2010, **12**, 5850-5860; (b) F. Mentink-Vigier, Ü. Akbey, Y. Hovav, S. Vega, H. Oschkinat and A. Feintuch, *J. Magn. Reson.*, 2012, **224**, 13-21.
7. C. Sauvée, M. Rosay, G. Casano, F. Aussenac, R. T. Weber, O. Ouari and P. Tordo, *Angew. Chem. Int. Ed.*, 2013, **52**, 10858-10861.

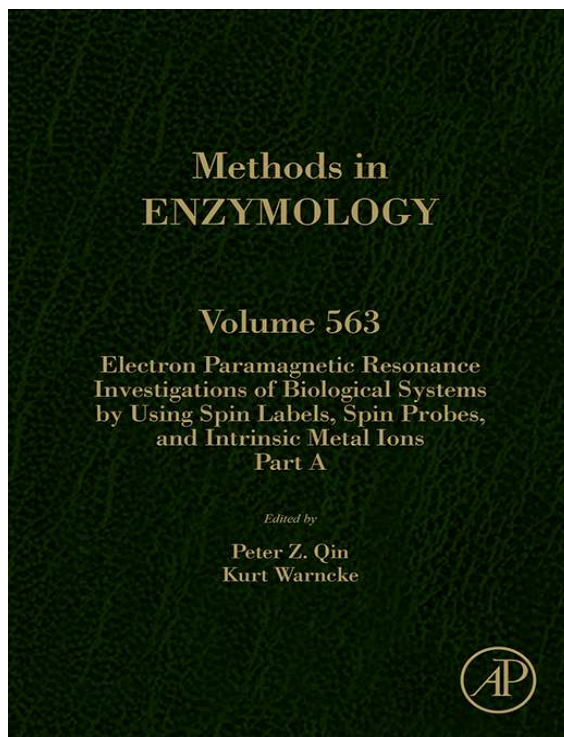
Article IV. Chapter 15 – SDSL of RNA by post-synthetic modification of 2'-amino groups

**Chapter fifteen - Site-directed spin labeling of RNA
by post-synthetic modification of 2'-amino groups**

Methods in Enzymol., Academic Press **2015**, 563, 397-414.

**Provided for non-commercial research and educational use only.
Not for reproduction, distribution or commercial use.**

This chapter was originally published in the book *Methods in Enzymology*, Vol. 563 published by Elsevier, and the attached copy is provided by Elsevier for the author's benefit and for the benefit of the author's institution, for non-commercial research and educational use including without limitation use in instruction at your institution, sending it to specific colleagues who know you, and providing a copy to your institution's administrator.



All other uses, reproduction and distribution, including without limitation commercial reprints, selling or licensing copies or access, or posting on open internet sites, your personal or institution's website or repository, are prohibited. For exceptions, permission may be sought for such use through Elsevier's permissions site at:

<http://www.elsevier.com/locate/permissionusematerial>

From Subham Saha, Anil P. Jagtap and Snorri Th. Sigurdsson, Site-Directed Spin Labeling of RNA by Postsynthetic Modification of 2'-Amino Groups. In: Peter Z. Qin and Kurt Warncke, editors, *Methods in Enzymology*, Vol. 563, Burlington: Academic Press, 2015, pp. 397-414.

ISBN: 978-0-12-802834-6

© Copyright 2015 Elsevier Inc.
Academic Press



Site-Directed Spin Labeling of RNA by Postsynthetic Modification of 2'-Amino Groups

Subham Saha, Anil P. Jagtap, Snorri Th. Sigurdsson¹

Department of Chemistry, Science Institute, University of Iceland, Reykjavik, Iceland

¹Corresponding author: e-mail address: snorrisi@hi.is

Contents

1. Introduction	398
1.1 The Phosphoramidite Method for SDSL	400
1.2 Postsynthetic Spin-Labeling	401
2. 2'-Amino Spin-Labeling with Aliphatic Isocyanates and Aromatic Isothiocyanates	404
2.1 Spin-Labeling of 2'-Amino Groups in RNA with 4-Isocyanato-TEMPO	405
2.2 Synthesis of Isothiocyanate-Containing Spin Labels	406
2.3 Spin Labeling of 2'-Amino Groups in RNA with Isothiocyanates	407
2.4 Analysis of Spin-Labeled Oligonucleotides	409
3. Summary and Conclusions	410
Acknowledgments	411
References	411

Abstract

To elucidate mechanisms that govern functions of nucleic acids, it is essential to understand their structure and dynamics. Electron paramagnetic resonance (EPR) spectroscopy is a valuable technique that is routinely used to study those aspects of nucleic acids. A prerequisite for most EPR studies of nucleic acids is incorporation of spin labels at specific sites, known as site-directed spin labeling (SDSL). There are two main strategies for SDSL through formation of covalent bonds, i.e., the phosphoramidite approach and postsynthetic spin-labeling. After describing briefly the advantages and disadvantages of these two strategies, postsynthetic labeling of 2'-amino groups in RNA is delineated. Postsynthetic labeling of 2'-amino groups in RNA using 4-isocyanato-TEMPO has long been established as a useful approach. However, this method has some drawbacks, both with regard to the spin-labeling protocol and the flexibility of the spin label itself. Recently reported isothiocyanate-substituted aromatic isoindoline-derived nitroxides can be used to quantitatively and selectively modify 2'-amino groups in RNA and do not have the drawbacks associated with 4-isocyanato-TEMPO. This chapter provides a detailed description of the postsynthetic spin-labeling methods of 2'-amino groups in RNA with a special focus on using the aromatic isothiocyanate spin labels.



1. INTRODUCTION

Nucleic acids are essential molecules for sustaining life. DNA and RNA are responsible for storage, expression, and transmission of genetic information—DNA carries the genetic information, whereas RNA has varied functions, such as transferring genetic information and acting as a chief constituent of ribonucleoprotein complexes involved with mRNA processing and translation. RNA can also catalyze reactions; a prominent example is formation of peptide bonds by the ribosome (Nissen, Hansen, Ban, Moore, & Steitz, 2000). RNA has also been implied in the catalytic function of the spliceosome (Fica et al., 2013). Recently discovered siRNAs play a notable role in RNA interference, where they inhibit particular gene expressions (Brummelkamp, Bernards, & Agami, 2002). Moreover, riboswitches have an important role in regulating gene expression (Mandal & Breaker, 2004).

It is of interest to know the structure and dynamics of nucleic acids, because these properties govern their functions. There are several biochemical and biophysical techniques that have been applied for the study of the structure and function of nucleic acids. The most powerful technique is undoubtedly X-ray crystallography, which is capable of providing a “photographic” representation of the three-dimensional molecular structure. However, this highly informative technique requires a sufficiently large and regular single crystal, which can be a daunting task to obtain for nucleic acids. In addition, a crystal structure might not represent a biologically active conformation. Moreover, an X-ray structure provides a static view, whereas conformational changes are usually required to carry out specific functions. Another high-resolution technique to study nucleic acid structure is nuclear magnetic resonance (NMR) spectroscopy, which provides structural information of the nucleic acid in solution, thus revealing their conformation under biologically relevant conditions. However, NMR of nucleic acids often requires relatively large amounts of isotopically labeled samples. Furthermore, NMR studies are usually restricted to nucleic acids that are smaller than 50 kDa (Xu & Matthews, 2013), because the increased anisotropy associated with slower tumbling of large molecules in solution causes peak broadening. Another common technique for studying nucleic acids is Förster resonance energy transfer, which is capable of measuring distances in the nanometer range. This technique can also be used to study nucleic acids under biologically relevant conditions, in addition to enabling

single-molecule studies (Roy, Hohng, & Ha, 2008; Sisamakris, Valeri, Kalinin, Rothwell, & Seidel, 2010). However, since natural nucleic acids do not possess any fluorescent chromophores, a prerequisite for this technique is the incorporation of a pair of rather bulky fluorophores.

The technique that will be addressed here is electron paramagnetic resonance (EPR) spectroscopy, which is applicable for the study of paramagnetic centers. EPR can provide structural information for biomolecules through measurement of distances between paramagnetic centers, using continuous wave (CW)- or pulsed EPR. CW EPR can be used to measure distances up to 25 Å through analysis of peak broadening (Kim, Murali, & DeRose, 2004; Macosko, Pio, Tinoco, & Shin, 1999). Pulsed EPR, such as pulsed electron-electron double resonance, also called double electron-electron resonance, can yield distances of 15–100 Å (Duss, Yulikov, Jeschke, & Allain, 2014; Jeschke, 2012; Milov, Salikhov, & Shirov, 1981; Reginsson & Schiemann, 2011; Schiemann & Prisner, 2007). EPR is also capable of probing the orientation of paramagnetic centers, which can provide information about both structure and dynamics (Denysenkov, Prisner, Stubbe, & Bennati, 2006; Marko et al., 2011; Schiemann, Cekan, Margraf, Prisner, & Sigurdsson, 2009). EPR is valuable for studying dynamics on a range of timescales (Marko et al., 2011; Nguyen & Qin, 2012; Sowa & Qin, 2008). Thus, EPR is a multifaceted tool that can provide valuable insights into both structure and dynamics of nucleic acids.

Nucleic acids are not inherently paramagnetic and, therefore, it is necessary to modify them with paramagnetic atoms or groups, referred to as spin labels. Although there are some examples of paramagnetic metal ions that have been used as spin probes (Goldfarb, 2014; Hunsicker-Wang, Vogt, & DeRose, 2009; Schiemann, Fritscher, Kisseleva, Sigurdsson, & Prisner, 2003), the most commonly used spin labels are aminoxyl radicals, usually called nitroxides. Many of these nitroxide radicals are commercially available or can be readily synthesized using standard techniques of organic synthesis. Therefore, nitroxides have found extensive use as spin labels. Although there are examples of noncovalent spin labeling of nucleic acids with nitroxides (Belmont et al., 1998; Chalmers et al., 2014; Maekawa et al., 2010; Shelke, Sandholt, & Sigurdsson, 2014; Shelke & Sigurdsson, 2010), the most common spin-labeling approach for nucleic acids is attachment of spin labels through covalent bonds.

There are several methods available for incorporation of spin labels at the end of nucleic acids (Shelke & Sigurdsson, 2012, 2013), but end-labeling has limited applicability for EPR studies. Therefore, this text focuses on

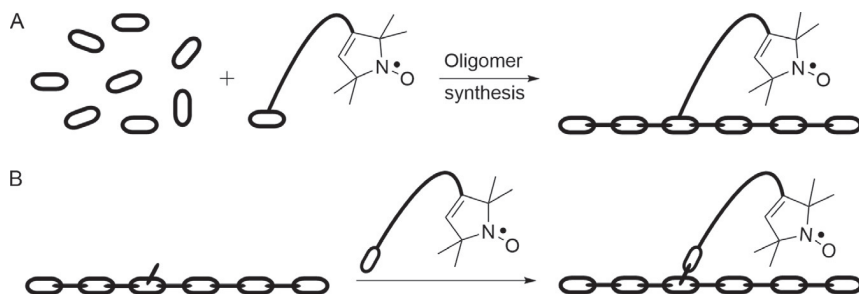


Figure 1 Strategies for site-directed spin labeling through covalent bonding. (A) The phosphoramidite approach. (B) Postsynthetic spin-labeling. A pyrrolidine-based spin label is used as a representative nitroxide spin label. Nucleotides are represented by links that form oligonucleotide chains.

methods for incorporation of spin labels at internal sites. Moreover, it will address how spin labels can be incorporated at specific sites of choice, referred to as site-directed spin labeling (SDSL). There are two main strategies that have been applied for covalent SDSL (Fig. 1). The first one utilizes spin-labeled phosphoramidites that are incorporated at specific positions during automated chemical synthesis of the nucleic acid (Shelke & Sigurdsson, 2012), shown schematically in Fig. 1A, and sometimes referred to as the phosphoramidite method. The second SDSL strategy is post-synthetic spin labeling, where spin labels are incorporated after the synthesis of the oligonucleotide, by either chemical or enzymatic methods (Fig. 1B).

The main features of these two spin-labeling strategies, the phosphoramidite method and postsynthetic labeling, will be described briefly below. Both of these SDSL routes are useful and complement each other. A facile approach for postsynthetic labeling of 2'-amino groups in RNA will subsequently be described in detail.

1.1 The Phosphoramidite Method for SDSL

Nucleoside phosphoramidites are derivatives of natural nucleosides and serve as building blocks in solid-phase synthesis of nucleic acids. A generic structure of a phosphoramidite is shown in Fig. 2A, where the 5'-hydroxyl group of a ribonucleoside is protected as a 5'-dimethoxytrityl (DMT) ether, while the phosphoramidite group is at the 3'-position. The 2'-position also needs to be protected when synthesizing RNA. The main advantage of the phosphoramidite method is that spin labels with specific and desired structural features can be inserted at chosen sites, which might not be possible using postsynthetic labeling.

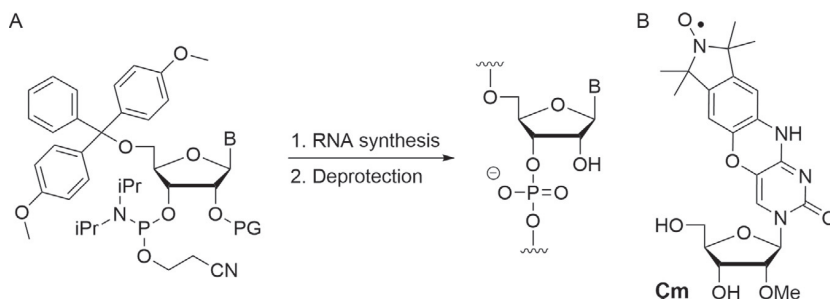


Figure 2 (A) Phosphoramidite monomer building block. PG is a protecting group for the 2'-hydroxy group. B is a nucleobase. (B) The rigid spin label **Çm** that has been incorporated into RNA by the phosphoramidite method.

There are several examples of spin labels that have been incorporated into DNA by the phosphoramidite method (Shelke & Sigurdsson, 2012). However, there is only one example of a spin-labeled nucleoside that has been incorporated into RNA by this method, the nucleoside **Çm** (Fig. 2B). **Çm** is a rigid spin label containing a nitroxide that has been fused to a nucleobase (Höbartner, Sicoli, Wachowius, Gophane, & Sigurdsson, 2012). Synthesis of spin-labeled phosphoramidites usually requires a substantial effort and involves a high degree of expertise in synthetic organic chemistry. Another drawback is the exposure of the spin labels to the reagents used during the oligonucleotide synthesis, which may result in partial reduction of the nitroxide radical. For example, iodine/water, which has traditionally been used to oxidize the phosphorous atoms from P(III) to P(V), needs to be replaced by *tert*-butyl hydroperoxide to avoid degradation of the radical (Cekan, Smith, Barhate, Robinson, & Sigurdsson, 2008; Piton et al., 2007). Moreover, the acid treatment, which removes the DMT groups from the 5'-end of the growing chain during elongation, can also result in decomposition of nitroxide spin labels, depending on their stability.

1.2 Postsynthetic Spin-Labeling

Postsynthetic spin labeling is the other main method of choice for incorporation of spin labels at specific sites (Fig. 1B). This strategy requires oligonucleotides that have uniquely reactive groups at specific sites where the spin label is to be incorporated. Such oligomers are normally prepared by the phosphoramidite method, often using commercially available reagents. This is a useful feature of this method, because both the modified oligonucleotide and a suitable spin label can often be either purchased or readily prepared. The other merit of this method is that the spin label does not get exposed

to the reagents used in the chemical synthesis of oligonucleotides. However, a drawback of this method is the possibility of nonspecific labeling due to the nucleophilic groups present in the nucleic acids, such as the exocyclic amino groups of the nucleobases, the N7 of purines, and nonbridging oxygen atoms of the phosphodiester. In addition, incomplete spin labeling is also a well-known drawback of this method.

There are a number of sites on a nucleotide in RNA that can in principle be spin labeled postsynthetically, namely the nucleobase, the sugar, and the phosphodiester backbone. Postsynthetic spin labeling of a nucleobase can, for example, be performed by the reaction of 4-thiouridine with a suitable spin-labeling reagent. [Figure 3A](#) shows such examples, where thiol-specific methane-thiosulfonate spin-labeling reagents have been reacted with 4-thiouridine in RNA to yield a variety of spin-labeled oligomers ([Qin, Hideg, Feigon, & Hubbell, 2003](#); [Qin, Iseri, & Oki, 2006](#)). 4-Thiouridine can also be spin labeled through alkylation ([Ramos & Varani, 1998](#)). Another facile postsynthetic method is the reaction of phosphorothioates, in which one of the nonbridging oxygen atoms has been replaced with sulfur by oxidation with a sulfurizing agent during oligonucleotide synthesis, with alkylating agents ([Fig. 3B](#); [Grant, Boyd, Herschlag, & Qin, 2009](#); [Qin, Butcher, Feigon, & Hubbell, 2001](#)). This method requires the use of a deoxynucleotide at the phosphorothioate site to prevent cleavage of the RNA strand. Exocyclic amino groups in RNA have also been modified with a spin label ([Sicoli, Wachowius, Bennati, & Höbartner, 2010](#)) using the “convertible nucleoside” approach ([Macmillan & Verdine, 1990](#)). In this method, a derivative of a nucleoside possessing a leaving group on its nucleobase (the convertible nucleoside) is

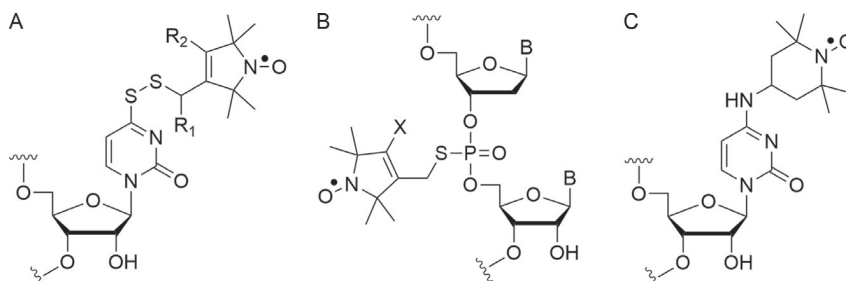


Figure 3 Representative examples of postsynthetic spin-labeling of nucleobases and phosphodiester. (A) Attachment of spin labels at 4-thiouridine. (B) Spin-labeling at phosphate backbone. (C) Labeling of exocyclic amino groups of cytosine through the convertible nucleoside approach. R₁ and R₂=H or CH₃, X=H or Br, and B is a nucleobase.

incorporated into RNA through solid-phase synthesis. After the synthesis of the full-length oligomer, it is treated with an amine-based nucleophile, which substitutes the leaving group on the nucleobase, and becomes covalently attached. [Figure 3C](#) shows an example, where TEMPO was utilized as the nucleophile ([Sicoli et al., 2010](#)).

Spin labels have also been incorporated at the 2'-position of sugars in oligonucleotides using postsynthetic methods ([Fig. 4](#)). The 2'-position is the only site that is readily available for labeling of sugars at internal positions of nucleic acids. Moreover, a spin label attached at the 2'-position gets projected out of the minor groove, causing minimal structural perturbation of the labeled RNA. Spin labels have been incorporated into 2'-positions of RNA using the Cu(I)-catalyzed Huisgen–Meldal–Sharpless [3+2] cycloaddition reaction (click chemistry), yielding triazole-linked spin labels ([Büttner, Javadi-Zarnaghi, & Höbartner, 2014; Flaender et al., 2008; Fig. 4A](#)).

Postsynthetic labeling of 2'-amino groups is another particularly facile and selective approach for labeling the 2'-position; the aliphatic 2'-amino group is more nucleophilic than the aromatic amines on the nucleobases or the hydroxyl groups on the phosphodiester and can be converted to ureas and esters ([Fig. 4B](#)). Moreover, RNA oligonucleotides having 2'-amino modification(s) are commercially available or can be synthesized in-house on an automated synthesizer using commercially available 2'-amino-modified phosphoramidites. Thus, easy availability of 2'-amino-modified RNAs makes this approach attractive. The 2'-amino group has been spin labeled through reaction with a succinimidyl ester of a pyrrolidine-derived

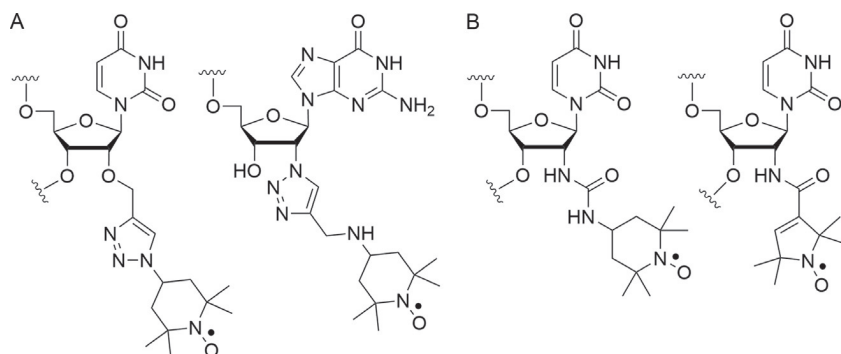


Figure 4 (A) Postsynthetic spin labeling of RNA at the 2'-position by using cycloaddition reaction between an azide and an alkyne. (B) Postsynthetic spin labeling at 2'-amino position through formation of urea or amide linkage.

nitroxide spin label to yield amide-modified spin label (Fig. 4B); however, this modification was found to cause considerable destabilization of RNA duplexes (Kim et al., 2004). Spin labeling of 2'-amino groups through reactions with aliphatic isocyanates and aromatic isothiocyanates is a more useful route than amide formation and is described in detail below.



2. 2'-AMINO SPIN-LABELING WITH ALIPHATIC ISOCYANATES AND AROMATIC ISOTHIOCYANATES

The first example of spin labeling of the 2'-position in RNA was the reaction of 4-isocyanato-TEMPO (**1**) with 2'-amino groups in RNA, forming a urea linkage (Fig. 5; Edwards, Okonogi, Robinson, & Sigurdsson, 2001). Spin-labeled oligonucleotides, prepared by this method, were used to study the structure-dependent dynamics of the transactivation response RNA (Edwards, Okonogi, & Sigurdsson, 2002; Edwards, Robinson, & Sigurdsson, 2005; Edwards & Sigurdsson, 2002, 2003) and the hammerhead ribozyme by EPR spectroscopy (Edwards & Sigurdsson, 2005). This spin-labeling method has been used by several other research groups and has the advantage that the starting materials are commercially available. However, it also has a few drawbacks. First, the isocyanate functional group is highly reactive and can lead to incomplete labeling in RNA due to a competing hydrolysis reaction, requiring a careful control of the reaction conditions. Second, at the low temperatures under which the spin-labeling reaction is performed, long RNAs sometimes form secondary structures that reduce

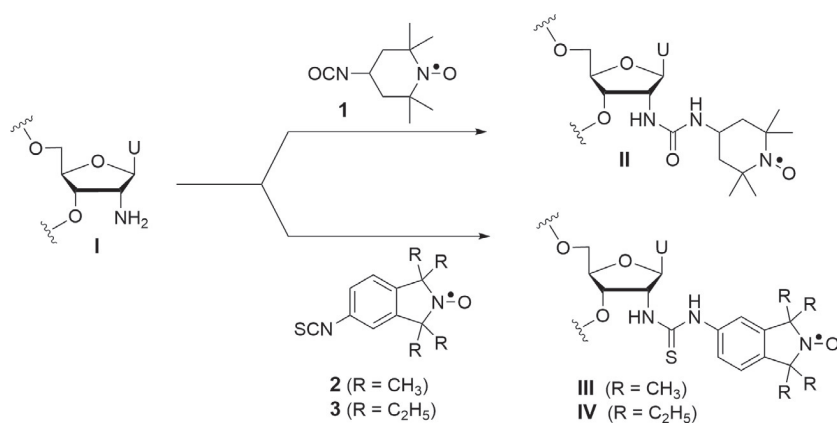


Figure 5 Spin labeling at the 2'-amino position of the oligonucleotide **I** by isocyanate **1** and isothiocyanate spin-labeling reagents **2** and **3**. U, uracil.

the reactivity of 2'-amino groups and result in low yields. In addition, TEMPO is not the optimal spin label for EPR studies due to its inherent flexibility.

To overcome these shortcomings of 4-isocyanato-TEMPO, a new class of spin labels for 2'-amino labeling has recently been introduced: isoindoline-derived nitroxides **2** and **3** have an aromatic isothiocyanate functional group, which forms a stable thiourea linker upon reaction with 2'-amino groups (Fig. 5; Saha, Jagtap, & Sigurdsson, 2015). Aromatic isothiocyanates are less reactive than aliphatic isocyanates, which allows the reaction to be carried out at a higher temperature without any nonspecific labeling. Performing these reactions at higher temperature in the presence of an organic cosolvent reduces RNA secondary structure and thus avoids potential reduced reactivity of the 2'-amino group. The detailed protocols of the preparation of these spin-labeling reagents and their incorporation into 2'-amino sites in RNA will be described in the latter part of this chapter.

2.1 Spin-Labeling of 2'-Amino Groups in RNA with 4-Isocyanato-TEMPO

Isocyanate **1**, the spin-labeling reagent for this protocol, can be either purchased (Toronto Research Chemicals) or synthesized using a previously reported protocol (Edwards et al., 2001; Edwards & Sigurdsson, 2007). As previously mentioned, the 2'-amino-modified oligonucleotides are also commercially available. A representative 2'-amino spin-labeling protocol (Edwards et al., 2001; Edwards & Sigurdsson, 2007, 2014) using isocyanate **1** is as follows:

- (1) To a solution of 2'-amino-modified RNA **I** (i.e., 5'-GACCUCG (2'-NH₂U)AUCGUG-3') (30 nmol), previously precipitated to exchange ammonium ions with sodium ions, in boric acid buffer (15 μ L, 70 mM, pH 8.6) was added formamide (9 μ L). The resulting solution was cooled in a rock salt/ice water bath (-8°C). It is recommended to perform this reaction in a cold room (4°C), which helps keeping the temperature low during transfer of reagents. The low temperature minimizes the competing isocyanate hydrolysis reaction and ensures the specificity of the labeling reaction toward the 2'-amino groups.
- (2) The solution was treated with freshly prepared **1** (9 μ L) in anhydrous *N,N*-dimethylformamide (DMF) and incubated for 1 h at -8°C . The solution of **1** was prepared by dissolving **1** (1 mg) in anhydrous DMF (67.6 μ L) to a final concentration 75 mM. Isocyanates are electrophilic functional groups and as such they are reactive toward a variety of

nucleophiles, including amines and water. Therefore, anhydrous and amine-free DMF should be used.

- (3) To ensure complete spin labeling, it is advisable to add a second aliquot of freshly prepared **1** in DMF (9 μL) after 1 h and a third aliquot after 2 h.
- (4) The extent of the spin-labeling reaction can be determined by a denaturing polyacrylamide gel electrophoresis (DPAGE) analysis. An aliquot from the reaction mixture (1 μL) was run on 20% DPAGE gel along with the starting RNA **I**; one lane contained an equimolar mixture of the starting RNA and the RNA present in the reaction. The spin-labeled RNA displays reduced mobility on DPAGE (see [Section 2.3](#) for an example of DPAGE analysis of 2'-amino spin labeling). DPAGE can be readily used to monitor the extent of spin labeling of oligonucleotides of up to ca. 20 nt long; for longer RNA sequences, it may be a challenge to gauge the difference in the mobilities of spin-labeled and unlabeled material. A quantitative conversion to spin-labeled RNA is usually observed. Non- or partial spin labeling indicates decomposition of isocyanate **1**. The purity of **1** can be examined by thin-layer chromatography (TLC) (silica gel, 5% MeOH:CH₂Cl₂, R_f (**1**) = 0.7) and IR spectroscopy (RNCO stretching at 2100–2270 cm^{-1}).
- (5) On completion of the reaction, H₂O (100 μL) was added to the reaction mixture, the solution was washed with CHCl₃ (4 \times 300 μL), and the solvent was removed *in vacuo*.
- (6) The spin-labeled RNA was precipitated in EtOH (NaOAc (5 μL , 3 M, pH 4.6) and EtOH (300 μL), -80°C , 4 h) and purified by 20% DPAGE. The gel slices containing spin-labeled material were excised, extracted using the “crush and soak method” with Tris buffer (250 mM NaCl, 10 mM Tris, 1 mM Na₂EDTA, pH 7.5), and subsequently desalted using Sep-pak C18 cartridges following the manufacturer's instructions, to obtain the final product (28 nmol).

2.2 Synthesis of Isothiocyanate-Containing Spin Labels

Spin labeling with **2** and **3** is a newly published method at the time of this writing and thus, these reagents are not yet commercially available. Therefore, the protocol for their preparation has been included. In short, **2** and **3** were prepared by reaction of their corresponding amino derivatives **4** and **5** with thiophosgene ([Fig. 6](#)), according to the following representative protocol for the synthesis of **2**:

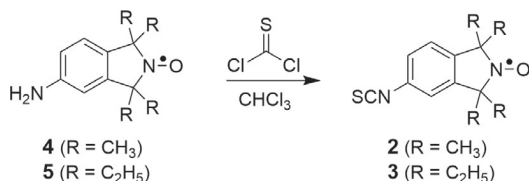


Figure 6 Synthesis of isothiocyanate spin-labeling reagents **2** and **3**.

- (1) A solution of 1,1,3,3-tetramethylisoindoline-5-amine-2-oxyl (**4**) (Jagtap et al., 2015; Mileo et al., 2013) (100 mg, 0.49 mmol) in CHCl_3 (3.5 mL) was treated dropwise with a solution of thiophosgene (0.041 mL, 0.54 mmol) in CHCl_3 (1 mL) at 24 °C. (Note: Thiophosgene is a toxic reagent and it is strongly recommended to perform the reaction in an efficiently ventilated fume hood.) The progress of the reaction was monitored by TLC (20% EtOAc:pet. ether, R_f (**4**) = 0.2, R_f (**2**) = 0.8).
- (2) After stirring for 2 h at 24 °C, the reaction mixture was washed successively with aq. NaOH (4 mL, 1 M), H_2O (2×5 mL) and brine (5 mL).
- (3) The organic layer was dried over anhydrous sodium sulfate, filtered, and concentrated *in vacuo*. The crude product was purified by flash column chromatography using a gradient elution (EtOAc:pet. ether from 0:100 to 5:95) to give **2** as a yellow solid (98 mg, 82%).

Spin-labeling reagent **3** was prepared from its corresponding amino derivative **5** (1,1,3,3-tetraethylisoindoline-5-amine-2-oxyl) (Jagtap et al., 2015) in the same manner. Isothiocyanates **2** and **3** are stable solids that have not shown any detectable decomposition after storing at -20 °C for several months.

2.3 Spin Labeling of 2'-Amino Groups in RNA with Isothiocyanates

The main difference between the protocols for spin labeling with isothiocyanates **2** and **3** and isocyanate **1** is that the spin-labeling reactions were performed at 37 °C for **2** and **3**, compared with -8 °C for **1**. A detailed representative protocol for this spin-labeling method is as follows:

- (1) A solution of an isothiocyanate spin label (**2** or **3**) (2 μmol) in DMF (20 μL) was added to a solution of RNA oligonucleotide **I** (40 nmol) in borate buffer (20 μL , 100 mM, pH 8.6) and heated at 37 °C for 8 h. For isothiocyanate **2**, we observed a precipitate at the end of the reaction which was extracted into an organic solvent (see next step).

- (2) Sterile water was added (200 μL) and the excess labeling reagent was removed by extracting the aqueous reaction mixture with EtOAc ($6 \times 500 \mu\text{L}$). Each of the EtOAc washings was collected separately, and the presence of excess unreacted spin label was monitored. TLC (silica gel, 20% EtOAc:pet. ether, R_f (**2** or **3**) = 0.8) could only be used to detect the presence of spin label in the first two rounds of extraction. In addition, EPR spectroscopy could be used to monitor the whole extraction process; the last EtOAc washing should not show any EPR activity.
- (3) In spite of the washings in step 2, we have observed traces of unattached spin contaminants in the spin-labeled RNA (especially using **2**), which were removed by EtOH precipitation: (NaOAc (5 μL , 3 M, pH 4.6) and EtOH (300 μL), -80°C , 4 h) to yield 30–34 nmol of spin-labeled RNA. Note: Further purification of the spin-labeled RNA from the precipitation by DPAGE yielded a product which was of similar purity as the precipitated RNA as judged by EPR and DPAGE.

As mentioned in the spin-labeling protocol of **1**, DPAGE is a useful method to ascertain the extent of RNA spin labeling with **1**, **2**, and **3**. It is also useful for determining the time course of a spin-labeling reaction, just as TLC is useful for monitoring the extent of chemical reactions. Figure 7 shows a DPAGE analysis of samples taken from the spin-labeling reaction mixtures (1 μL) after specific intervals of time. The spin-labeled oligonucleotide showed reduced mobility as compared to the starting 2'-amino RNA, owing to its increased mass. For example, the sample containing **2**, which

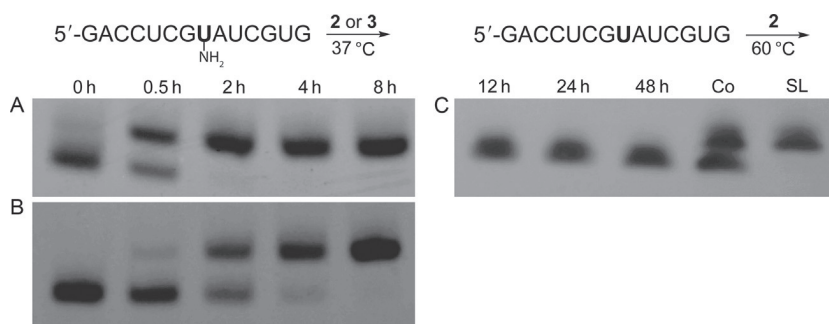


Figure 7 (A) Time course of spin-labeling reaction of RNA sequence I with **2**. (B) Time course of spin-labeling reaction of RNA sequence I with **3**. (C) Control reaction on unmodified sequence for checking out specificity of the labeling reaction with isothiocyanate spin label **2**. Lane SL contains spin-labeled RNA III, and Co is an equimolar mixture of SL and reaction mixture after 48 h.

was removed from the reaction mixture after 0.5 h, clearly showed two bands (Fig. 7A), indicating that the reaction was still not complete. However, the band corresponding to the starting oligonucleotide had disappeared after 2 h, showing that RNA **I** had been converted to its spin-labeled derivative **III**. In contrast, when tetraethyl-derivative **3** was used as the labeling reagent, 90% of the same RNA **I** was converted to **IV** in 4 h (Fig. 7B), showing that **2** was more reactive than **3**. All of the RNA for both reagents had fully reacted after 8 h.

One of the potential drawbacks of postsynthetic labeling is nonspecific reaction of reagents at unwanted sites in RNA. For example, reacting aliphatic isocyanates with unmodified RNA at 37 °C yields modified RNA (Sigurdsson & Eckstein, 1996). To determine specificity of the 2'-amino spin labeling with aromatic isothiocyanates, isothiocyanate **2** was reacted with an unmodified RNA oligonucleotide of the same sequence as 2'-amino-labeled oligomer **I**. Although the spin-labeling reactions of **I** were performed at 37 °C, the unmodified RNA was heated with **2** at 60 °C and reacted for 48 h to assess the degree of potential nonspecific labeling. Figure 7C shows no detectable conversion of the unlabeled RNA to slower moving products, demonstrating the selectivity of **2** for 2'-amino groups in RNA.

2.4 Analysis of Spin-Labeled Oligonucleotides

After the reaction of a 2'-amino-modified oligonucleotide with a spin-labeling reagent and isolation of the product, incorporation of the spin label into the RNA should be verified. Several techniques are routinely used for this purpose. Analysis by DPAGE and HPLC can be used to verify that the oligonucleotide has been modified, but other methods must be used to verify incorporation of an intact spin label (Edwards & Sigurdsson, 2014). Even mass spectrometry (MALDI-TOF) cannot distinguish between a nitroxide and its hydroxylamine derivative, which may result from an unlikely reduction of the spin label. Digestion of the oligonucleotide, followed by HPLC analysis and coinjection with an authentic sample of the spin label lesion, is a useful technique for that purpose (Edwards & Sigurdsson, 2014). However, the most direct method for detecting radicals is EPR spectroscopy.

Oligonucleotides labeled with a nitroxide radical show a characteristic three-peak pattern by EPR. EPR can also be used to detect and quantify free spin label contaminants. A free spin label tumbles rapidly in solution, giving a narrow EPR spectrum, but after attachment to RNA, the EPR lines

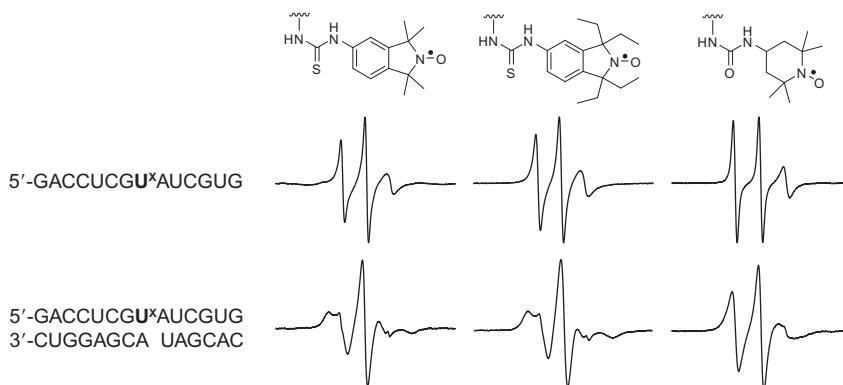


Figure 8 EPR spectra of the spin-labeled oligonucleotides at 10 °C (10 mM phosphate, 100 mM NaCl, 0.1 mM Na₂EDTA, pH 7.0). **U^x** indicates the position of the spin-labeled uridine.

become broader due to slower tumbling in solution. In the spin-labeling reaction with **2**, we detected the presence of an importunate unattached spin contaminant by EPR, which was still present after DPAGE purification. This impurity was removed by performing repeated ethyl acetate washes after the spin-labeling reaction, followed by ethanol precipitation. EPR can also be used to perform a spin-count experiment that quantifies the amount of nitroxide, which can be compared to the amount of oligonucleotides determined by UV spectroscopy.

In addition to verifying spin label incorporation, EPR spectroscopy gives valuable information about the mobility of the spin label, independent of the nucleic acid. Figure 8 shows the EPR spectra of oligonucleotides labeled with **1**, **2**, and **3**. It is noteworthy that the spectra of the isoindoline-derived spin labels are broader, compared to the TEMPO derivative, especially for the RNA duplexes. This shows that the isoindoline spin labels are less mobile and should, therefore, be more useful for studies of the structure and dynamics of nucleic acids.



3. SUMMARY AND CONCLUSIONS

Gaining understanding of RNA function through studies of structure and dynamics is an active area of research. SDSL, in combination with EPR spectroscopy, is fast turning out to be a valuable method for such studies. There are two main approaches for spin labeling, the phosphoramidite method and postsynthetic spin labeling. Among these, the latter strategy

requires minimal effort and is less time consuming. In this chapter, we have described postsynthetic spin labeling of 2'-amino groups in RNA using two classes of spin labels, aliphatic isocyanates and aromatic isothiocyanates. The aromatic isothiocyanates are particularly useful and do not suffer from any of the potential drawbacks associated with the postsynthetic labeling strategy, for example, incomplete and/or nonspecific labeling. Spin labeling with isothiocyanates is easy to perform and gives quantitative yields in a short period of time, with no detectable nonspecific labeling. These isoindoline-based spin labels are promising candidates for use in distance measurement with pulsed EPR as they showed reduced mobility by EPR, compared to a TEMPO-based spin label. Moreover, the isoindoline-derived spin labels are stable under reducing conditions (Saha et al., 2015), which makes them promising candidates for in-cell EPR spectroscopy.

ACKNOWLEDGMENTS

This research was supported by the Icelandic Research Fund. S.S. and A.P.J. gratefully acknowledge their doctoral fellowships provided by the University of Iceland. The authors would also like to thank members of the Sigurdsson research group for helpful discussions.

REFERENCES

- Belmont, P., Chapelle, C., Demeunynck, M., Michon, J., Michon, P., & Lhomme, J. (1998). Introduction of a nitroxide group on position 2 of 9-phenoxyacridine: Easy access to spin labelled DNA-binding conjugates. *Bioorganic and Medicinal Chemistry Letters*, 8(6), 669–674.
- Brummelkamp, T. R., Bernards, R., & Agami, R. (2002). A system for stable expression of short interfering RNAs in mammalian cells. *Science*, 296(5567), 550–553.
- Büttner, L., Javadi-Zarnaghi, F., & Höbartner, C. (2014). Site-specific labeling of RNA at internal ribose hydroxyl groups: Terbium-assisted deoxyribozymes at work. *Journal of the American Chemical Society*, 136(22), 8131–8137.
- Cekan, P., Smith, A. L., Barhate, N., Robinson, B. H., & Sigurdsson, S. T. (2008). Rigid spin-labeled nucleoside Ç: A nonperturbing EPR probe of nucleic acid conformation. *Nucleic Acids Research*, 36(18), 5946–5954.
- Chalmers, B. A., Saha, S., Nguyen, T., McMurtrie, J., Sigurdsson, S. T., Bottle, S. E., et al. (2014). TMIO-Pyrlmid hybrids are profluorescent, site-directed spin labels for nucleic acids. *Organic Letters*, 16(21), 5528–5531.
- Denysenkov, V. P., Prisner, T. F., Stubbe, J., & Bennati, M. (2006). High-field pulsed electron-electron double resonance spectroscopy to determine the orientation of the tyrosyl radicals in ribonucleotide reductase. *Proceedings of the National academy of Sciences of the United States of America*, 103(36), 13386–13390.
- Duss, O., Yulikov, M., Jeschke, G., & Allain, F. H. T. (2014). EPR-aided approach for solution structure determination of large RNAs or protein-RNA complexes. *Nature Communications*, 5, 3669.

- Edwards, T. E., Okonogi, T. M., Robinson, B. H., & Sigurdsson, S. T. (2001). Site-specific incorporation of nitroxide spin-labels into internal sites of the TAR RNA; structure-dependent dynamics of RNA by EPR spectroscopy. *Journal of the American Chemical Society*, 123(7), 1527–1528.
- Edwards, T. E., Okonogi, T. M., & Sigurdsson, S. T. (2002). Investigation of RNA-protein and RNA-metal ion interactions by electron paramagnetic resonance spectroscopy: The HIV TAR-Tat motif. *Chemistry and Biology*, 9(6), 699–706.
- Edwards, T. E., Robinson, B. H., & Sigurdsson, S. T. (2005). Identification of amino acids that promote specific and rigid TAR RNA-tat protein complex formation. *Chemistry and Biology*, 12(3), 329–337.
- Edwards, T. E., & Sigurdsson, S. T. (2002). Electron paramagnetic resonance dynamic signatures of TAR RNA—Small molecule complexes provide insight into RNA structure and recognition. *Biochemistry*, 41(50), 14843–14847.
- Edwards, T. E., & Sigurdsson, S. T. (2003). EPR spectroscopic analysis of TAR RNA-metal ion interactions. *Biochemical and Biophysical Research Communications*, 303(2), 721–725.
- Edwards, T. E., & Sigurdsson, S. T. (2005). EPR spectroscopic analysis of U7 hammerhead ribozyme dynamics during metal ion induced folding. *Biochemistry*, 44(38), 12870–12878.
- Edwards, T. E., & Sigurdsson, S. T. (2007). Site-specific incorporation of nitroxide spin-labels into 2'-positions of nucleic acids. *Nature Protocols*, 2(8), 1954–1962.
- Edwards, T. E., & Sigurdsson, S. T. (2014). Modified RNAs as tools in RNA biochemistry. In R. K. Hartmann, A. Bindereif, A. Schön, & E. Westhof (Eds.), *Handbook of RNA biochemistry* (pp. 151–172). Germany: Wiley: Wiley-VCH Verlag GmbH & Co. KGaA.
- Fica, S. M., Tuttle, N., Novak, T., Li, N. S., Lu, J., Koodathingal, P., et al. (2013). RNA catalyses nuclear pre-mRNA splicing. *Nature*, 503(7475), 229–234.
- Flaender, M., Sicoli, G., Fontecave, T., Mathis, G., Saint-Pierre, C., Boulard, Y., et al. (2008). Site-specific insertion of nitroxide-spin labels into DNA probes by click chemistry for structural analyses by ELDOR spectroscopy. *Nucleic Acids Symposium Series (Oxford)*, 52(1), 147–148.
- Goldfarb, D. (2014). Gd^{3+} spin labeling for distance measurements by pulse EPR spectroscopy. *Physical Chemistry Chemical Physics*, 16(21), 9685–9699.
- Grant, G. P. G., Boyd, N., Herschlag, D., & Qin, P. Z. (2009). Motions of the substrate recognition duplex in a group I intron assessed by site-directed spin labeling. *Journal of the American Chemical Society*, 131(9), 3136–3137.
- Höbartner, C., Sicoli, G., Wachowius, F., Gophane, D. B., & Sigurdsson, S. T. (2012). Synthesis and characterization of RNA containing a rigid and nonperturbing cytidine-derived spin label. *Journal of Organic Chemistry*, 77(17), 7749–7754.
- Hunsicker-Wang, L., Vogt, M., & DeRose, V. J. (2009). EPR methods to study specific metal-ion binding sites in RNA. *Methods in Enzymology*, 468, 335–367.
- Jagtap, A. P., Krstić, I., Kunjir, N. C., Hänsel, R., Prisner, T. F., & Sigurdsson, S. T. (2015). Sterically shielded spin labels for in-cell EPR spectroscopy: Analysis of stability in reducing environment. *Free Radical Research*, 49(1), 78–85.
- Jeschke, G. (2012). DEER distance measurements on proteins. *Annual Review of Physical Chemistry*, 63, 419–446.
- Kim, N. K., Murali, A., & DeRose, V. J. (2004). A distance ruler for RNA using EPR and site-directed spin labeling. *Chemistry and Biology*, 11(7), 939–948.
- Macmillan, A. M., & Verdine, G. L. (1990). Synthesis of functionally tethered oligodeoxynucleotides by the convertible nucleoside approach. *Journal of Organic Chemistry*, 55(24), 5931–5933.
- Macosko, J. C., Pio, M. S., Tinoco, I., & Shin, Y. K. (1999). A novel 5' displacement spin-labeling technique for electron paramagnetic resonance spectroscopy of RNA. *RNA*, 5(9), 1158–1166.

- Maekawa, K., Nakazawa, S., Atsumi, H., Shiomi, D., Sato, K., Kitagawa, M., et al. (2010). Programmed assembly of organic radicals on DNA. *Chemical Communications*, 46(8), 1247–1249.
- Mandal, M., & Breaker, R. R. (2004). Gene regulation by riboswitches. *Nature Reviews. Molecular Cell Biology*, 5(6), 451–463.
- Marko, A., Denysenkov, V., Margraft, D., Cekan, P., Schiemann, O., Sigurdsson, S. T., et al. (2011). Conformational flexibility of DNA. *Journal of the American Chemical Society*, 133(34), 13375–13379.
- Mileo, E., Etienne, E., Martinho, M., Lebrun, R., Roubaud, V., Tordo, P., et al. (2013). Enlarging the panoply of site-directed spin labeling electron paramagnetic resonance (SDSL-EPR): Sensitive and selective spin-labeling of tyrosine using an isoindoline-based nitroxide. *Bioconjugate Chemistry*, 24(6), 1110–1117.
- Milov, A., Salikhov, K., & Shirov, M. (1981). Application of the double resonance method to electron spin echo in a study of the spatial distribution of paramagnetic centers in solids. *Soviet Physics—Solid State*, 23, 565–569.
- Nguyen, P., & Qin, P. Z. (2012). RNA dynamics: Perspectives from spin labels. *Wiley Interdisciplinary Reviews RNA*, 3(1), 62–72.
- Nissen, P., Hansen, J., Ban, N., Moore, P. B., & Steitz, T. A. (2000). The structural basis of ribosome activity in peptide bond synthesis. *Science*, 289(5481), 920–930.
- Piton, N., Mu, Y., Stock, G., Prisner, T. F., Schiemann, O., & Engels, J. W. (2007). Base-specific spin-labeling of RNA for structure determination. *Nucleic Acids Research*, 35(9), 3128–3143.
- Qin, P. Z., Butcher, S. E., Feigon, J., & Hubbell, W. L. (2001). Quantitative analysis of the isolated GAAA tetraloop/receptor interaction in solution: A site-directed spin labeling study. *Biochemistry*, 40(23), 6929–6936.
- Qin, P. Z., Hideg, K., Feigon, J., & Hubbell, W. L. (2003). Monitoring RNA base structure and dynamics using site-directed spin labeling. *Biochemistry*, 42(22), 6772–6783.
- Qin, P. Z., Iseri, J., & Oki, A. (2006). A model system for investigating lineshape/structure correlations in RNA site-directed spin labeling. *Biochemical and Biophysical Research Communications*, 343(1), 117–124.
- Ramos, A., & Varani, G. (1998). A new method to detect long-range protein–RNA contacts: NMR detection of electron–proton relaxation induced by nitroxide spin-labeled RNA. *Journal of the American Chemical Society*, 120(42), 10992–10993.
- Reginsson, G. W., & Schiemann, O. (2011). Studying bimolecular complexes with pulsed electron–electron double resonance spectroscopy. *Biochemical Society Transactions*, 39, 128–139.
- Roy, R., Hohng, S., & Ha, T. (2008). A practical guide to single-molecule FRET. *Nature Methods*, 5(6), 507–516.
- Saha, S., Jagtap, A. P., & Sigurdsson, S. T. (2015). Site-directed spin labeling of 2'-amino groups in RNA with isoindoline nitroxides that are resistant to reduction. *Chemical Communications*, 51, 13142–13145.
- Schiemann, O., Cekan, P., Margraf, D., Prisner, T. F., & Sigurdsson, S. T. (2009). Relative orientation of rigid nitroxides by PELDOR: Beyond distance measurements in nucleic acids. *Angewandte Chemie, International Edition*, 48(18), 3292–3295.
- Schiemann, O., Fritscher, J., Kisseleva, N., Sigurdsson, S. T., & Prisner, T. F. (2003). Structural investigation of a high-affinity Mn–II binding site in the hammerhead ribozyme by EPR spectroscopy and DFT calculations. Effects of neomycin B on metal-ion binding. *ChemBioChem*, 4(10), 1057–1065.
- Schiemann, O., & Prisner, T. F. (2007). Long-range distance determinations in biomacromolecules by EPR spectroscopy. *Quarterly Reviews of Biophysics*, 40(1), 1–53.
- Shelke, S. A., Sandholt, G. B., & Sigurdsson, S. T. (2014). Nitroxide-labeled pyrimidines for non-covalent spin-labeling of abasic sites in DNA and RNA duplexes. *Organic & Biomolecular Chemistry*, 12(37), 7366–7374.

- Shelke, S. A., & Sigurdsson, S. T. (2010). Noncovalent and site-directed spin labeling of nucleic acids. *Angewandte Chemie, International Edition*, 49(43), 7984–7986.
- Shelke, S. A., & Sigurdsson, S. T. (2012). Site-directed spin labelling of nucleic acids. *European Journal of Organic Chemistry*, 2012(12), 2291–2301.
- Shelke, S. A., & Sigurdsson, S. T. (2013). Site-directed nitroxide spin labeling of biopolymers. In C. R. Timmel & J. R. Harmer (Eds.), *Structural information from spin-labels and intrinsic paramagnetic centres in the biosciences*, (pp. 121–162). Germany: Springer.
- Sicoli, G., Wachowius, F., Bennati, M., & Höbartner, C. (2010). Probing secondary structures of spin-labeled RNA by pulsed EPR spectroscopy. *Angewandte Chemie, International Edition*, 49(36), 6443–6447.
- Sigurdsson, S. T., & Eckstein, F. (1996). Site specific labelling of sugar residues in oligoribonucleotides: Reactions of aliphatic isocyanates with 2' amino groups. *Nucleic Acids Research*, 24(16), 3129–3133.
- Sisamakris, E., Valeri, A., Kalinin, S., Rothwell, P. J., & Seidel, C. A. M. (2010). Accurate single-molecule FRET studies using multiparameter fluorescence detection. *Methods in Enzymology*, 475, 455–514.
- Sowa, G. Z., & Qin, P. Z. (2008). Site-directed spin labeling studies on nucleic acid structure and dynamics. *Progress in Nucleic Acid Research and Molecular Biology*, 82, 147–197.
- Xu, Y., & Matthews, S. (2013). TROSY NMR spectroscopy of large soluble proteins. *Topics in Current Chemistry*, 335, 97–119.

